

43333

437353

64-17



MICROWAVE ASSOCIATES, INC.

1

129. p. 10.10

Handbook on
**HIGH POWER
CAPABILITIES
of
WAVEGUIDE
SYSTEMS**

M. GILDEN L. GOULD

This Document Contains
Missing Page/s That Are
Unavailable In The
Original Document

NOTICE: When government or other drawings, specifications or other data are used for any purpose other than in connection with a definitely related government procurement operation, the U. S. Government thereby incurs no responsibility, nor any obligation whatsoever; and the fact that the Government may have formulated, furnished, or in any way supplied the said drawings, specifications, or other data is not to be regarded by implication or otherwise as in any manner licensing the holder or any other person or corporation, or conveying any rights or permission to manufacture, use or sell any patented invention that may in any way be related thereto.

514 490



MICROWAVE ASSOCIATES, INC.

BURLINGTON, MASS.

Contract NObr # 85190
Index No. SRO080302, ST 9604
DEPARTMENT OF THE NAVY, BUREAU OF SHIPS,
ELECTRONICS DIVISION

JUN 1963

Handbook on

HIGH POWER CAPABILITIES of WAVEGUIDE SYSTEMS

M. GILDEN, L. GOULD,

REPRINTED JANUARY 1964



ABSTRACT

The high power capabilities of waveguide systems are specified, for the commonly used waveguide modes of propagation, in terms of electrical breakdown at high peak powers and excessive temperature rise at high average power. The material includes the characteristics of various gases and the effects of such factors as pulse length, repetition rate, gas temperature, harmonics, spurious modes and standing waves. Also included are the effects resulting from non-uniform conditions in electric field and gas which the values of power can be readily obtained. A section also discusses the problems associated with reducing the likelihood of the occurrence of failures in high power waveguide systems.




TABLE OF CONTENTS

	<u>Page No.</u>
ABSTRACT	i
TABLE OF CONTENTS	ii
LIST OF ILLUSTRATIONS	iv
LIST OF TABLES	viii
LIST OF SYMBOLS	ix
PURPOSE	xi
ACKNOWLEDGEMENTS	xii
I. THEORY OF BREAKDOWN	1
General Consideration	1
CW Breakdown	8
Non-Uniform Breakdown	8
Single-Pulse Breakdown	10
Dielectric Strength of Gases	11
Effects of an External Radioactive Source on Breakdown	16
II. ADDITIONAL FACTORS INFLUENCING WAVEGUIDE FAILURE	19
Gas Temperature	19
Waveguide Temperature	19
Effect of Altitude on Breakdown	22
Effect of the High Power Signal Characteristics	22
Effect of VSWR on Breakdown	32
Effect of Harmonic Power and Spurious Mode Power on Breakdown	34

	<u>Page No.</u>
III. WAVEGUIDE CHARACTERISTICS	38
Rectangular Waveguide - Standard and Tall	41
Circular Waveguide - TE_{11} Mode	55
Circular Waveguide - TE_{01} Mode	60
Circular Waveguide - TM_{01} Mode	67
Coaxial Waveguides	72
IV. HIGHLY LOCALIZED BREAKDOWN, NON-UNIFORM CONDITIONS	77
V. DESIGN CONSIDERATION FOR HIGH POWER WAVEGUIDE SYSTEMS	88

REFERENCES

APPENDIX I - Numerical Examples and Non-Standard Conditions

APPENDIX II - Diffusion Lengths

LIST OF ILLUSTRATIONS

	<u>Page No.</u>
Figure 1 Ratio of rms to effective value of electric field for air as a function of pressure times wavelength	4
Figure 2 Time average of $(v_1 - v_2)/p_0$ as a function of E_0/p_0 for air	5
Figure 3 Additive term for E_0/p_0 in air as a function of $p_0\lambda$	7
Figure 4 Universal breakdown curve for air	9
Figure 5 Normalized single-pulse breakdown curves for air in a parallel plane configuration	12
Figure 6 Extrapolation of pulse-breakdown curve to large values of E/p for air	13
Figure 7 Dielectric strength of gases	15
Figure 8 Sparking probability as a function of incident power	17
Figure 9 Relative breakdown power as a function of relative temperature rise	20
Figure 10 Density - equivalent pressure (p_0) as a function of altitude	25
Figure 11 Normalized breakdown field strength as a function of repetition rate for air	27
Figure 12 Region of repetition rate in which single pulse breakdown conditions are valid in air	28
Figure 13 Arcing rate as a function of pulse length in air with very long pulse lengths	29
Figure 14 Typical envelope of microwave power and equivalent trapezoidal approximation	31
Figure 15 Degradation of breakdown power by VSWR	33
Figure 16 Fractional reduction in breakdown power by harmonic power (no energy modulation)	36

	<u>Page No.</u>
Figure 17 Fraction reduction in breakdown power by harmonic and spurious mode power (full energy modulation)	37
Figure 18 CW breakdown power for air filled standard rectangular waveguides ($a/b = 2$)	45
Figure 19 CW breakdown power for air filled tall waveguides ($a/b = 0.5$)	46
Figure 20 CW breakdown power for air filled square waveguides ($a/b = 1$)	47
Figure 21 CW breakdown power for air filled narrow height waveguides ($a/b = 10$)	48
Figure 22 Single pulse breakdown power for air filled standard waveguides	49
Figure 23 Single pulse breakdown power for air filled narrow height waveguides	50
Figure 24 Average power capability of standard waveguides as a function of waveguide temperature	51
Figure 25 Average power capability of standard waveguides as a function of frequency	52
Figure 26 Average power capability of tall waveguides ($a/b = 0.5$) as a function of waveguide temperature	53
Figure 27 Average power capability of tall waveguides ($a/b = 0.5$) as a function of frequency	54
Figure 28 CW breakdown power for air filled circular waveguides TE_{01}^0 mode	58
Figure 29 Single pulse breakdown power for air filled circular waveguides, TE_{11}^0 mode	59
Figure 30 CW breakdown power for air filled circular waveguides TE_{01}^0 mode	63
Figure 31 Single pulse breakdown power for air filled circular waveguides, TE_{01}^0 mode	64

	<u>Page No.</u>
Figure 32 Average power capability of circular waveguides, TE ₀₁ mode, as a function of temperature	65
Figure 33 Average power capability of circular waveguides, TE ₀₁ mode, as a function of frequency	66
Figure 34 CW breakdown power for air filled circular waveguides, TM ₀₁ mode	70
Figure 35 Single pulse breakdown power for air filled circular waveguides, TM ₀₁ mode	71
Figure 36 CW breakdown power for air filled coaxial lines, TEM mode	75
Figure 37 Single pulse breakdown power for air filled coaxial lines, TEM mode	76
Figure 38 Transition pressure for hemispherical discontinuity in an air filled waveguide	80
Figure 39 Temperature of foreign particle in a waveguide	81
Figure 40 Normalized solution for breakdown at a hot surface (exact digital computer solution)	82
Figure 41 Breakdown of air in TM ₀₁₀ cavity, .025 hemisphere on floor	84
Figure 42 Uniform field breakdown characteristic for air, Freon 12, and SF ₆	85
Figure 43 Results of breakdown measurements with a hot wire in the presence of gas flow	86
Figure 44 Relative attenuation of modes for rectangular waveguides	91
Figure 45 Relative attenuation of modes in circular waveguide	92
Figure 46 Velocity of a traveling arc for several different gases,	97
Figure 47 Ratio of normalized single pulse breakdown field to pressure as a function of pressure times pulse width for various values of pressure times waveguide height and for a/b = 2	I-4

	<u>Page No.</u>
Figure 48 Ratio of normalized single pulse breakdown field to pressure as a function of pressure times pulse width for various values of pressure times waveguide height and for $a/b > 8$	I-5
Figure 49 Ratio of normalized single pulse breakdown field to pressure as a function of pressure times pulse width for various values of pressure times inner conductor radius	I-6
Figure 50 Ratio of normalized single pulse breakdown field to pressure as a function of pressure times pulse width for various values of pressure times radius for circular waveguides operating in the TE_{11} mode	I-7
Figure 51 Ratio of normalized single pulse breakdown field to pressure as a function of pressure times pulse width for various values of pressure times radius for circular waveguides operating in the TE_{01} mode	I-8
Figure 52 Ratio of normalized single pulse breakdown field to pressure as a function of pressure times pulse width for various values of pressure times radius for circular waveguides operating in the TM_{01} mode	I-9
Figure 53 λ/λ_g as a function of λ/λ_c	I-10
Figure 54 Diffusion lengths for air filled rectangular waveguide TE_{10} mode	II-3
Figure 55 Diffusion lengths for air filled circular waveguide	II-4

LIST OF TABLES

	<u>Page No.</u>
Table I Relative breakdown strength of gases	14
Table II Table of resistivity of common metals as a function of absolute temperature	23
Table III Formula for waveguide attenuation (cast into form for comparing the different modes of propagation)	24
Table IV Standard rectangular waveguides; TE_{10} mode	44
Table V Standard circular waveguides, TE_{11}^0 mode	57
Table VI Standard circular waveguides, TE_{01}^0 mode	62
Table VII Standard circular waveguides, TM_{01}^0 mode	69
Table VIII Standard coaxial waveguides, TEM mode	74
Table IX Comparison of breakdown power for various modes	89
Table X Relative peak power capabilities of high power components	98

LIST OF SYMBOLS

a	Waveguide width
A	Area
b	Waveguide height
C	Constant use in equation for E_e
d	Gap spacing
D	Diffusion coefficient
E_e	Effective electric field strength
E_{rms}	rms value of electric field strength
f	Frequency; also used as a correction factor for geometry
H	Ratio of net power transmitted by harmonic or spurious mode to fundamental or main mode power
K	$H^2 f^2 Z_H / Z_f$, f is a geometric factor
L	Waveguide length
n	Electron density
p	Pressure
p_0	$p T_0 / T$, density equivalent pressure
P	Power (subscripts as indicated in text)
r_0	Waveguide radius
t	Time
T	Temperature (units as indicated in text)
T_0	Reference temperature 20°C (293°K)
WR	Rectangular waveguide designation, width in inches x 100
WC	Circular waveguide designation, diameter in inches x 100
WX	Coaxial waveguide designation, inner conductor diameter in inches x 100

Z_h	Waveguide impedance at harmonic or spurious mode
Z_f	Waveguide impedance at fundamental or main mode
A	Additive term for energy modulation
λ	Wavelength
A	Characteristic diffusion length
ν_c	Electron collision frequency
ν_a	Electron attachment frequency
ν_i	Electron ionization frequency
ν_{net}	$\nu_i - \nu_a$
$\frac{1}{\rho}$	Inverse of the relative gas density
$\frac{1}{2}$	$Dn/\frac{1}{2}$, normalized electron density
ω	Angular frequency, radian

PURPOSE

The purpose of this handbook is to bring together currently available information in order to specify the high power capabilities of waveguide systems. Thus the earlier "Handbook on Breakdown of Air in Waveguide Systems"* has been extended to cover additional subjects and new results, but the same theory on breakdown of air has served as the basis and is retained as an important section. The form of presentation has also been modified for more readily determining the peak power and average power limits. Among the items added are the characteristics of those high dielectric strength gases which have been finding application in high power systems and the characteristics of components which find use in high power systems. Many components are obviously not suited for high power and are not discussed. Additional material that has been added or expanded include gas temperature, standing wave, harmonics, spurious modes, gradients in electric field and gas temperature. Another purpose is to provide specific recommendations for obtaining good performance of high power microwave transmission lines. Finally, material is included from which non-standard cases can be calculated.

*L. Gould, Microwave Associates 1956; Work performed for Navy Department, Bureau of Ships, Electronics Division NObsr 63295, "Microwave High Power Breakdown Study" April 1956.

ACKNOWLEDGEMENTS

Contributions to this work, including experimentation and preparation of material, were made by Mr. John Antonucci, Mr. Joseph Pergola and Mr. Burt Salkins.

The sponsorship of a concurrent program by Rome Air Development Center resulted in additional useful material which was included in this report.

I. THEORY OF BREAKDOWN

General Consideration

A satisfactory theory of high frequency gas discharge breakdown requires only a production mechanism due to primary ionization of the gas molecules by electrons and breakdown occurs when the production rate of electrons becomes greater than or equal to the loss of electrons by diffusion to the surrounding walls and attachment to neutral gas molecules. A detailed study of the build-up of the discharge is obtained from considering the continuity equation for electrons¹

$$\partial n / \partial t = \nu_1 n - \nu_a n + \nabla^2 (Dn) \quad (1)$$

Equation (1) states that the net number of electrons produced per second, $\partial n / \partial t$, is equal to the number of electrons produced per second by ionization, $\nu_1 n$, less the number of electrons lost per second by attachment, $\nu_a n$, and the number of electrons lost per second by diffusion, $-\nabla^2 (Dn)$. The coefficients ν_1 , ν_a , and D can be obtained as a function of applied electric field or average electron energy from dc measurements of drift velocity, average energy, Townsend ionization coefficient, and attachment coefficient².

A solution of Equation (1) is feasible provided the correlation between electron energy and the applied microwave field has been established. A study of the electron motion in a microwave field

shows that the electron average energy will be modulated in time at a frequency which is twice the applied frequency¹. The degree of energy modulation depends upon the ratio of the electron energy relaxation time to the period of oscillation. In air and in high dielectric strength gases the electron energy losses due to excitation of molecular vibration and rotation, inelastic collisions, are large compared to the energy losses due to elastic collisions. The electrons, therefore, lose their energy very rapidly in these gases at high pressures so that the electron energy relaxation time can be comparable and even smaller than the period of rf oscillation. For small values of relaxation time the mean electron energy literally follows the instantaneous value of electric field. At low pressures or short wavelengths, the energy relaxation time is large compared to a period so that the degree of energy modulation is negligible and the mean electron energy can be considered as independent of time. In this case, the high frequency field can be related to an effective dc field^{2,3} defined as

$$E_e = E_{rms} / [1 + (u/v_c)^2]^{1/2} = E_{rms} / [1 + (C/p_0 \lambda)^2]^{1/2} \quad (2)$$

The coefficient C has different values for each gas and for air is 36. The factor $[1 + (u/v_c)^2]^{-1/2}$ is a measure of the efficiency of energy transfer from the microwave field to an electron. The efficiency of energy transfer decreases as the pressure or wavelength decreases, with the efficiency factor becoming significantly smaller

than unity for $p_0\lambda$ less than 200 in air. A plot of E_{rme}/E_0 for air as a function of $p_0\lambda$ is shown in Figure 1. The coefficients in Equation 1 can be determined from dc measured values by considering E_0 as an equivalent dc field.

The degree of energy modulation becomes important for values of $p_0\lambda$ larger than 250 in air, that is the energy relaxation time becomes comparable to the rf period. The actual time variation of the electron energy in a given microwave field is determined from a solution of the energy balance equation¹. This solution coupled with the known dependence of v_1 , v_a , and D upon mean energy then yields the time variation of v_1 , v_a and D . These quantities are now averaged over an rf cycle, since it is the average value of the coefficients which is important. The diffusion coefficient is fairly independent of the degree of energy modulation and can be determined directly from the value of E_0 as in the low pressure-wavelength case; however, this is not the situation for the frequencies of ionization and attachment. The time average of $(v_1 - v_a)/p_0$ as a function of E_0/p_0 is shown in Figure 2 for air for various values of $p_0\lambda$. The effect of energy modulation is to significantly increase the net average rate of the electron production. This occurs because the ionization rate increases very rapidly with the electron energy so that during the peaks of energy in the modulation cycle large ionization rates occur. For simplicity, it is desirable to normalize the values of E_0/p_0 so that only a single curve of (v_{net}) vs. E_0/p_0 , that for $p_0\lambda = 0$, is required. This is

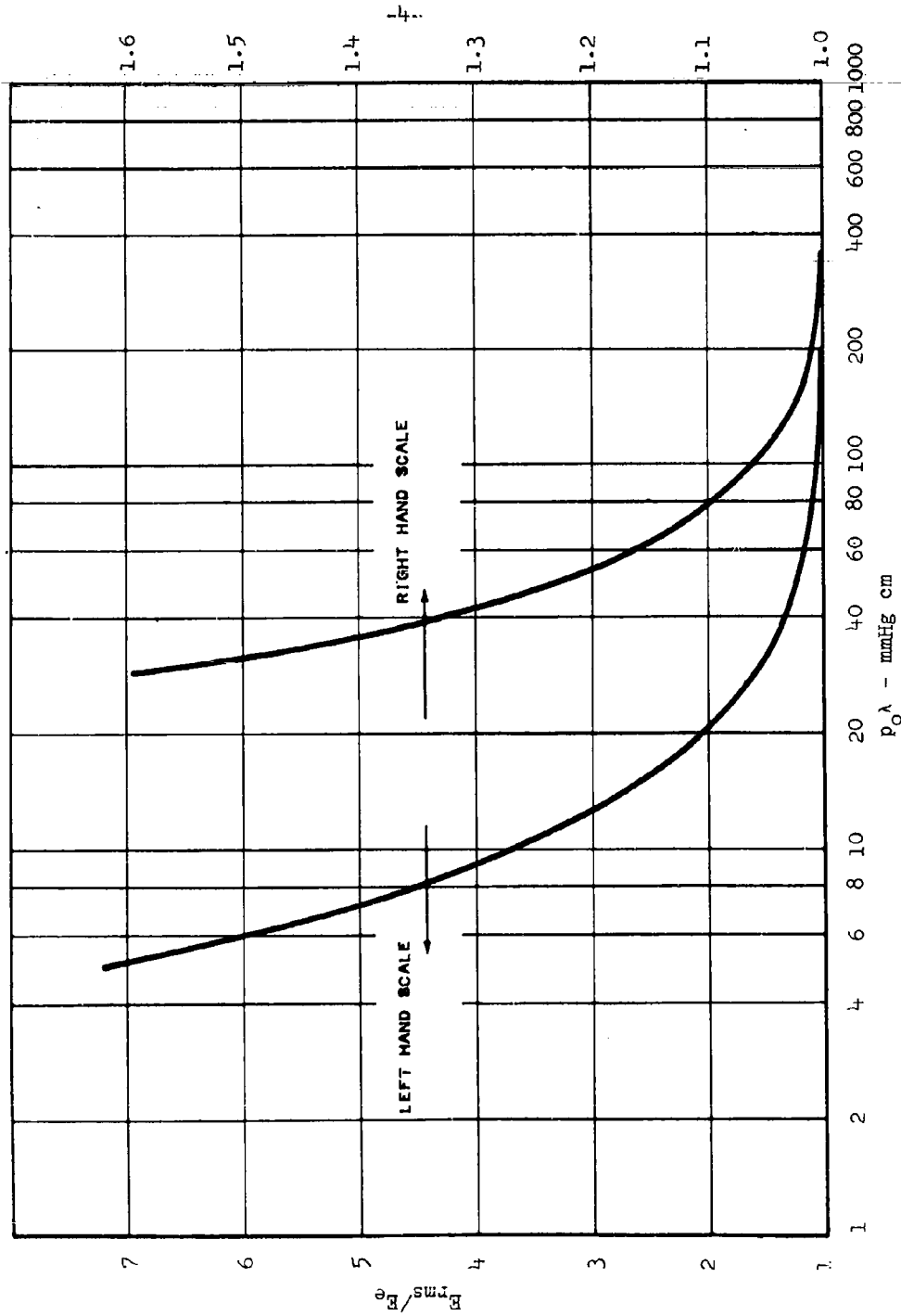


Figure 1 Ratio of rms to effective value of electric field for air as a function of pressure times wavelength

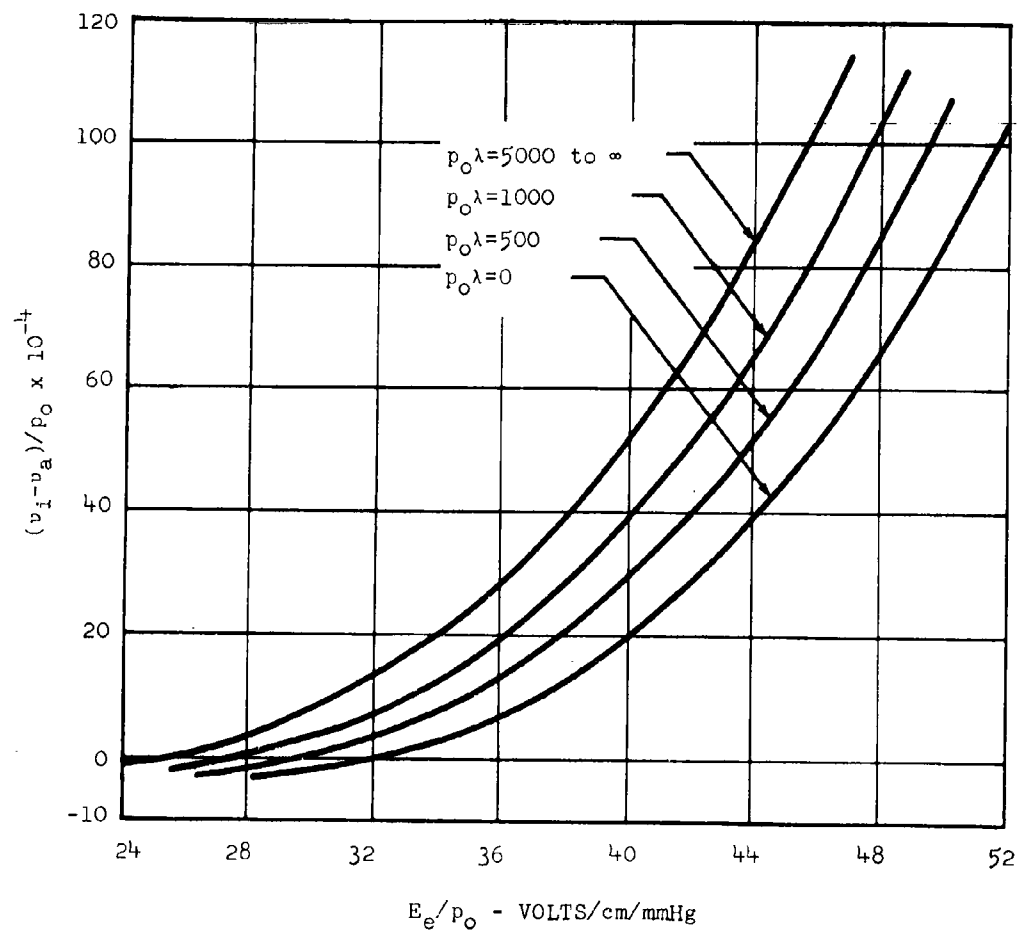


Figure 2 Time average of $(v_i - v_a)/p_0$ as a function of E_e/p_0 for air

accomplished by introducing an additive term, Δ , defined by

$$(E_e/p_o)_n = E_e/p_o + \Delta \quad (3)$$

which only depends upon $p_o \lambda$, as shown in Figure 3. When the term Δ is added to E_e/p_o (as computed from Equation 2) the resulting value is used with the $p_o \lambda = 0$ curve of Figure 2 to determine the average value of the ionizing frequency. The above analysis shows that the actual rf field strengths can be equated to dc fields in terms of the parameter $p_o \lambda$, the product of pressure and wavelength.

The electron continuity equation, Equation (1), can be solved for the breakdown conditions in waveguide systems. The boundary conditions are that the electron density is zero on the waveguide walls. For compactness $(v_i - v_g)$ in Equation (2) is replaced by $(v_i - v_g) = v_{net}$. For uniform conditions, i.e., v_{net} and D constant in space, functions are sought for n such that

$$\frac{V^2 n}{n} = - \frac{1}{\Lambda^2} \quad (4)$$

where Λ is a constant dependent upon the size of the volume and is called the characteristic diffusion length. Typical values of Λ will be discussed in a following section; however, for illustration $\Lambda = d/\pi$ for a parallel plane region. With the above assumptions and definitions the solution to Equation (1) becomes

$$n = n_o \exp \left[\frac{v_{net}}{p_o} - \frac{D p_o}{p_o^2 \Lambda^2} \right] p_o t. \quad (5)$$

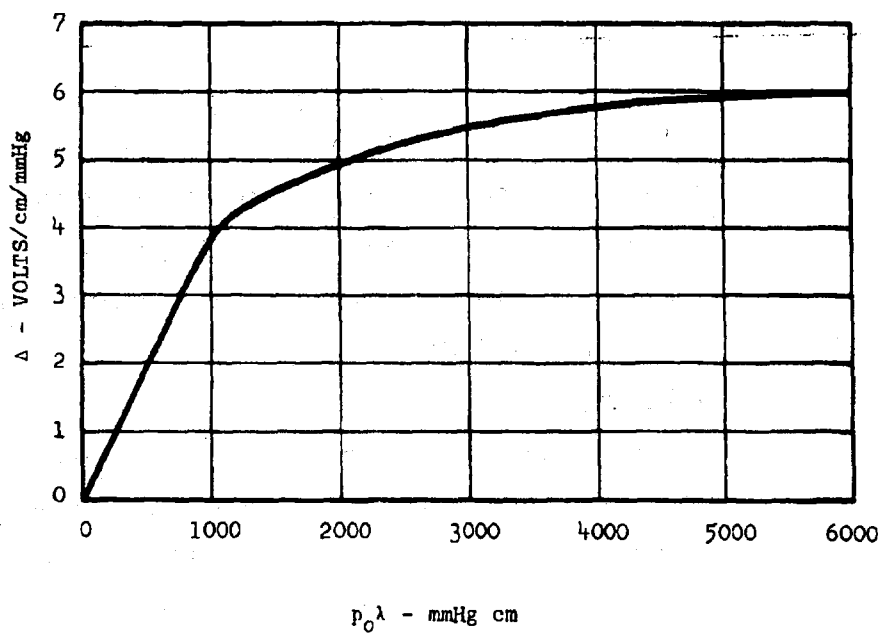


Figure 3 Additive term for E_e/p_0 in air as a function of $p_0\lambda$

It is seen that n can grow exponentially when the exponential growth factor, the quantity in the brackets, is positive. Thus a necessary condition for breakdown is

$$\left[\frac{v_{\text{net}}}{p_0} - \frac{Dp_0}{p_0^2 \Lambda^2} \right] > 0. \quad (6)$$

The grouping of terms is consistent with scaling laws for gases, i.e., v/p_0 is a single valued function of E/p_0 and Dp_0 is also a function of E_e/p_0 but essentially constant. Likewise $p_0 \Lambda$ and $p_0 t$ are also suitable normalized variables.

CW Breakdown

The cw breakdown condition, since the time for the exponential growth can be infinity long, is that the left hand side of Equation (6) be identically zero. Since both v_{net}/p_0 and Dp_0 are functions of $(E_e/p_0)_n$, Equation (6) defines a relationship between $(E_e/p)_n$ and $p_0 \Lambda$. This relationship is shown in Figure 4 for air. For large values of $p_0 \Lambda$, where attachment is the dominant loss mechanism, $v_{\text{net}}/p_0 = 0$ and the value of $(E_e/p_0)_n$ becomes independent of the dimensions of the volume. In the pressure range where Λ is constant and attachment dominates, the familiar linear relationship between breakdown field strength and pressure (or breakdown power and the square of pressure) holds. As diffusion becomes important or as the value of Λ depends upon pressure this linear relationship falls.

Non-Uniform Breakdown

In most practical situations the electric field intensity is not uniform within the volume and at certain walls the values are zero.

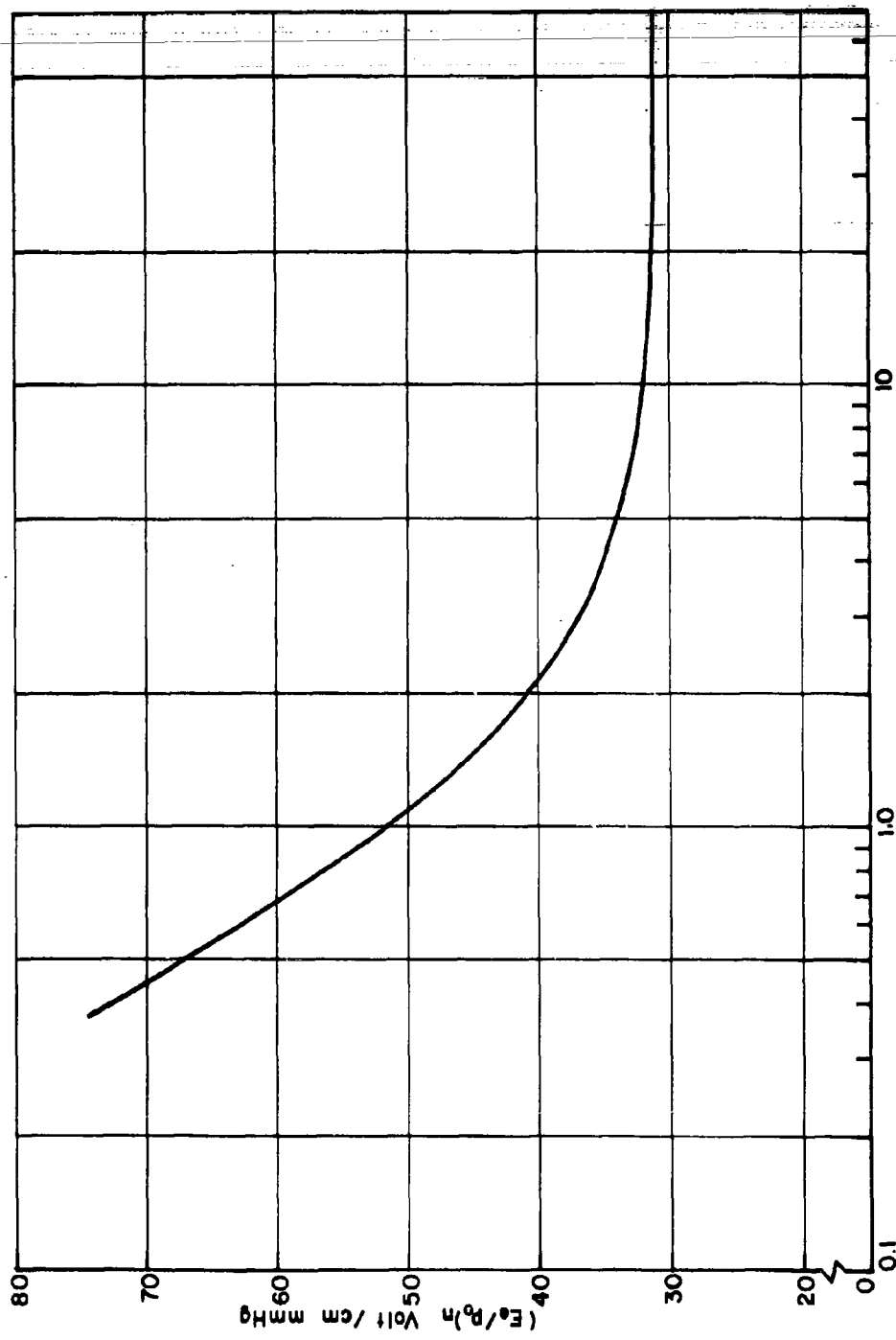


Figure 4 Universal breakdown curve for air

$$\left[\frac{v_{net}}{p_0} - \frac{Dp_0}{p_0^2 \Lambda^2} \right] = \frac{\ln(n_b/n_0)}{p\tau} \quad (7)$$

Empirically it has been found that a value of n_b/n_0 of 10^8 yields good agreement between theory and experiment. Because the logarithm of this ratio appears in Equation 7, the values of breakdown field strength are insensitive to this ratio. An order of magnitude change in n_b/n_0 changes the breakdown field by only a few percent. Figure 5 shows a normalized single-pulse breakdown curve for a parallel plane gap for various values of $p_0 d$. The normalized effective field is plotted as a function of $p_0 \tau$. For large values of $p_0 \tau$, the values of $(E_e/p_0)_n$ approach the cw values. For small values of $p_0 \tau$, $(E_e/p_0)_n$ rises indicating that greater peak powers can be handled in a given geometry with decreasing values of $p_0 \tau$. In addition, for small values of $p_0 \tau$ Figure 5 shows that breakdown becomes independent of values of $p_0 d$ (i.e., electron diffusion become unimportant). This can be seen from Equation 7 by noting that as τ is decreased the left hand side of the equation can only increase significantly through an increase in v_{net}/p_0 ; therefore, the term involving $p_0 \Lambda$ eventually becomes negligible. A theoretical extension of Figure 5 using available data and some approximation is given in Figure 6 for $p_0 d \rightarrow \infty$.⁴

Dielectric Strength of Gases

A number of gases in addition to air are used in waveguide systems, primarily, to increase the power handling capability. Although these gases intrinsically have relatively high dielectric strength,

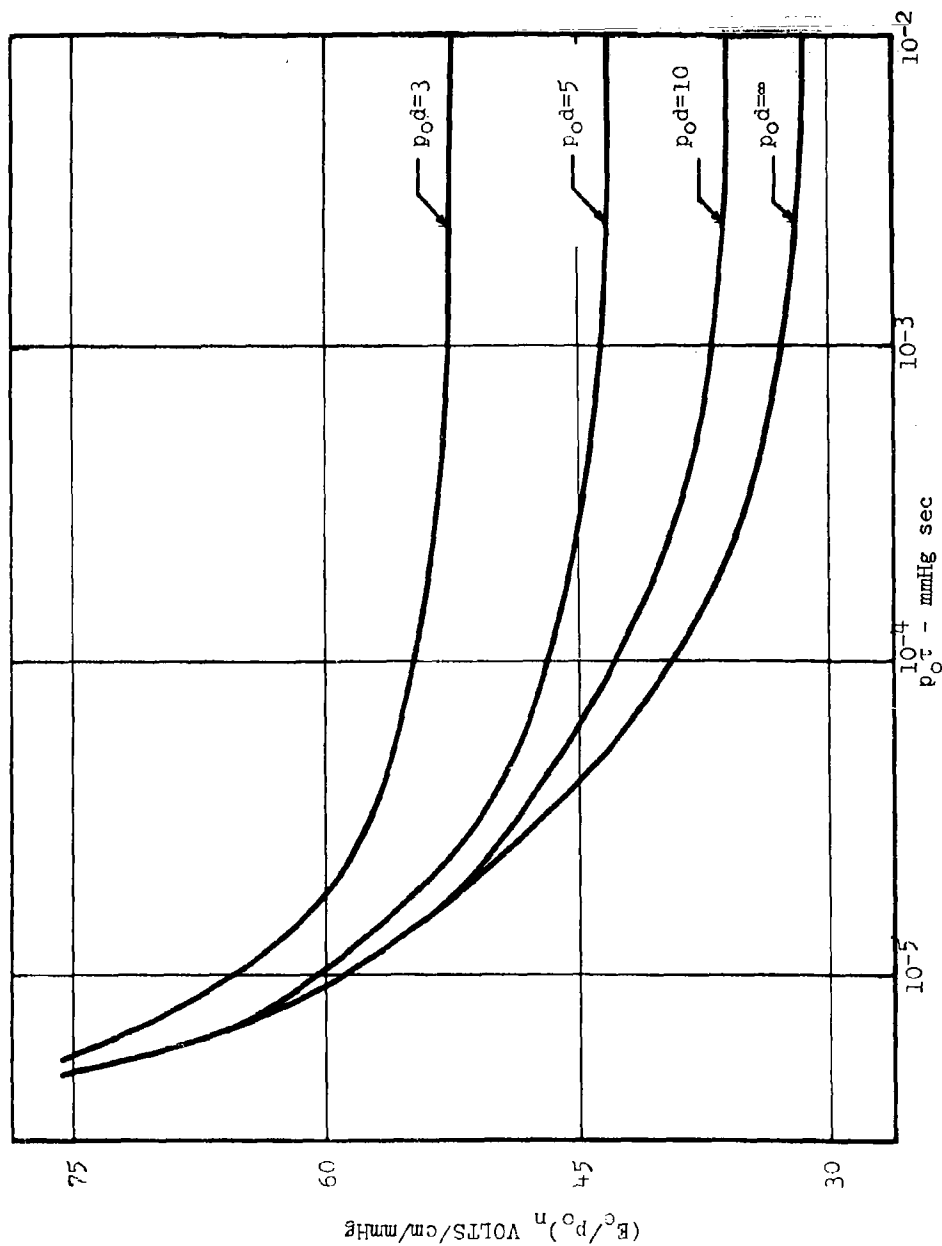


Figure 5 Normalized single-pulse breakdown curves
for air in a parallel plane configuration

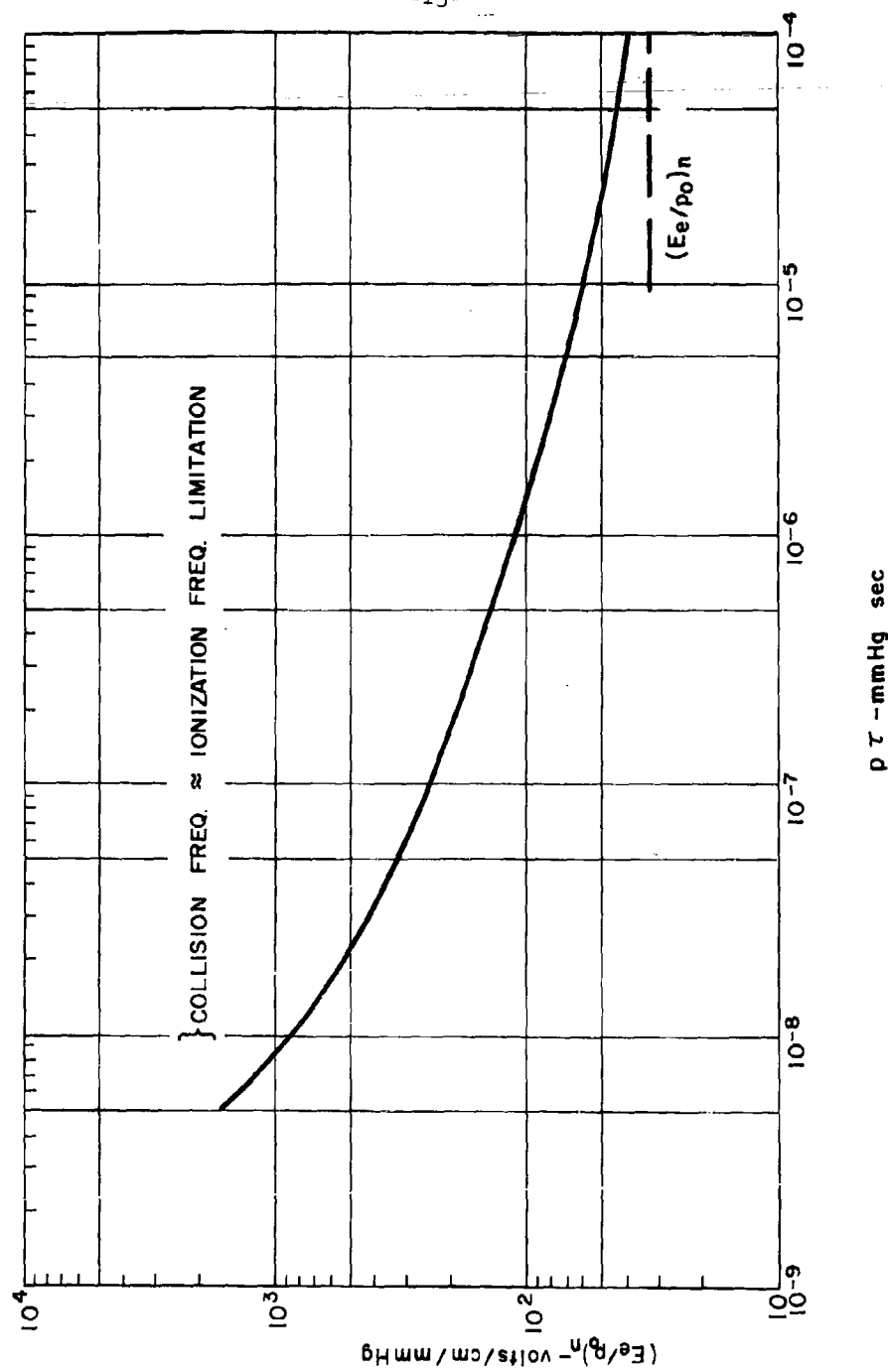


Figure 6 Extrapolation of pulse-breakdown curve to large values of E/p for air

they are seldom realized in practice. Results of microwave measurements on breakdown in a parallel plane geometry are given in Figure 7. Values of E_{rms}/P_0 are used because insufficient data is available to compute $(E_e/p_0)_n$. The normalized breakdown field strengths are indicated in Figure 7 and the relative power handling capability of the gases are tabulated below.

TABLE I

Relative Breakdown Strength of Gases

<u>Gas</u>	<u>Relative Breakdown Power</u>
Air	1.0
Nitrogen	0.9
Freon 12	18
SF ₆	20
Freon 114	49
Freon C318	60

The values for Freon 12 and SF₆ are substantiated by ionization and attachment data^{2,5}; however, none was available for Freon 114 and Freon C318. For the pressure ranges covered in the experiments the above ratios are relative to air with full energy modulation of the electrons and very likely the same condition exists in high dielectric strength gases. Data to extend the curves to the right could not be obtained in the set of experiments because of other failure mechanisms (see Section IV).

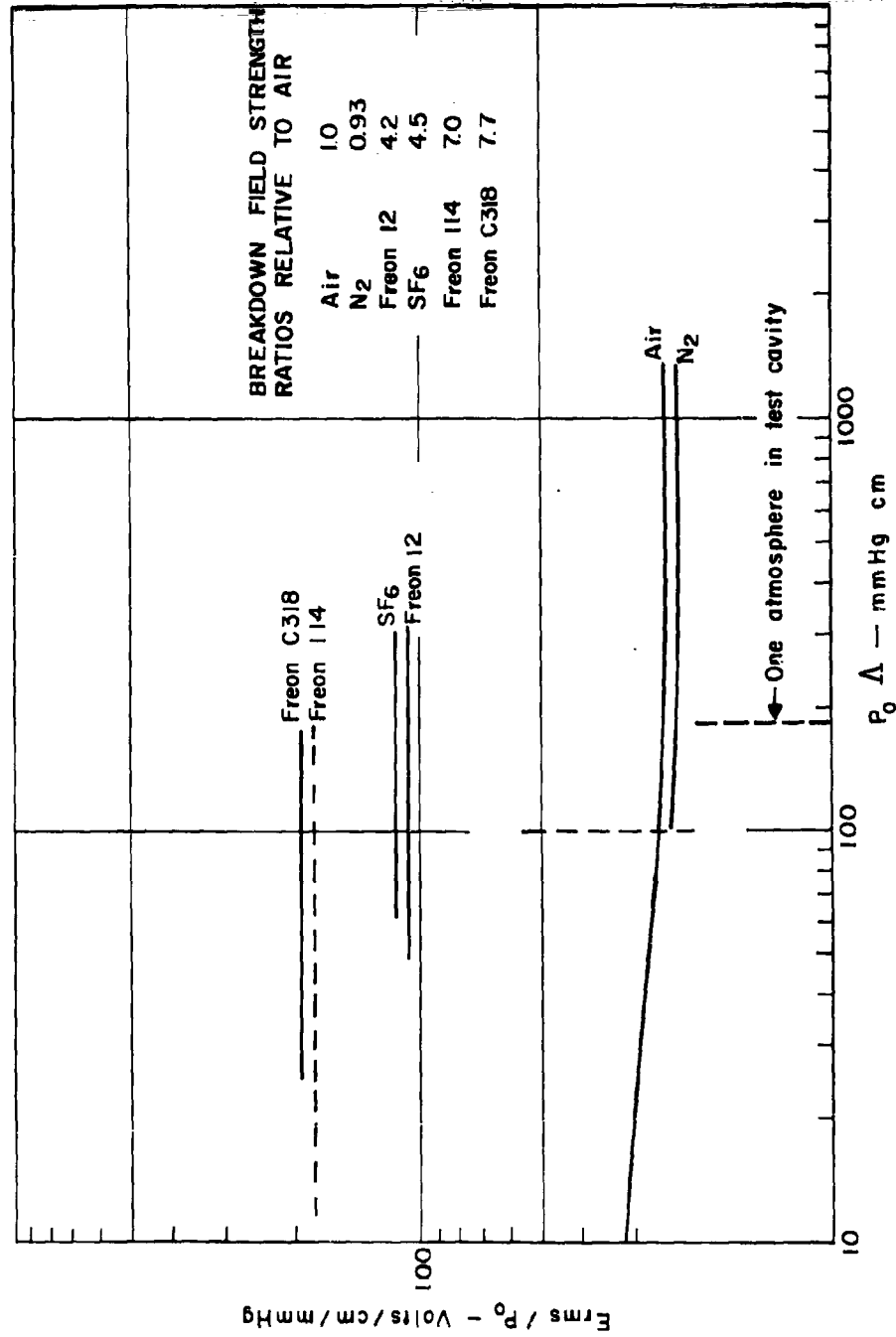


Figure 7 Dielectric strength of gases

Effects of an External Radioactive Source on Breakdown

A sufficiently strong radioactive source is necessary in order to insure that a sufficient number of electrons are present in the discharge region so that the statistical fluctuations in the breakdown field are minimized. In the experiments at Microwave Associates, Inc. an 80 millicurie source of cobalt 60 was used. A typical curve of the sparking probability, i.e., the number of breakdowns per pulse, as a function of relative incident power for various values of lead thickness between the source and the discharge region is shown in Figure 8. The conditions of the measurements are atmospheric pressure, 0.8 microsecond pulse width, and 1000 cps repetition rate. The number of breakdowns is determined from the number of light impulses detected by a photomultiplier which are counted on a standard Berkeley counter. This work and the results reported by Cooper⁶ demonstrate that the sparking probability is a function of the irradiation conditions of the discharge region and microwave field; whereas, there exists a threshold value of breakdown field which is fairly insensitive to the irradiation conditions. The theoretical pulsed breakdown field represents the minimum field necessary for breakdown and, consequently, is associated with the threshold value of breakdown. Rather than establishing the threshold field from curves as shown in Figure 8, which can present a tedious task, the threshold field can be assumed when a sparking probability of 10^{-3} exists. Another factor influencing the reproducibility of breakdown measurements is the size of the breakdown region. For example, a radioactive source sufficient for study

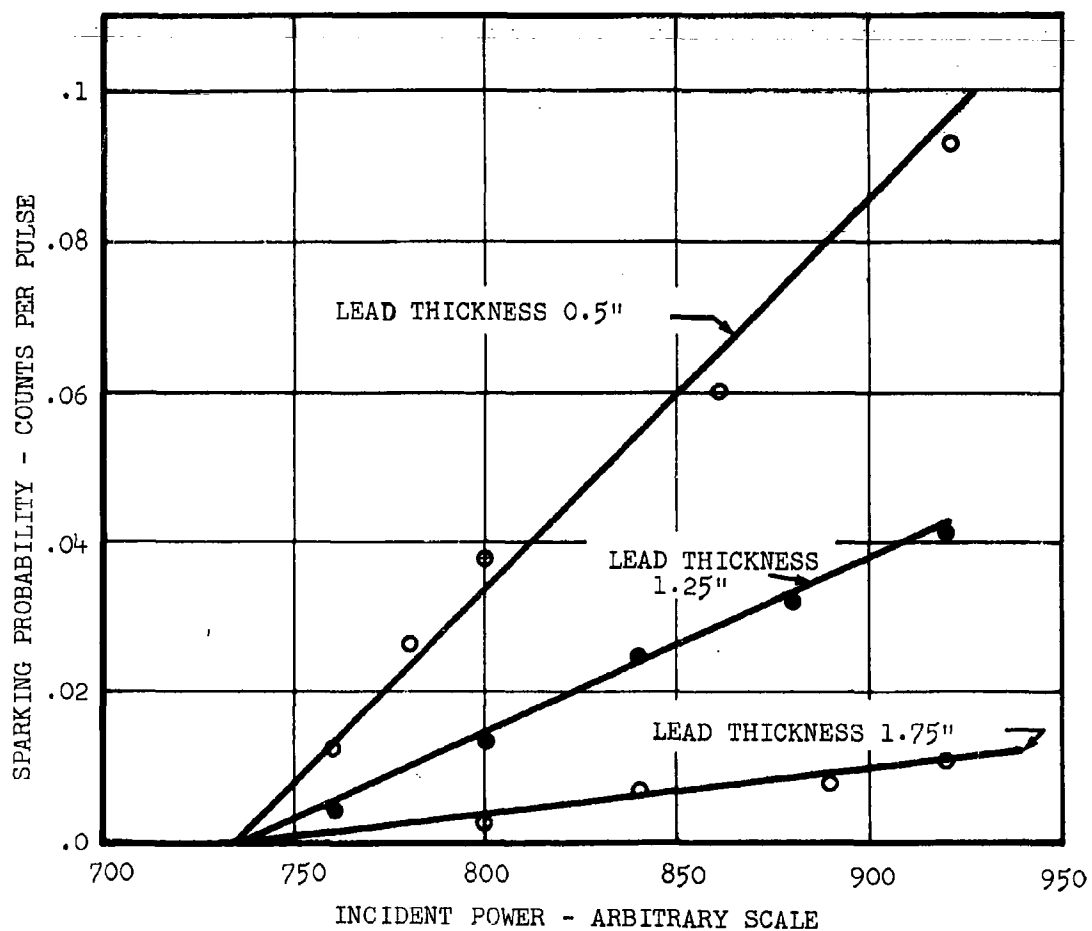


Figure 8 Sparking probability as a function of incident power

of a uniform parallel-plane region proved to be inadequate when a small hemisphere was introduced to study breakdown at a discontinuity. Other useful sources for creating initial ionization are ultraviolet light and X-rays. Thus a strong source of radiation in the immediate breakdown region is desirable in order to eliminate the necessity of determining sparking probability curves for every experimental condition and to enhance the accuracy and reproducibility of the threshold field measurements.

II. ADDITIONAL FACTORS INFLUENCING WAVEGUIDE FAILURE

There are other factors which influence microwave breakdown in waveguides. These factors include the gas temperature, the characteristics of the high power signal and the conditions of the transmission line.

Gas Temperature

One of the factors important in the breakdown theory is the gas density. For convenience, however, the gas density is expressed in terms of an equivalent pressure at a particular reference temperature. In this handbook the reference temperature is 20°C or 293°K. The equivalent pressure, from the ideal gas law, is

$$P_0 = p \frac{T_0}{T} \quad (8)$$

where the temperatures are expressed in absolute units. To facilitate applying Equation 8, Figure 9 contains a curve showing the relative breakdown power of any gas as a function of the relative temperature rise. This curve is only valid where E/p is independent of pressure variations. Although the reference temperature is indicated, this curve is also applicable for an arbitrary reference temperature.

Waveguide Temperature

In general the gas in a section of waveguide will be in thermal equilibrium with the walls. At high average power levels where the

condition imposes an upper limit on the breakdown power whereas the cw breakdown condition imposes a lower limit on the breakdown power. Measurements of breakdown power as a function of repetition rate indicate that there exists a wide range of repetition rates in which the single pulse breakdown conditions are valid, Figure 11. This range of repetition rate is given approximately by the condition that the repetition rate be less than three times the pressure. Figure 12 shows the range of repetition rate in which the single pulse breakdown conditions are valid. For the range in which single pulse breakdown conditions are not valid, the variation of breakdown power with repetition rate must be determined experimentally in order to obtain an accurate value of breakdown power.

The effect of pulse length was discussed in Section I and it was seen that for pulse lengths greater than 2 to 3 microseconds the breakdown threshold was essentially cw in air at atmospheric pressure. This has been verified experimentally also. Deviations from these results have been found at very long pulse lengths and consequently high average power^u. Experimental measurements are shown in Figure 13 in terms of arcing rate as a function of pulse length for pulse lengths in the range of 50 to 1000 microseconds. The number of arcs per pulse increase both with pulse repetition rate and pulse length. For constant arcing rate the peak power decreases with pulse length. The measurements were made at a hemisphere in a waveguide and the arcing rate was measured with a photo detector and a counter. A satisfactory explanation has not been found; however, it is likely that the results are related

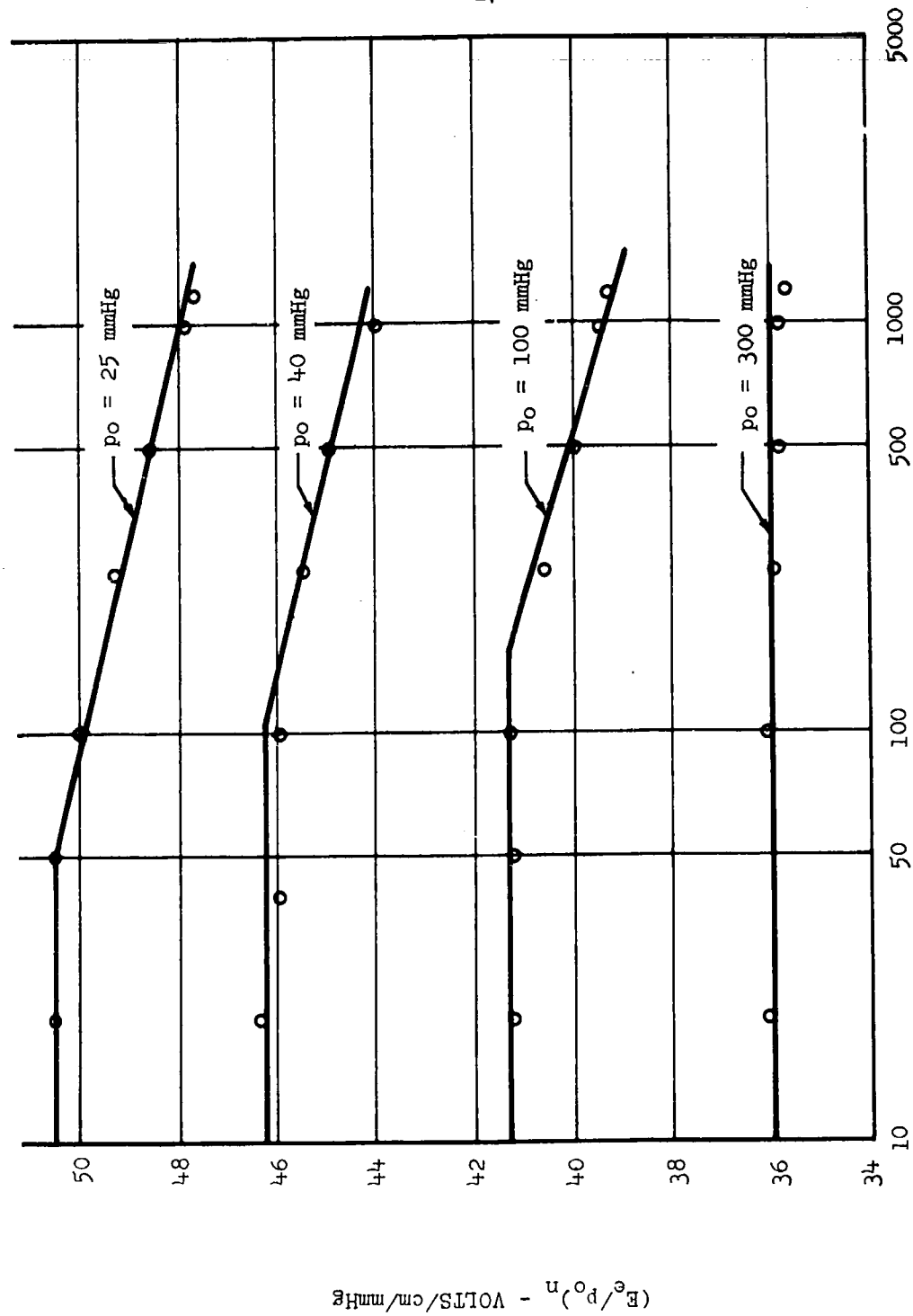


Figure 11 Normalized breakdown field strength as a function of repetition rate for air

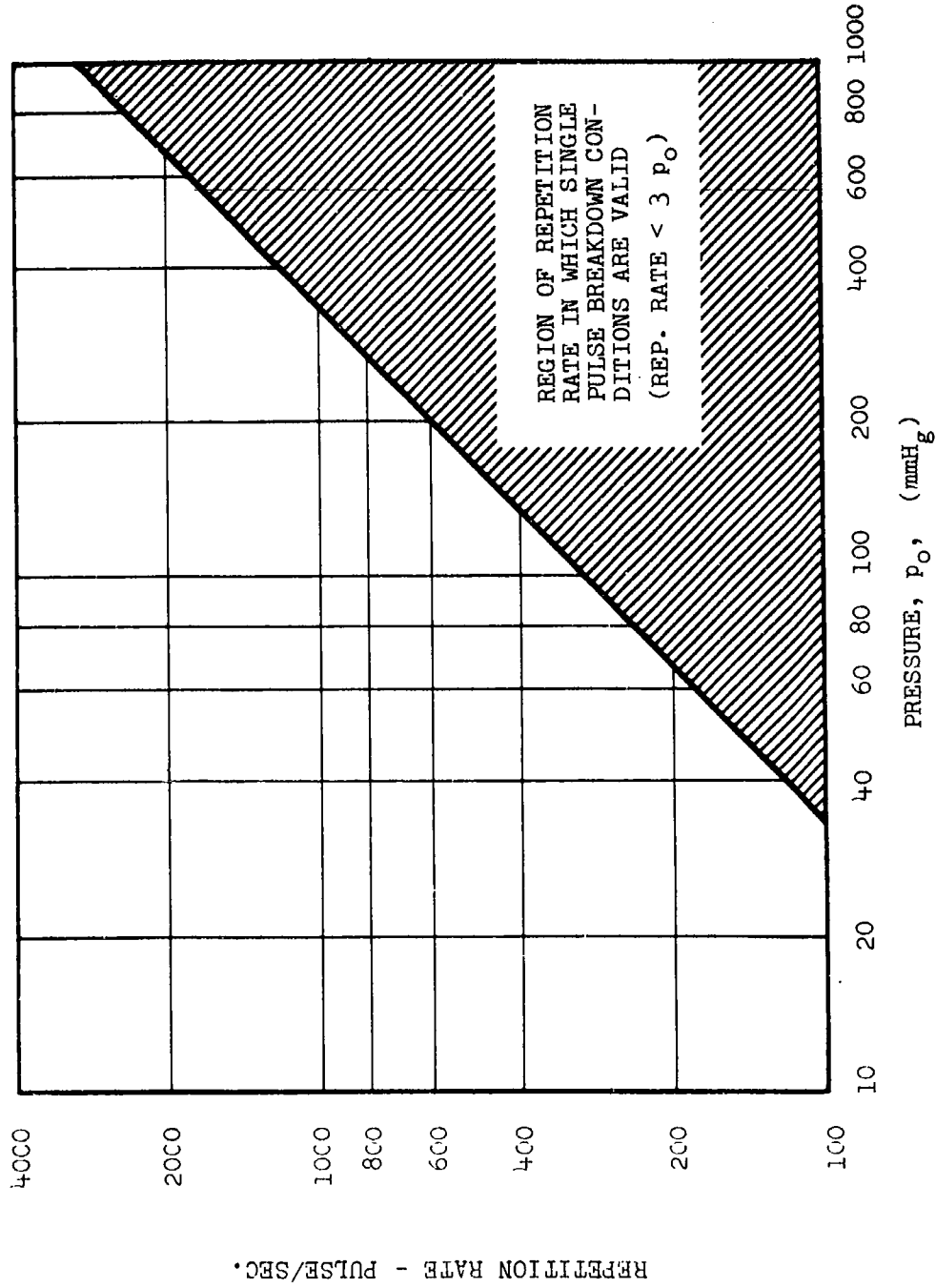
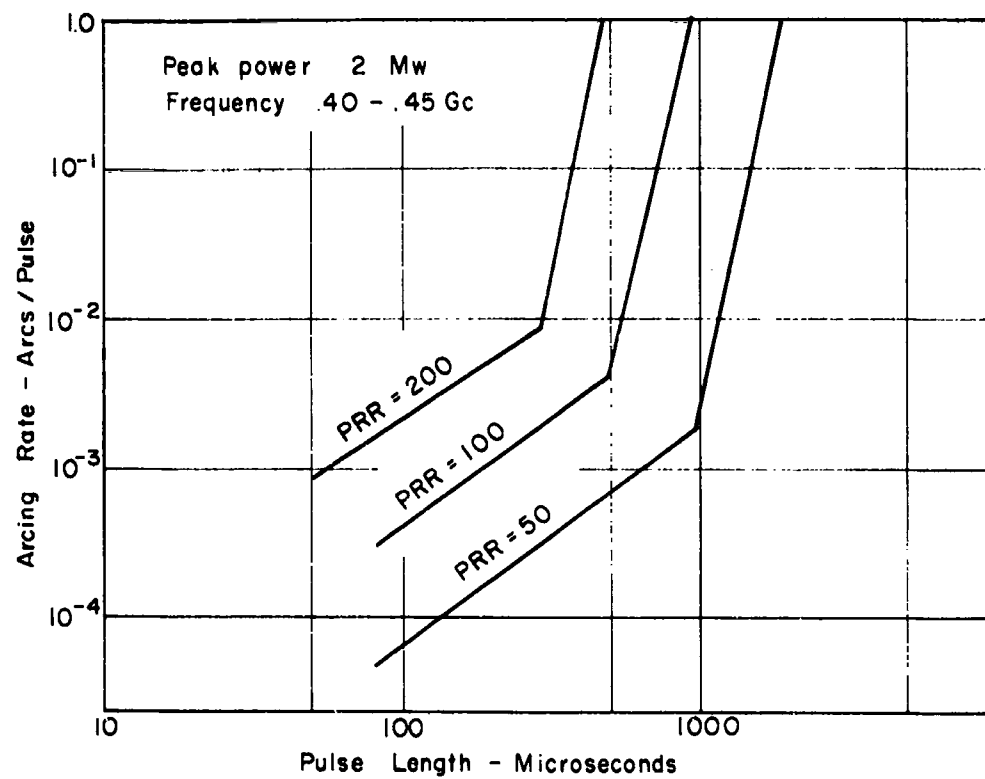
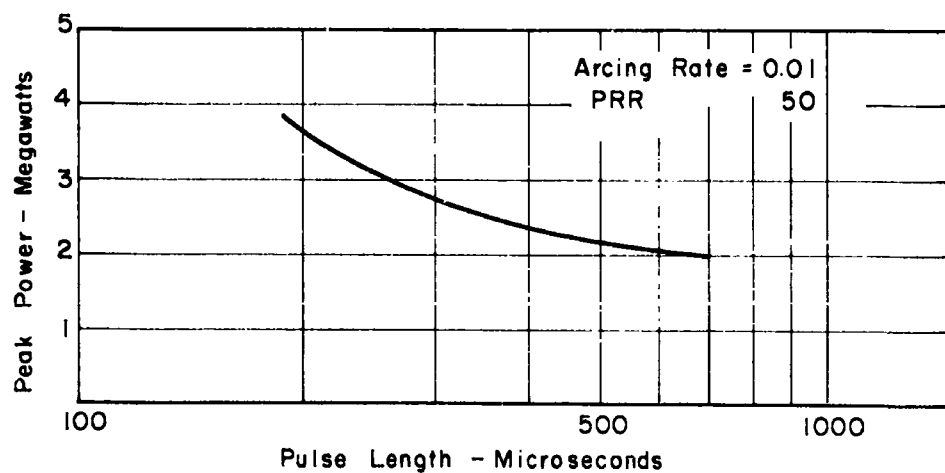


Figure 12 Region of repetition rate in which single pulse breakdown conditions are valid in air



a.) Arcing Rate As A Function Of Pulse Length



b.) Peak Power As A Function Of Pulse Length

Figure 13 Arcing rate as a function of pulse length in air with very long pulse lengths

to the highly localized breakdown effects discussed in Section IV. In any event, the breakdown results in Figure 13 indicate that system failure problems can arise at lower thresholds than expected with very long pulses.

In developing the theory of pulsed breakdown, it has been assumed that the pulses of microwave power are rectangular in shape. In practice, such is not the case. However, most pulses can be represented to the first approximation as trapezoidal in shape. A typical envelope of a microwave pulse is shown in Figure 14 as the solid line. The equivalent trapezoid used to approximate this pulse is represented by the dotted line. The hatched area depicts that portion of the pulse which will contribute to breakdown; i.e., that portion of the pulse in which the electric field is larger than the cw value. Calculations show that for t_1/t_2 and t_3/t_2 less than one, the trapezoid pulse may be replaced by an equivalent rectangular pulse of width t_2 seconds. For example, the equivalent rectangular pulse in Figure 14 is 0.8 microseconds. Therefore, in interpreting the theoretical breakdown curves, the equivalent rectangular pulse width of the power pulse should be used. In general, for more complicated pulse shapes, the value of the breakdown field must be computed numerically from Equation 1. For this case, a definition of pulse width is no longer applicable and each case of breakdown must be computed individually.

The calculations of peak power from average power measurements involves a different definition of pulse width. For an arbitrary pulse shape the relation between average power and peak power is given by

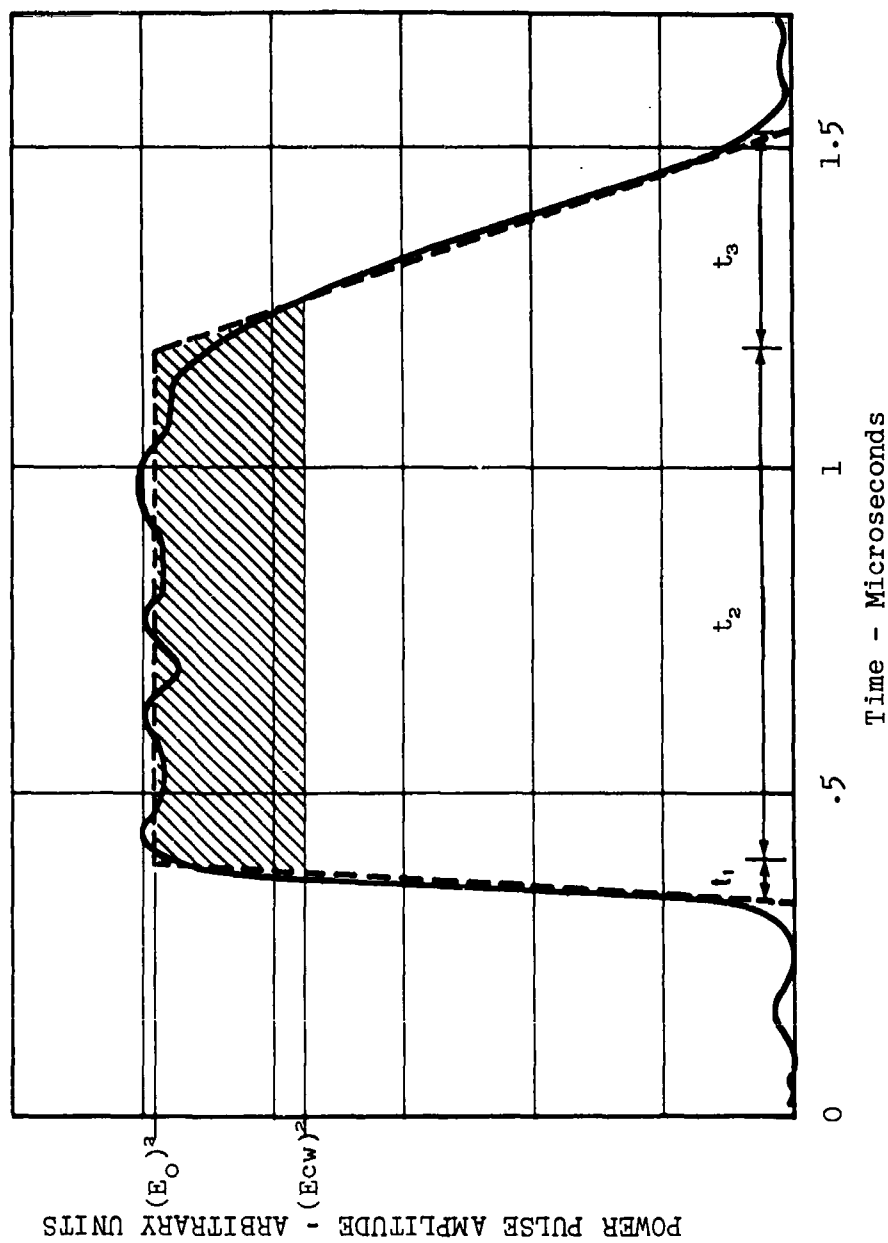


Figure 14 Typical envelope of microwave power and equivalent trapezoidal approximation

$$P_{\text{average}} = \text{repetition rate} \times \int P_{\text{peak}} dt \quad (12)$$

The peak power is integrated over the time of the pulse. For the trapezoidal pulse, the time $[t_n + (t_1 + t_2)/2]$ is the corresponding rectangular pulse width which is used in interpreting the power measurements. In Figure 14, the actual area under the pulse was measured yielding a pulse width of one microsecond to be used in the calculation of peak power. This differentiation in the definition of pulse width must be considered for proper interpretation of the experimental measurements.

Effect of VSWR on Breakdown

A standing wave degrades the power handling capability of a transmission line. The amount of degradation may be derived from two different points of view depending upon whether the breakdown power is taken as 1) the net transmitted power or 2) simply the power carried by the forward component of the standing wave. If the net transmitted power is used (where $P_t = P_f - P_r$), then as the value of VSWR increases the relative transmitted power or degradation ratio continues to decrease as shown in Figure 15 by curve 1. Basically this continuous decrease occurs because the breakdown is determined by the sum of the field strengths in the forward and reflected waves. The transmitted power, on the other hand, is determined by the difference in the square of the field strengths which continues to decrease with increasing VSWR. If the power carried by the forward

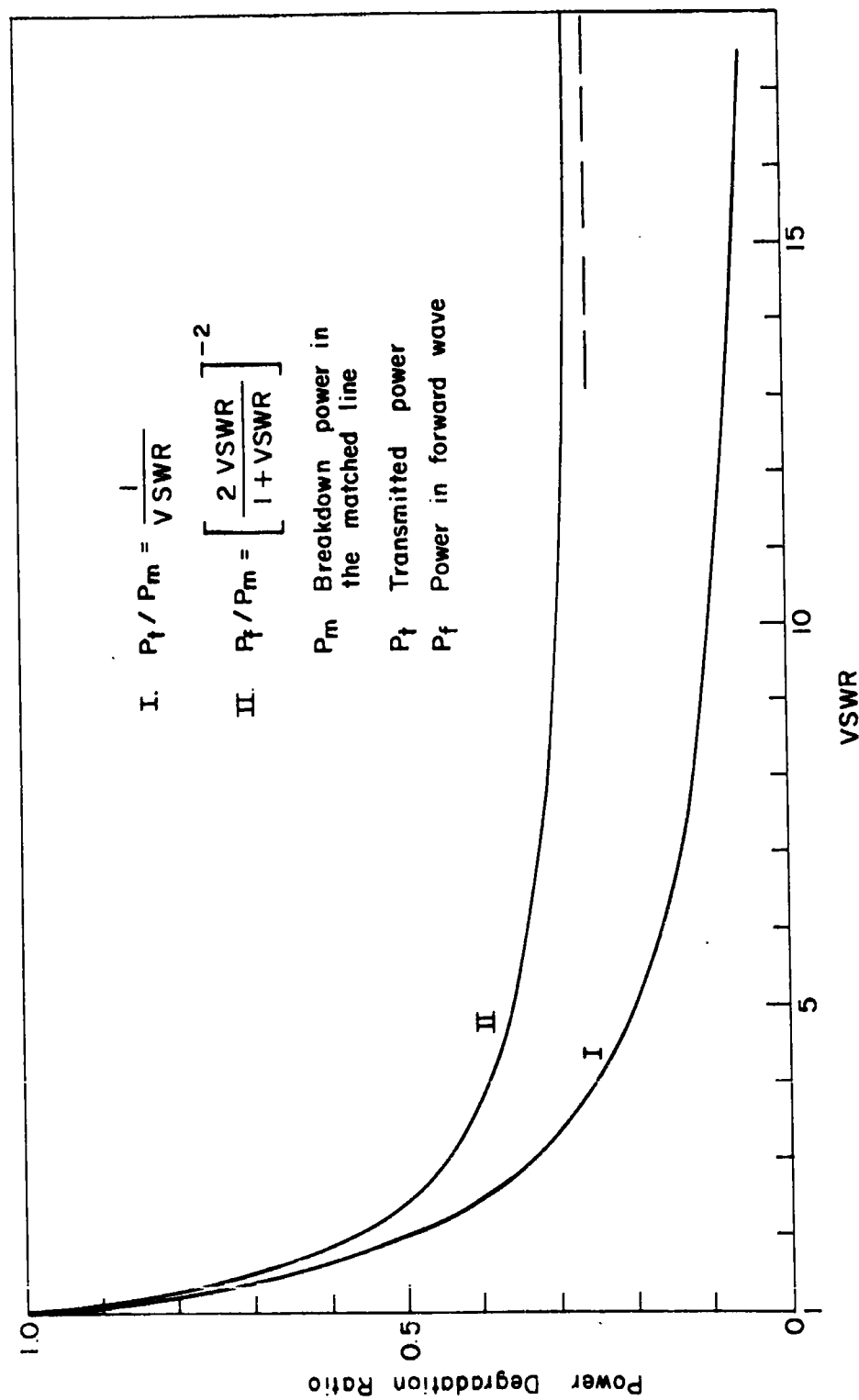


Figure 15 Degradation of breakdown power by VSWR

component is used to indicate breakdown, the degradation ratio decreases to a lower limit of only 0.25 as shown in Figure 15 by curve II. This lower limit occurs because the square of the maximum electric field can be increased by only a factor of four relative to the forward wave at large values of VSWR. The first view is useful in considering a complete transmission system in which the actual transmitted power is important. The second point of view is useful where the forward power is being monitored in the presence of a standing wave (e.g. high power levels being simulated in a resonant structure).

Effect of Harmonic Power and Spurious Mode Power on Breakdown

The effects of harmonic power and spurious power are a reduction in the breakdown threshold. The two effects are discussed together because of their similarity. In general only when resonances occur do harmonics or spurious modes become troublesome. It is difficult to be precise in analyzing this problem because the power is distributed in an arbitrary way among the possible harmonics and among the possible modes of propagation. For purposes of discussion the worst case is selected, that case in which all the power is in one mode and in one frequency. To indicate the relative power in the harmonic or spurious mode a factor H is defined as the ratio of the net power transmitted to that transmitted by the main mode at the fundamental frequency. It should be noted that the net power transmitted in a system is different than what would be measured if the transmitter in question were connected directly to a matched multimode load. In Figure 16 the fractional reduction in breakdown power due to harmonics

is given assuming no energy modulation (see Section I). The factor K is the fractional power in the harmonic multiplied by the impedance ratio and f^2 which corrects for geometric factors. In Figure 17 the fractional reduction in breakdown power due to harmonics or spurious modes (at the fundamental frequency) is given assuming full energy modulation. Since the latter cases involve direct addition of field strengths, even a few percent of relative power in a harmonic or spurious causes a significant reduction in the breakdown threshold for values of VSWR above 10.

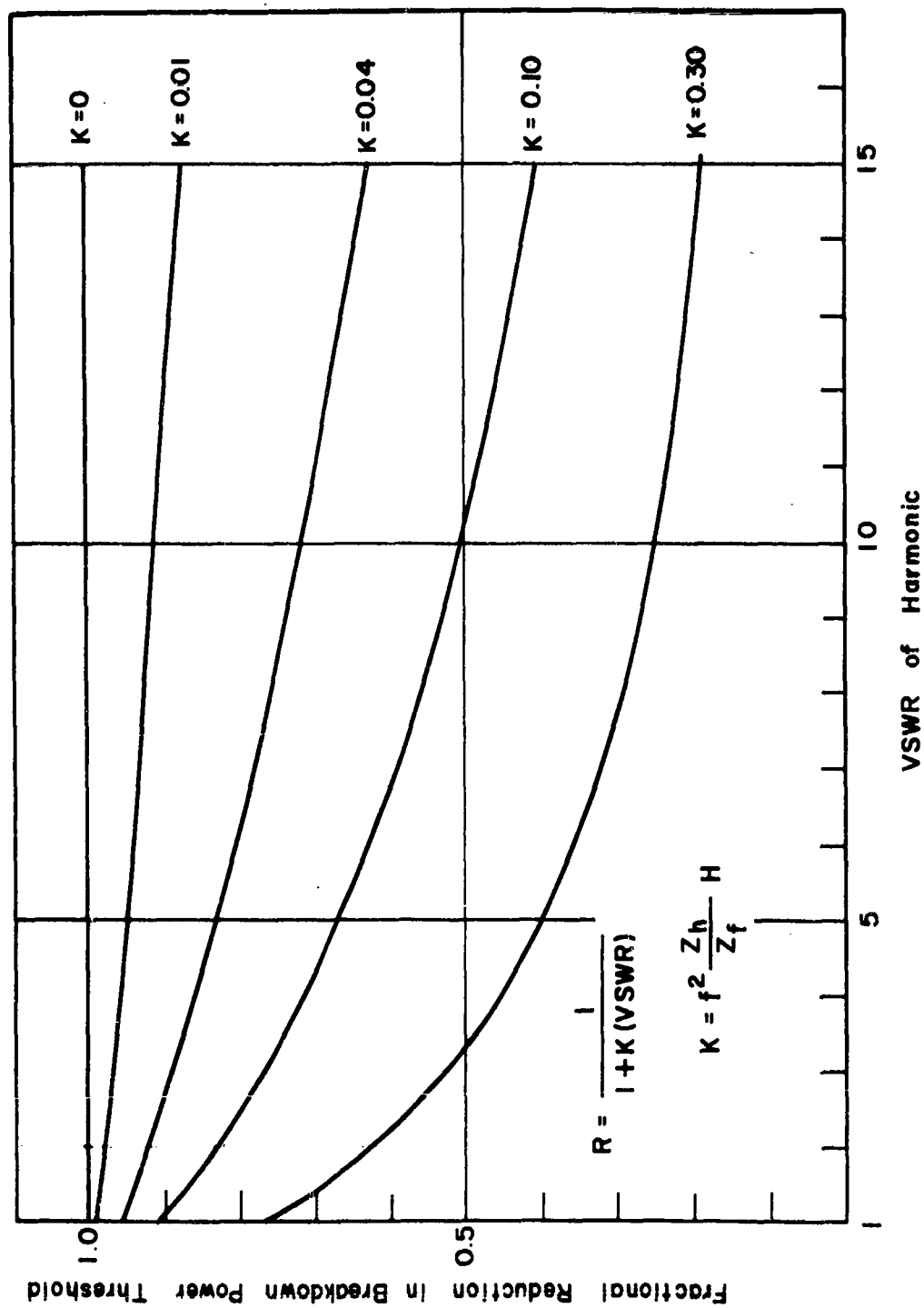
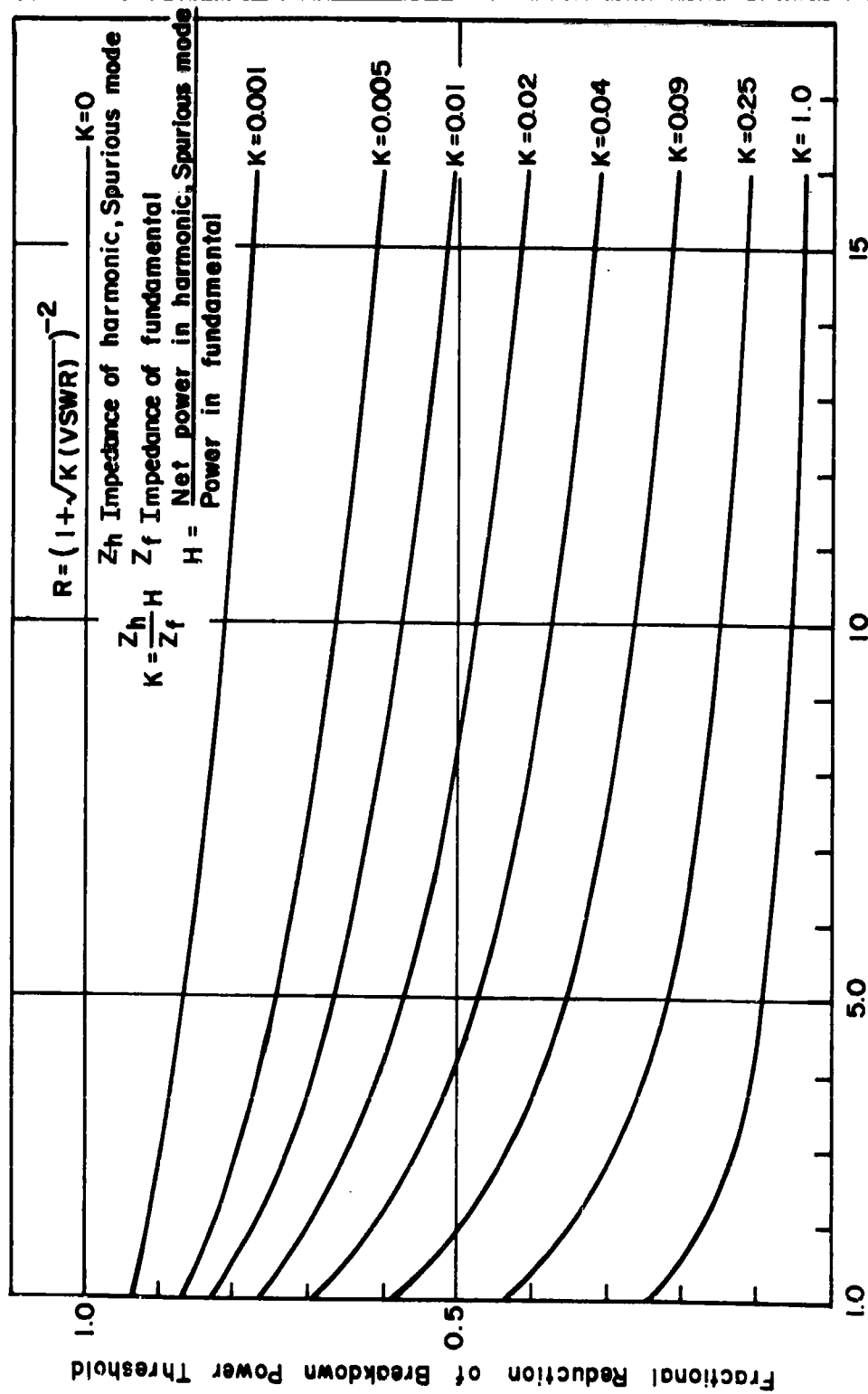
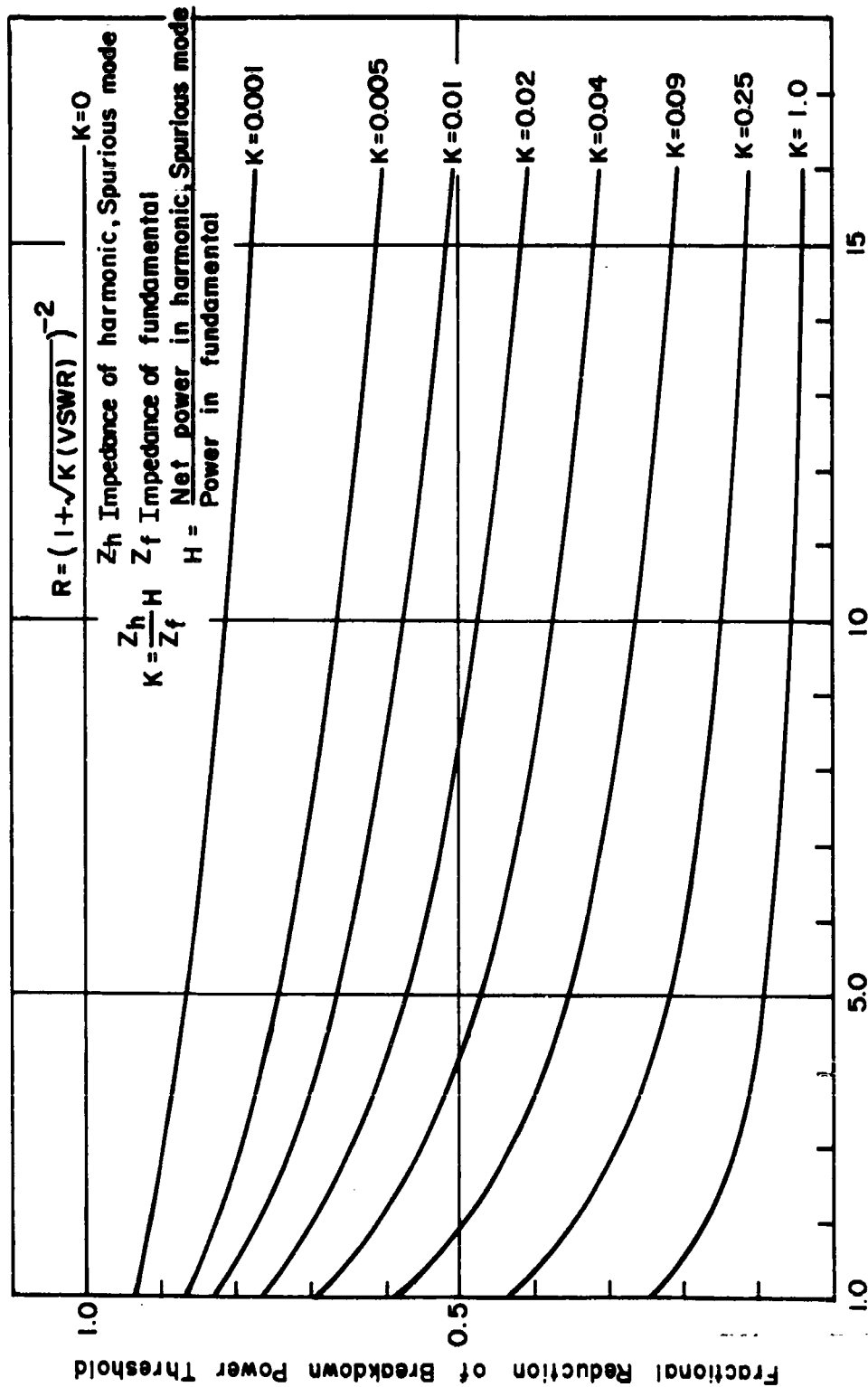


Figure 16 Fractional reduction in breakdown power by harmonic power (no energy modulation)



VSWR of harmonic, Spurious mode

Figure 17 Fraction reduction in breakdown power by harmonic and spurious mode power (full energy modulation)



VSWR of harmonic, Spurious mode

Figure 17 Fraction reduction in breakdown power by harmonic and spurious mode power (full energy modulation)

III. WAVEGUIDE CHARACTERISTICS

The analysis of waveguide characteristics discussed in Sections I and II are applied in this section to common structures and the information is presented in graphical form. Rectangular, circular and coaxial structures are included, in that order, and for each structure there are curves for cw breakdown, single-pulse breakdown and waveguide temperature (for circular and rectangular structures only). For reference purposes the pertinent formulae are included. In order to compute non-standard cases the appendix contains sample calculations.

All of the curves for breakdown are for air since the basic parameters are reasonably well known. In order to determine the breakdown characteristics for other gases the scaling factors relative to air given in Section I should be used. They, however, can be applied only in the high pressure ranges where the air breakdown power is linearly proportional to pressure squared (see Section I). With some discretion the scaling factors can also be applied to values found on a straight line extrapolation of the linear portion of the breakdown curve to lower values of pb, see Figure 18 as an example. Pulse breakdown information on the high dielectric strength gases has not been studied systematically and so no attempt has been made to discuss the subject at this time.

The cw and single-pulse breakdown curves found in this section require some explanation. First the curves show breakdown power as a function of the product of pressure and a significant dimension of the

waveguide cross section. For definiteness the discussion will be concerned with Figure 18 where the waveguide height, b , is used. The breakdown curves are general in that they apply to any fixed cross section and mode, regardless of size, provided that the frequency of operation falls in the prescribed band as determined by waveguide size. In terms of $p_0 b$ there is an absolute minimum value of breakdown power (about one kilowatt for standard rectangular waveguide) for each type of waveguide structure. This means that below the critical value of power, this type of waveguide will not breakdown regardless of frequency of operation or degree of pressurization. For large values of $p_0 b$ the simple linear dependence of power upon pressure squared applies. Also at large values of $p_0 b$, if the frequency is increased well above the prescribed operating band, a slight increase in power is found. The limiting values for increasing frequency are essentially those on the curve $f/f_c = 5.73$ (Figure 18). For low pressures or low values of $p_0 b$ deviation from linearity occurs because of energy modulation (in air), the ratio of E_{rms}/E_e and electron diffusion. It is interesting to note that in this $p_0 b$ range, because of the two latter effects, at a frequency 5.73 times above cutoff (Figure 18) the absolute minimum breakdown is almost an order of magnitude higher than for frequencies in the prescribed band.

Application of the breakdown curves is greatly facilitated by the use of the additional scales, upper right hand portion of the figures, showing the size of waveguide. For rectangular waveguide the size is given in a WR scale which is the width of the waveguide in inches

multiplied by 100. For circular waveguide WC is the diameter multiplied by 100 and for coaxial waveguide the WX scale is the inner conductor diameter multiplied by 100. The scale is used by locating the waveguide size and then following a vertical line to where it intersects with the breakdown curves. This intersection gives the breakdown power at one atmosphere of air. Continuing the vertical line to the $p_0 b$ axis also gives the corresponding value of $(p_0 b)_a$. To find the breakdown power at some other pressure the new value of $p_0 b$ is calculated by multiplying $(p_0 b)_a$ by the ratio of the new pressure to atmospheric pressure, all in absolute units. An identical procedure is used for all of the breakdown curves.

One caution should be kept in mind when using the breakdown curves. When the value of $p_0 b$ is varied through changes in b , the corresponding frequency of operation also varies. Thus reducing b by a factor of 2 corresponds to increasing the frequency by a factor of 2 and appropriately using a waveguide size reduced by a factor of 2.

Rectangular Waveguide - Standard and Tall

The characteristics of rigid rectangular waveguide operating in the dominant TE_{10} mode will be considered in this section. The electric field configuration for this mode in terms of rms values is

$$E = E_{rms} \cos (\pi x/a) \quad (13)$$

where a is the width and b will be the height. The maximum field intensity occurs midway between the side walls and is parallel to the b dimension of the waveguide and independent of distance measured parallel to the b dimension. The relationship between the power carried by the waveguide and the maximum rms electric field is

$$P = 1.33 \times 10^{-3} a b (\lambda/\lambda_g) E_{rms}^2 \text{ (watts)} \quad (14)$$

If the same units of length are used in the electric field strength and in the waveguide dimensions, the power is obtained in watts.

The guide wavelength is given by

$$\lambda_g/\lambda = [1 - (\lambda/\lambda_c)^2]^{-1/2}$$

where $\lambda_c = 2a$ is the cutoff wavelength. A plot of λ_g/λ is included

in the Appendix I, Figure 53.

The breakdown curves on the following pages were developed from the differential equations given in Section I subject to the boundary conditions that the electron density vanish at the walls. The solutions, obtained by numerical integration, take into account the spatial variation of quantities v_i , v_a and D resulting from the above spatial variation in electric field strength. To apply the universal breakdown curve, Figure 4, an approximate value for the diffusion length assuming that the above quantities are constant is

$$\frac{1}{\Lambda^2} = \frac{\pi^2}{a^2} + \frac{\pi^2}{b^2} \quad (15)$$

Values for Λ taking into account non-uniform field conditions are given in Appendix II.

The waveguide temperature curves were obtained from the material given in Section II.

The rectangular waveguide characteristics are given in Table IV and in Figures 18 through 27. The breakdown characteristics are based upon the theory and are given with no safety factor. These values may be used, with some restrictions as discussed earlier and also in Section I, as a basis for scaling to other pressures by the square of the pressure ratio or the relative dielectric strengths given in Table I.

- 43 -

Generally for pressures above one atmosphere for air the scaling is valid.

TABLE IV

STANDARD RECTANGULAR WAVEGUIDES; TE₁₀ MODE
Dimensions, Recommended Frequencies and Breakdown Power

RETMA DESIGNATION	FREQUENCY RANGE (kmc/s)		INSIDE DIMENSIONS				CUT-OFF WAVELENGTH (cm)	CW BREAKDOWN*	
			(inches)		(centimeter)			POWER-760 mm Hg	
	WIDTH	HEIGHT	WIDTH	HEIGHT	(megawatts)				
	f_1	f_2						f_1	f_2
WR2300	0.32	0.49	23.00	11.50	54.42	29.21	116.8	510	727
WR1800	0.41	0.625	18.00	9.00	45.72	22.86	91.44	313	435
WR1150	0.64	0.96	11.50	5.75	29.21	14.61	58.42	128	180
WR770	0.96	1.45	7.70	3.85	19.6	9.78	39.1	57.5	81.5
WR650	1.12	1.70	6.50	3.25	16.5	8.26	33.0	40.2	58.0
WR510	1.45	2.20	5.10	2.55	12.9	6.48	25.9	25.3	35.8
WR430	1.70	2.60	4.30	2.15	10.9	5.46	21.8	17.5	25.2
WR340	2.20	3.30	3.40	1.70	8.64	4.32	17.3	11.5	16.0
WR284	2.60	3.95	2.84	1.34	7.21	3.40	14.4	7.30	10.4
WR229	3.30	4.90	2.29	1.14	5.82	2.91	11.6	5.30	7.30
WR187	3.95	5.85	1.87	0.872	4.76	2.22	9.51	3.20	4.50
WR159	4.90	7.05	1.59	0.795	4.04	2.02	8.08	2.70	3.50
WR137	5.85	8.20	1.37	0.622	3.49	1.58	6.97	1.90	2.50
WR112	7.05	10.0	1.12	0.497	2.85	1.26	5.70	1.24	1.64
WR90	8.20	12.4	0.900	0.400	2.29	1.02	4.57	0.730	1.10
WR75	10.0	15.0	0.750	0.375	1.91	0.953	3.81	0.600	0.860
WR62	12.4	18.0	0.622	0.311	1.58	0.790	3.16	0.440	0.600
WR51	15.0	22.0	0.510	0.255	1.30	0.648	2.59	0.300	0.410
WR42	18.0	26.5	0.420	0.170	1.07	0.432	2.13	0.160	0.240
WR34	22.0	33.0	0.340	0.170	0.866	0.432	1.73	0.130	0.185
WR28	26.5	40.0	0.280	0.140	0.711	0.356	1.42	0.095	0.145
WR22	33.0	50.0	0.224	0.112	0.569	0.284	1.14	0.062	0.090
WR19	40.0	60.0	0.188	0.094	0.487	0.239	0.974	0.047	0.064
WR15	50.0	75.0	0.148	0.074	0.376	0.188	0.752	0.029	0.042
WR12	60.0	90.0	0.122	0.061	0.310	0.155	0.620	0.020	0.029
WR10	75.0	110.0	0.100	0.050	0.254	0.127	0.508	0.014	0.020

*These values are for atmospheric air; but they may be scaled for high dielectric strength gases as shown in Section I.

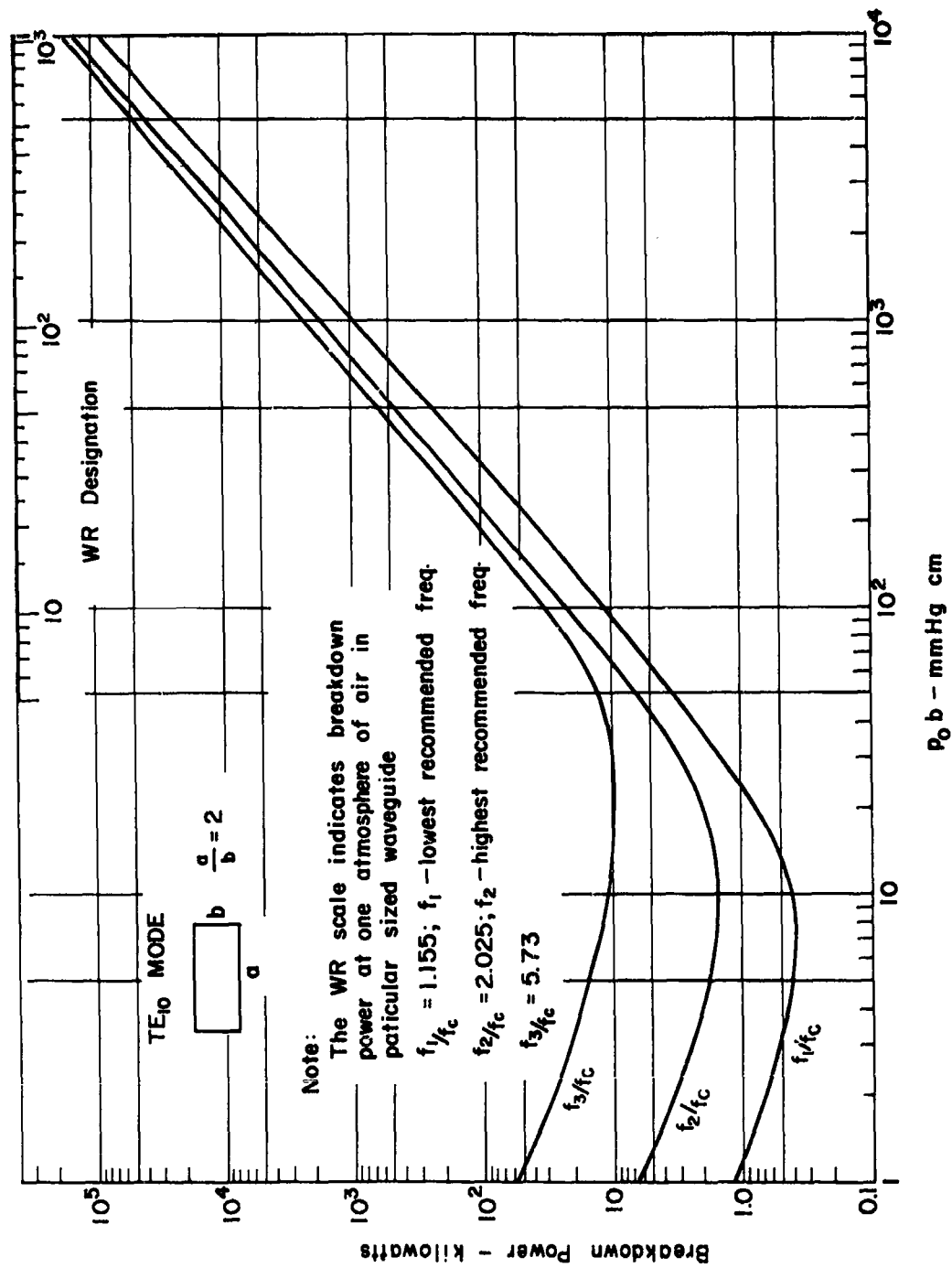


Figure 18 CW breakdown power for air filled standard rectangular waveguides ($a/b = 2$)

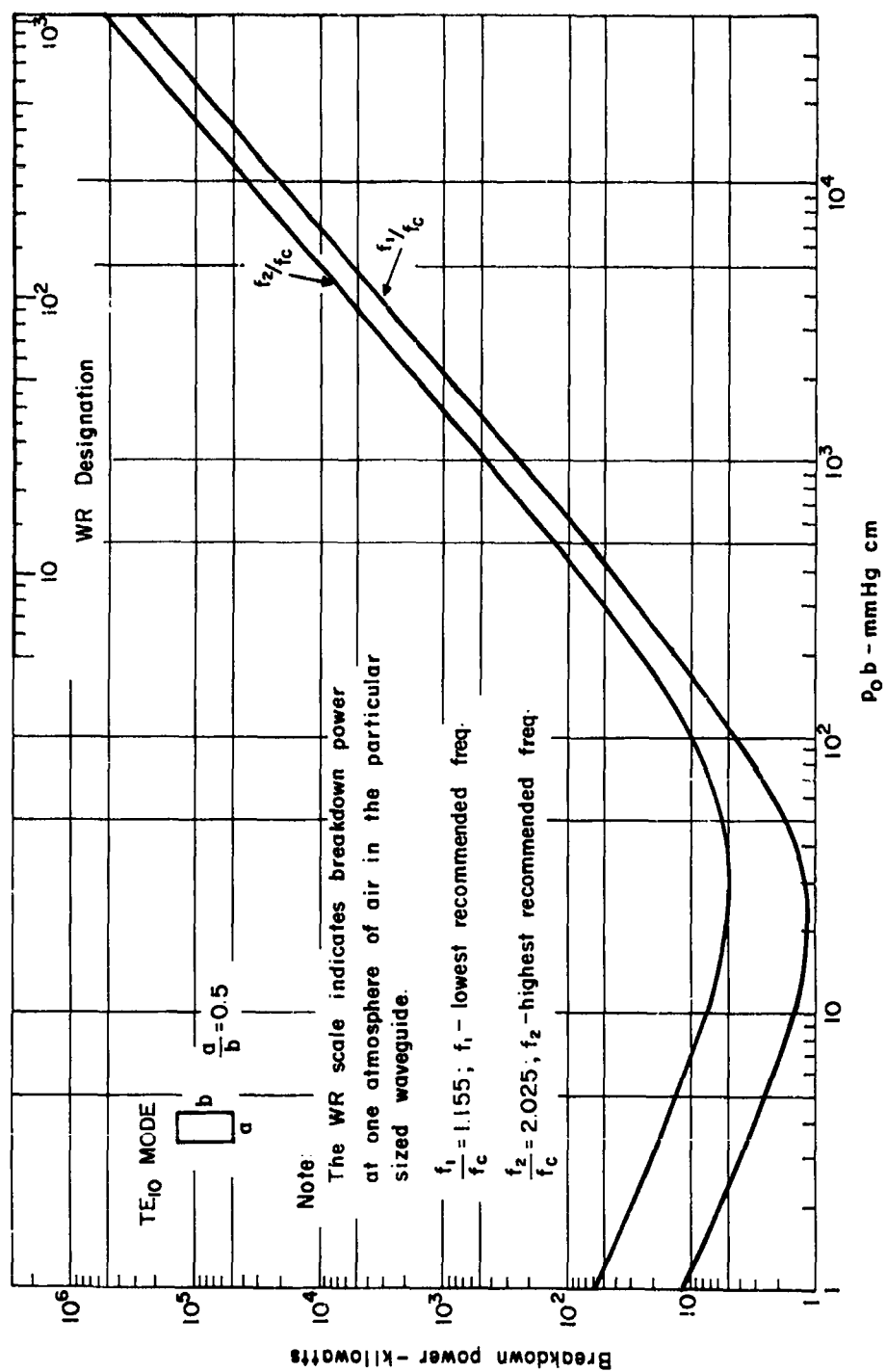


Figure 19 CW breakdown power for air filled tall waveguides
($a/b = 0.5$)

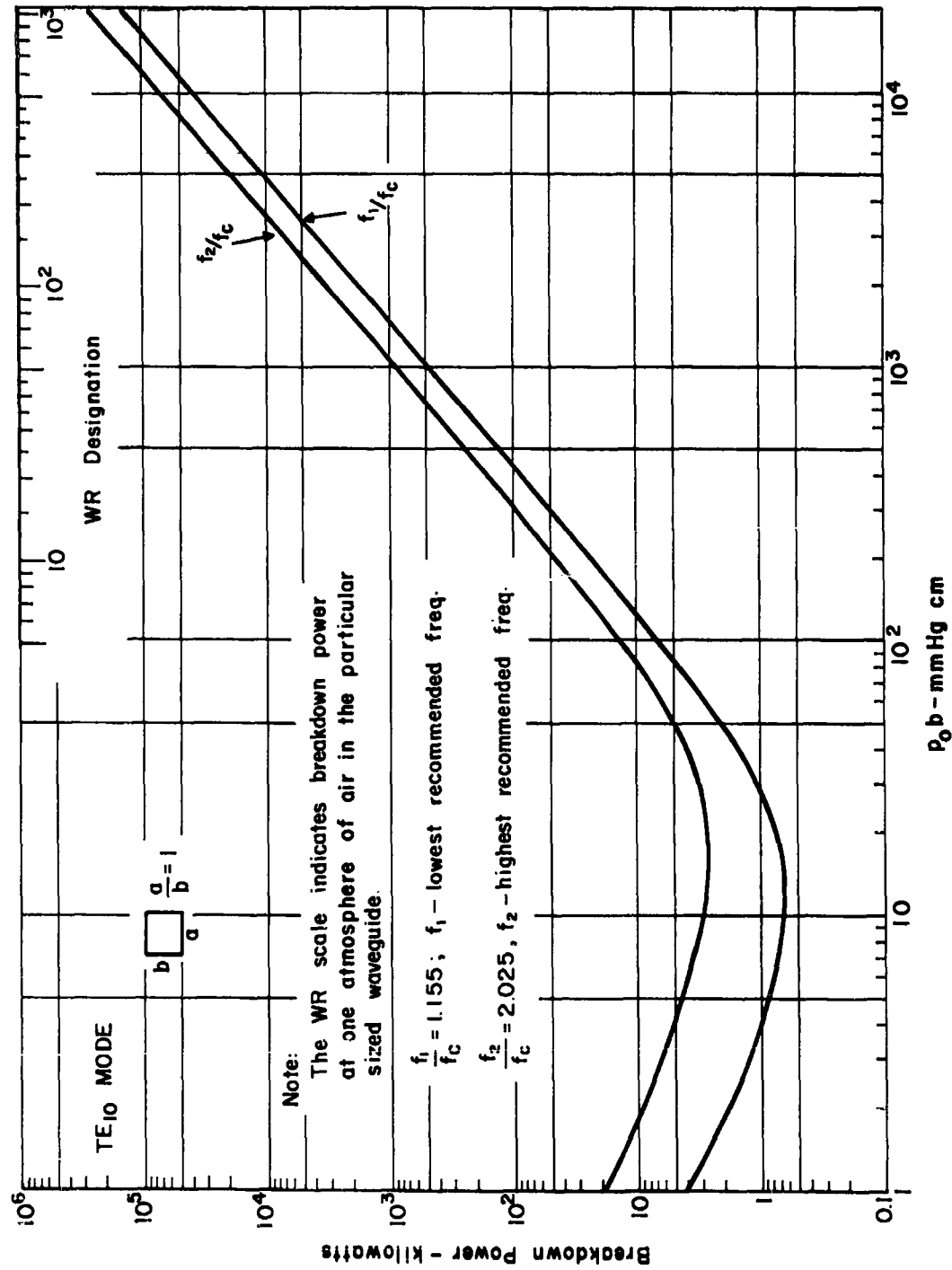


Figure 20 CW breakdown power for air filled square waveguides
($a/b = 1$)

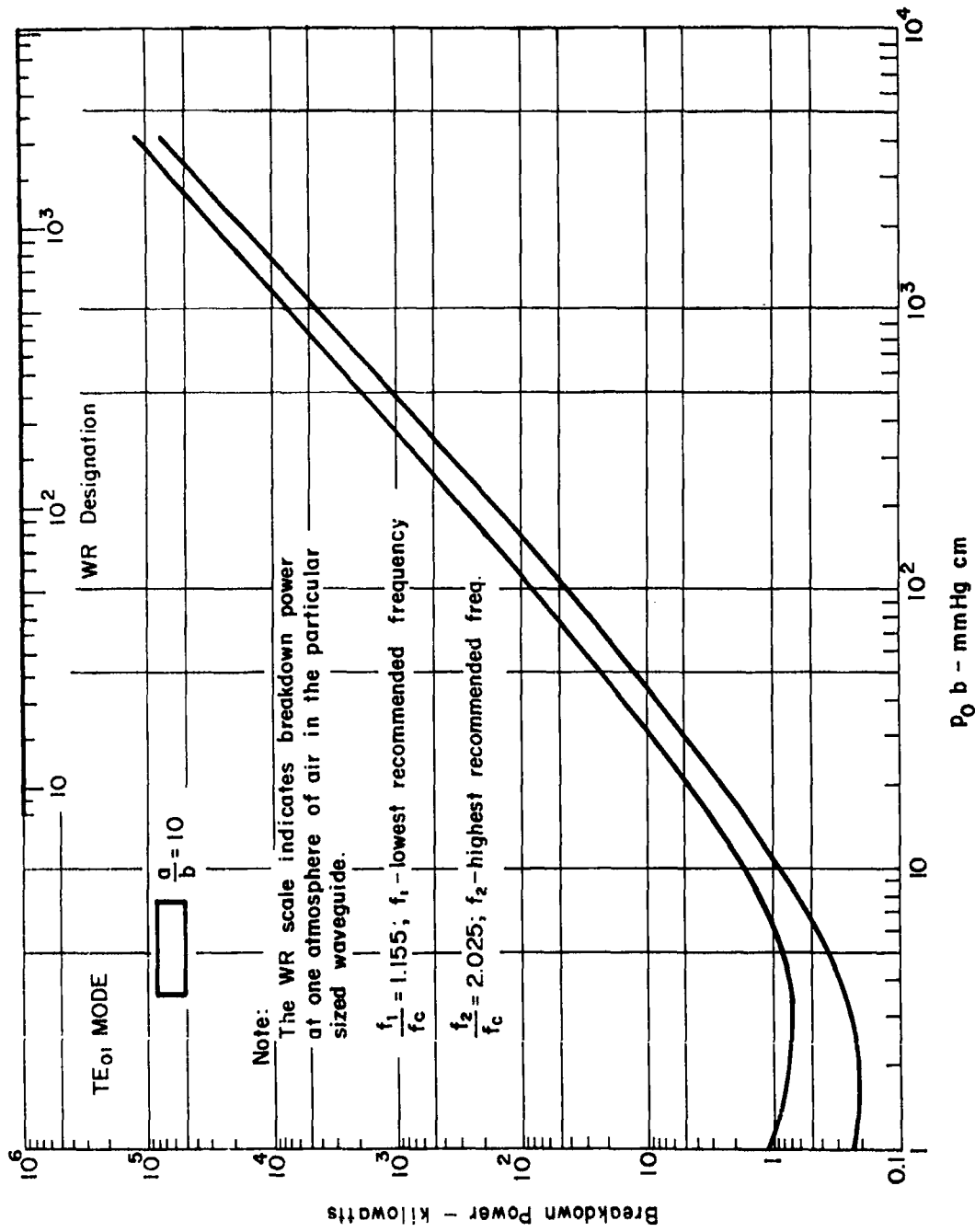


Figure 21 CW breakdown power for air filled narrow height waveguides
($a/b = 10$)

Figure 22 Single pulse breakdown power for air filled standard waveguides

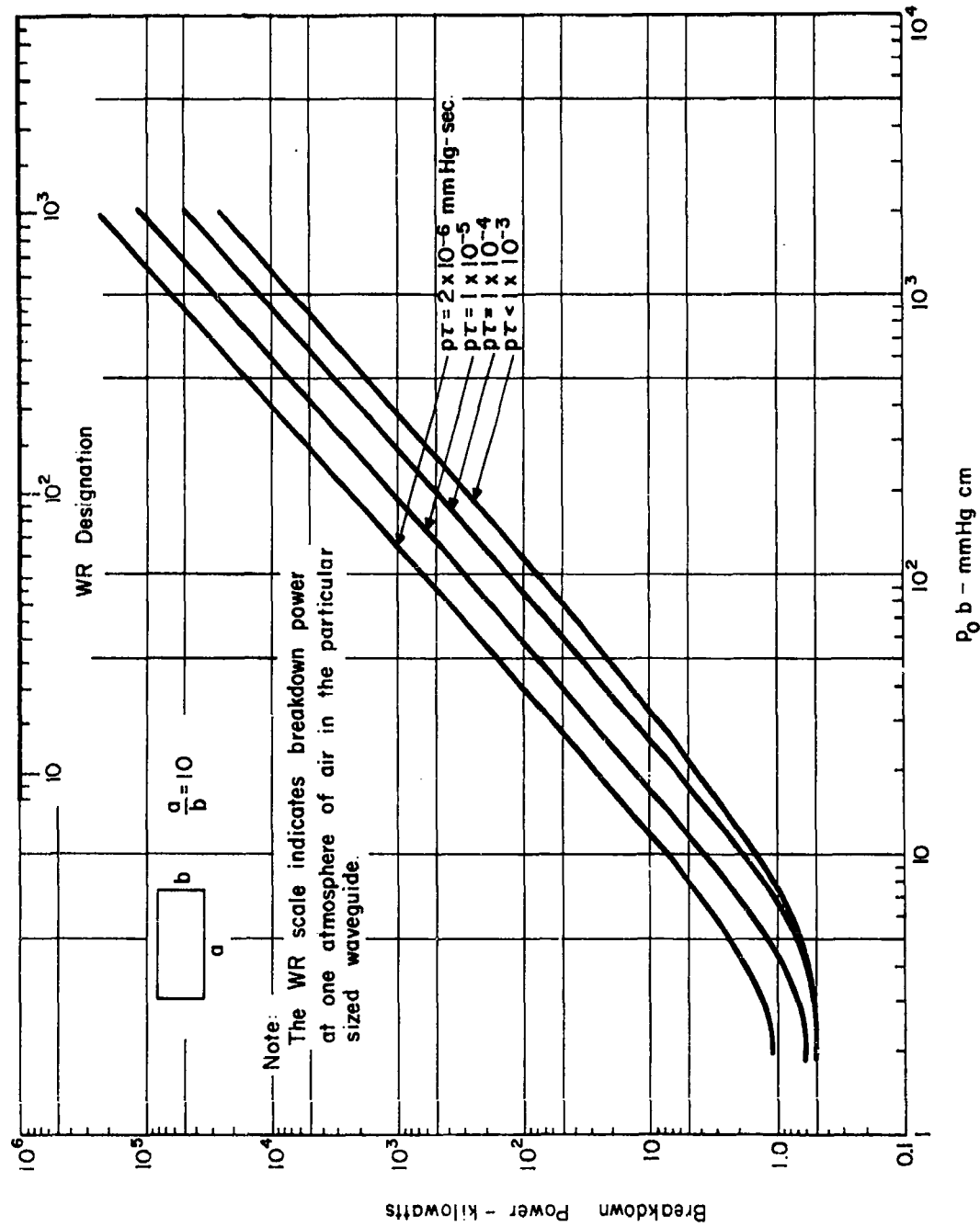


Figure 23 Single pulse breakdown power for air filled narrow height waveguides

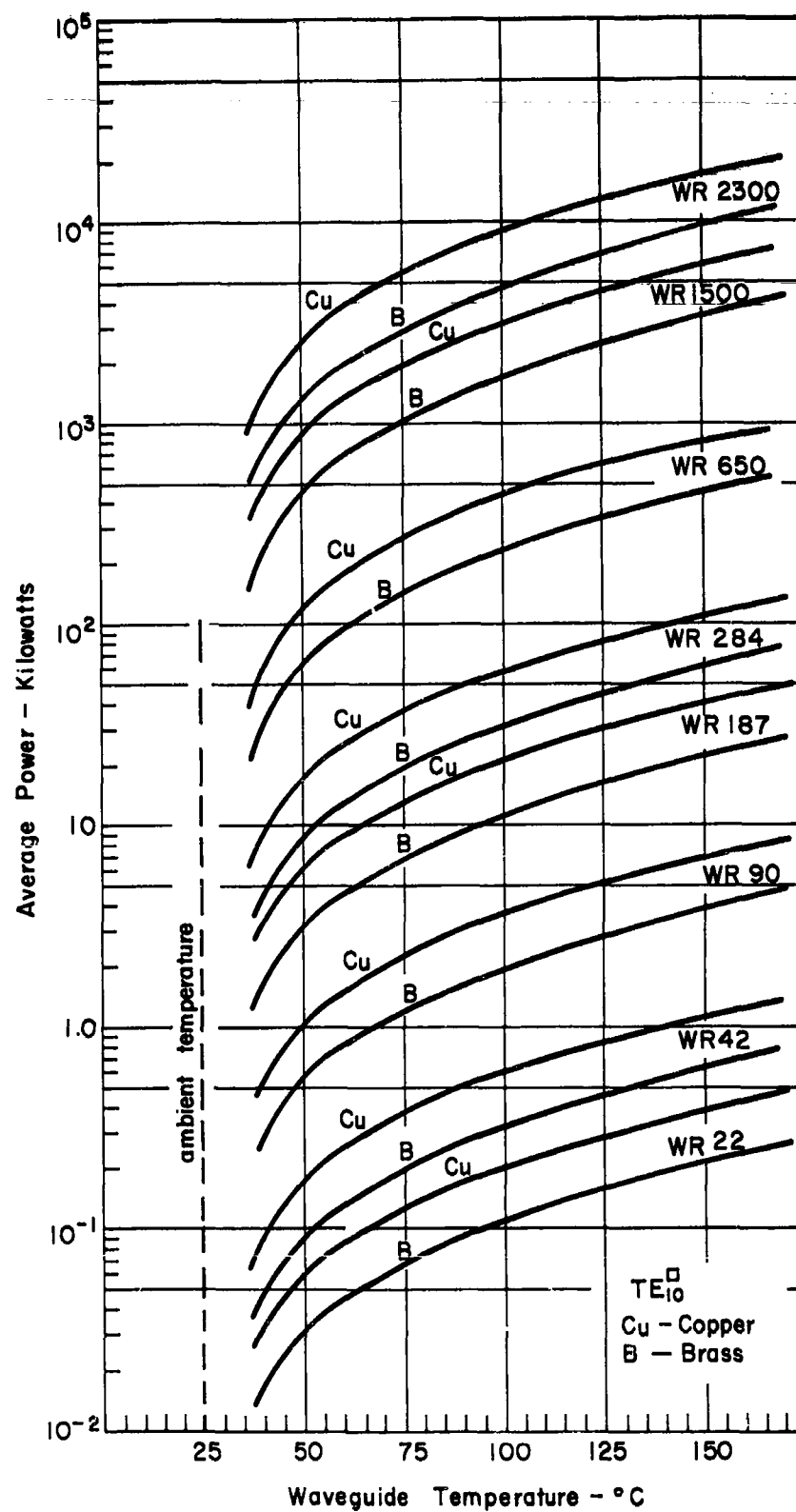


Figure 24 Average power capability of standard waveguides as a function of waveguide temperature

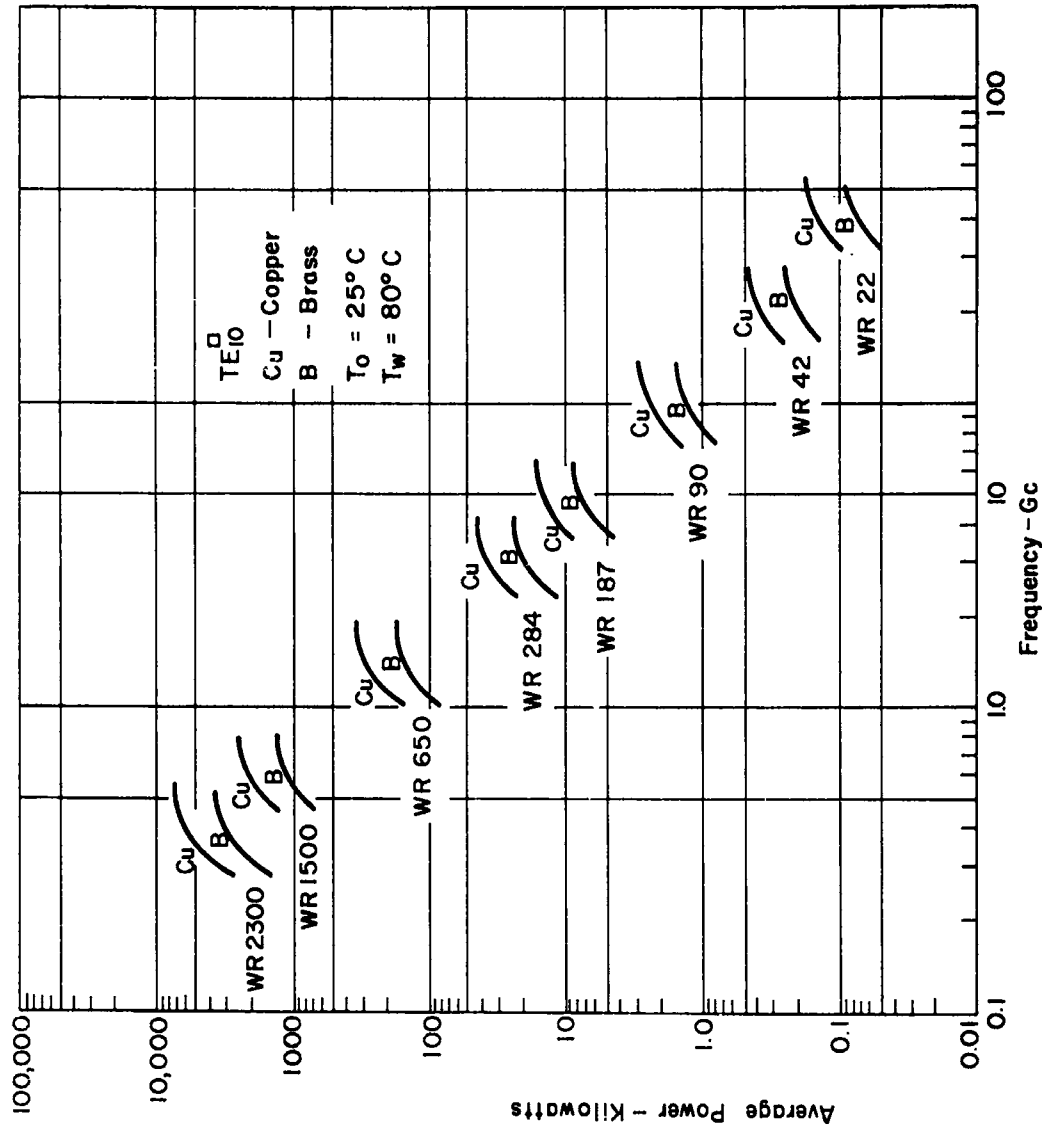


Figure 25 Average power capability of standard waveguides as a function of frequency

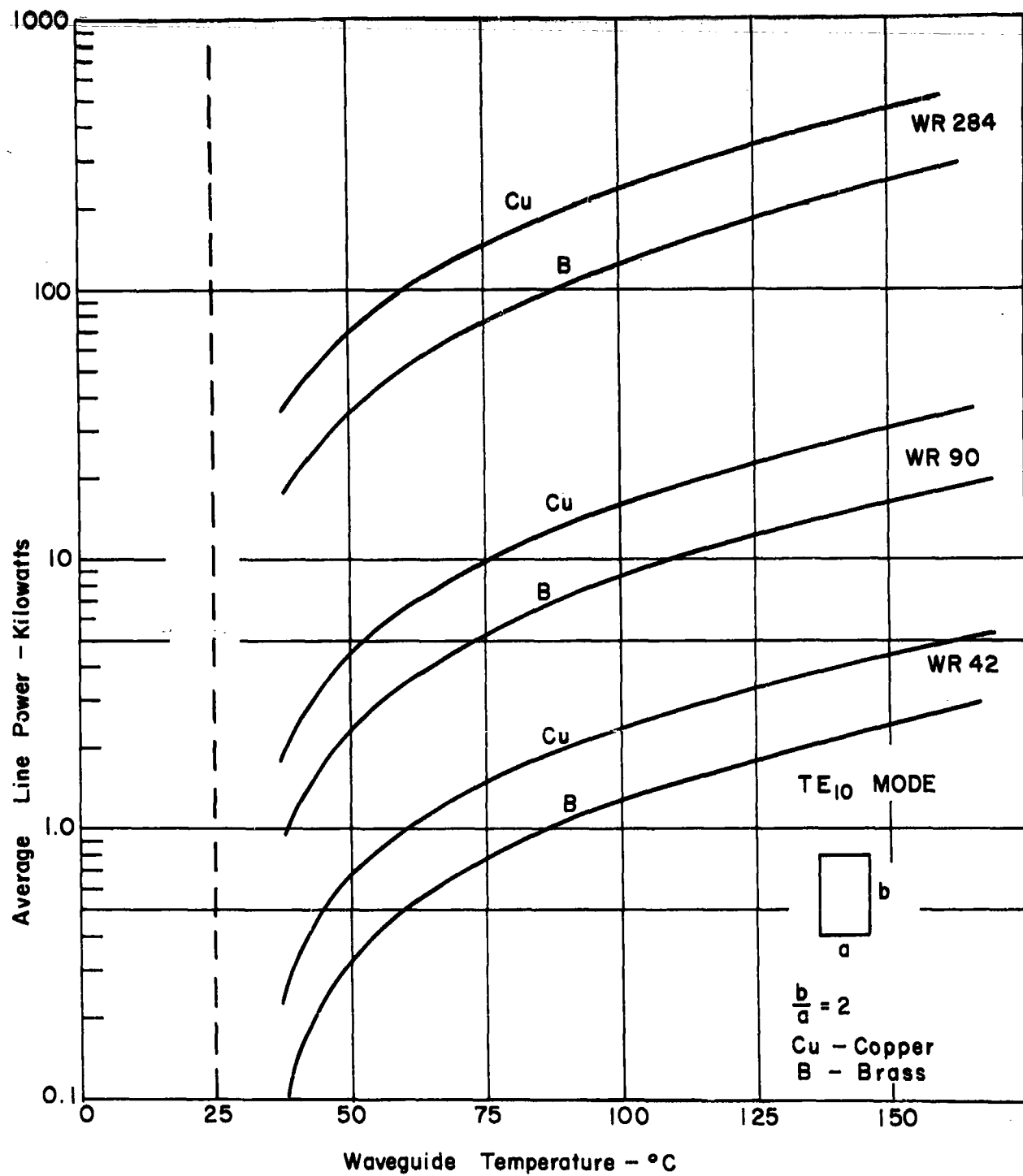


Figure 26 Average power capability of tall waveguides ($a/b = 0.5$) as a function of waveguide temperature

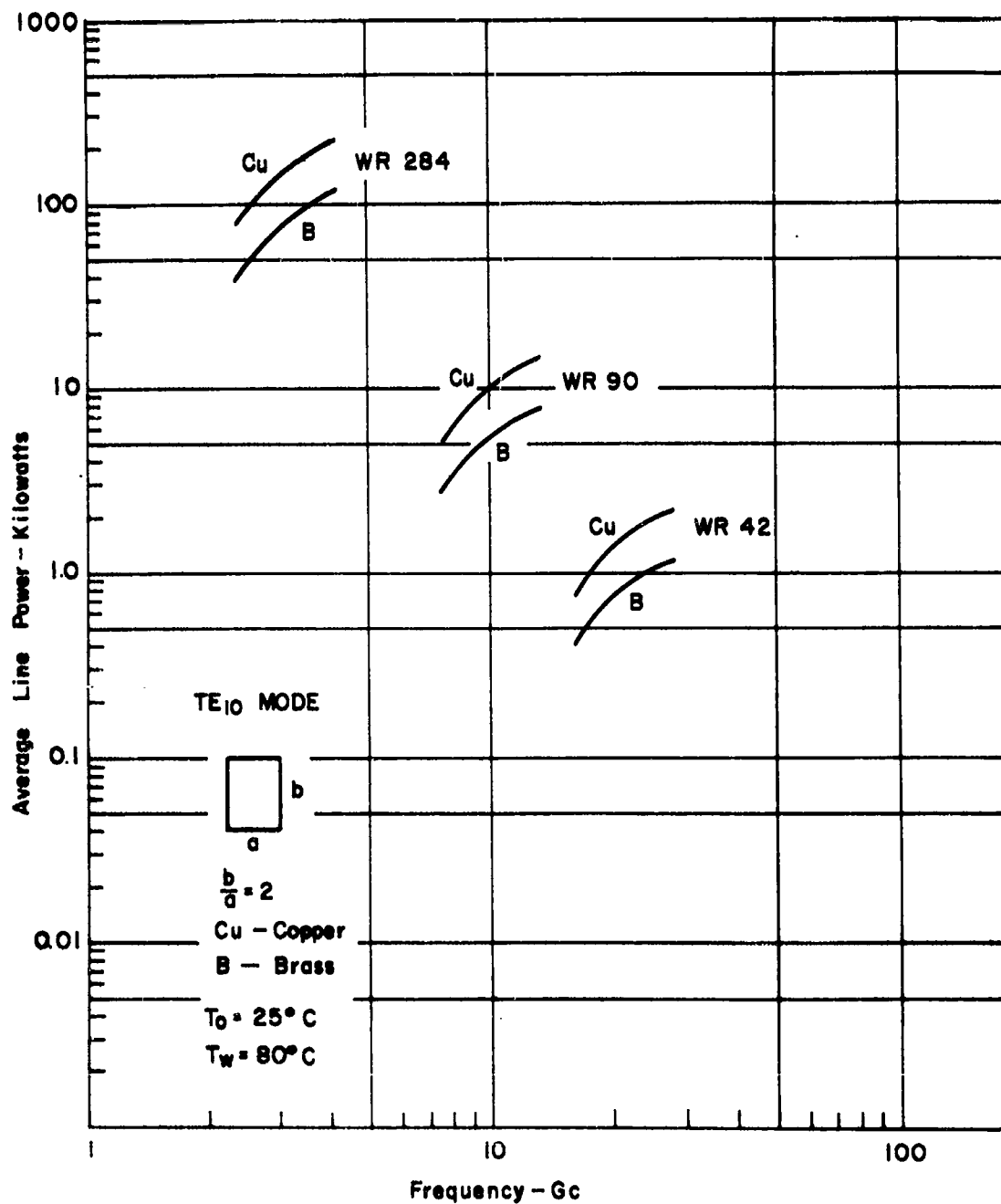


Figure 27 Average power capability of tall waveguides
($a/b = 0.5$) as a function of frequency

Circular Waveguide - TE₁₁ Mode

The characteristics of rigid circular waveguide operating in the dominant or TE₁₁ mode will be considered in this section. The electric field configuration for this mode in terms of the maximum value of rms field is

$$E_r = E_{rms} \left[\frac{2J_1(1.84r/r_0)}{(1.84r/r_0)} \right] \sin \theta \quad (16)$$

$$E_\theta = E_{rms} \left[J_0(1.84r/r_0) - J_2(1.84r/r_0) \right] \cos \theta \quad (17)$$

where r_0 is the radius of the circular conductor. The electric field has components in the radial direction, E_r , and in the angular direction, E_θ , and is a function of radius and angle within the circular cross-section. For simplicity in solving the continuity equation for the breakdown conditions, the angular dependence of the electric field is removed by considering a value of electric field averaged with respect to angle. With this simplification the magnitude of the electric field at a given radius is expressed by

$$E = \frac{E_{rms}}{1.41} \left\{ \left[\frac{2J_1(1.84r/r_0)}{1.84r/r_0} \right]^2 + \left[J_0(1.84r/r_0) - J_2(1.84r/r_0) \right]^2 \right\}^{1/2} \quad (18)$$

The relationship between the power carried by the waveguide and the maximum rms electric field is

$$P = 3.98 \times 10^{-3} (r_0)^2 (\lambda/\lambda_g) (E_{rms})^2 \quad (19)$$

The guide wavelength is determined from Eq. 14 where the cutoff wavelength for this mode is λ_c equal to $3.41 r_0$.

The conditions of breakdown were determined from a numerical solution of the continuity equation, Equation 1, subject to the boundary condition that the electron density vanish along the inside walls of the circular guide. The coefficients v_1 , v_g , and D are functions of radius because of the radial variation of the electric field as determined by Equation 18. An approximate value for the diffusion length assuming that the coefficients are constant is

$$\Lambda = r_0/2.405. \quad (20)$$

More exact values for Λ are found in Appendix III.

Waveguide temperature curves are not given for this mode since the values are close to those for the TE_{10} mode.

The dimensions, recommended frequencies and breakdown power at one atmosphere of air are given in Table V. These values may be used, with some restrictions as discussed in Section I, as a basis for scaling to other pressures by the square of the pressure ratio or the relative dielectric strength for gases given in Table I. Generally for pressures above one atmosphere for air the scaling is valid. Additional information is given in Figures 28 and 29.

TABLE V
STANDARD CIRCULAR WAVEGUIDES, TE_{11}^0 MODE
Dimensions, Recommended Frequencies and Breakdown Power

RETMA DESIGNATION	FREQUENCY RANGE (kmc/sec)		INSIDE DIAMETER (inches)	INSIDE RADIUS (cm)	CUT-OFF WAVELENGTH (cm)	CW BREAKDOWN POWER-760 mm Hg (megawatts)	
	f_1	f_2				f_1	f_2
WC-724	1.10	1.51	7.24	9.19	31.4	63	98
WC-329	2.42	3.31	3.30	4.18	14.3	13	20
WC-94	8.49	11.6	0.938	1.19	4.06	1.1	1.78
WC-59	13.4	18.4	0.594	0.754	2.57	0.46	0.75
WC-38	21.2	29.1	0.375	0.476	1.62	0.19	0.33
WC-28	28.3	38.8	0.281	0.356	1.21	0.11	0.19
WC-14	56.6	77.5	0.141	0.179	0.610	0.033	0.053

TABLE V
STANDARD CIRCULAR WAVEGUIDES, TE_{11}^0 MODE
Dimensions, Recommended Frequencies and Breakdown Power

RETMA DESIGNATION	FREQUENCY RANGE (kmc/sec)		INSIDE DIAMETER (inches)	INSIDE RADIUS (cm)	CUT-OFF WAVELENGTH (cm)	CW BREAKDOWN POWER-760 mm Hg (megawatts)	
	f_1	f_2				f_1	f_2
WC-724	1.10	1.51	7.24	9.19	31.4	63	98
WC-329	2.42	3.31	3.30	4.18	14.3	13	20
WC-94	8.49	11.6	0.938	1.19	4.06	1.1	1.78
WC-59	13.4	18.4	0.594	0.754	2.57	0.46	0.75
WC-38	21.2	29.1	0.375	0.476	1.62	0.19	0.33
WC-28	28.3	38.8	0.281	0.356	1.21	0.11	0.19
WC-14	56.6	77.5	0.141	0.179	0.610	0.033	0.053

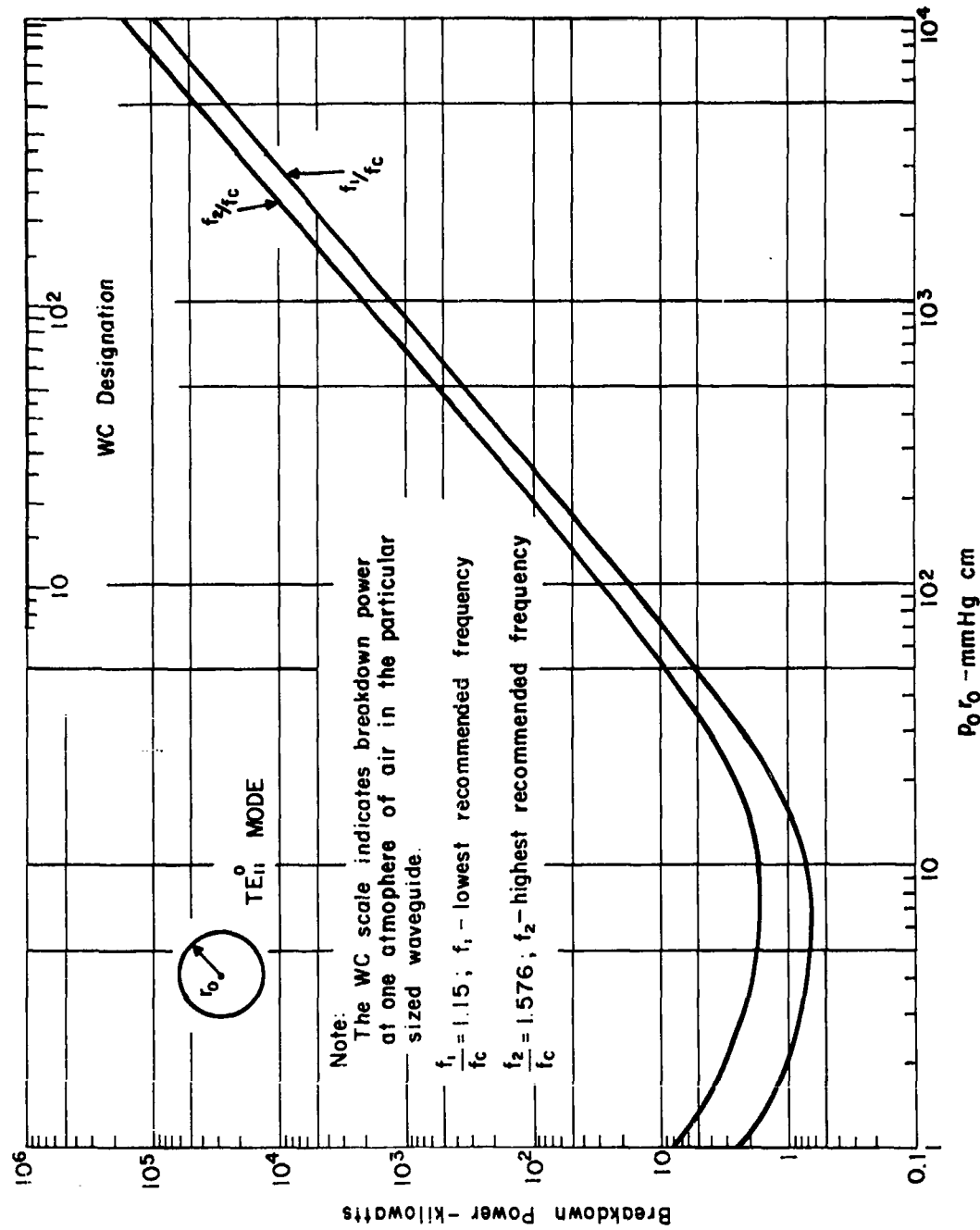


Figure 28 CW breakdown power for air filled circular waveguides, TE₁₁ mode

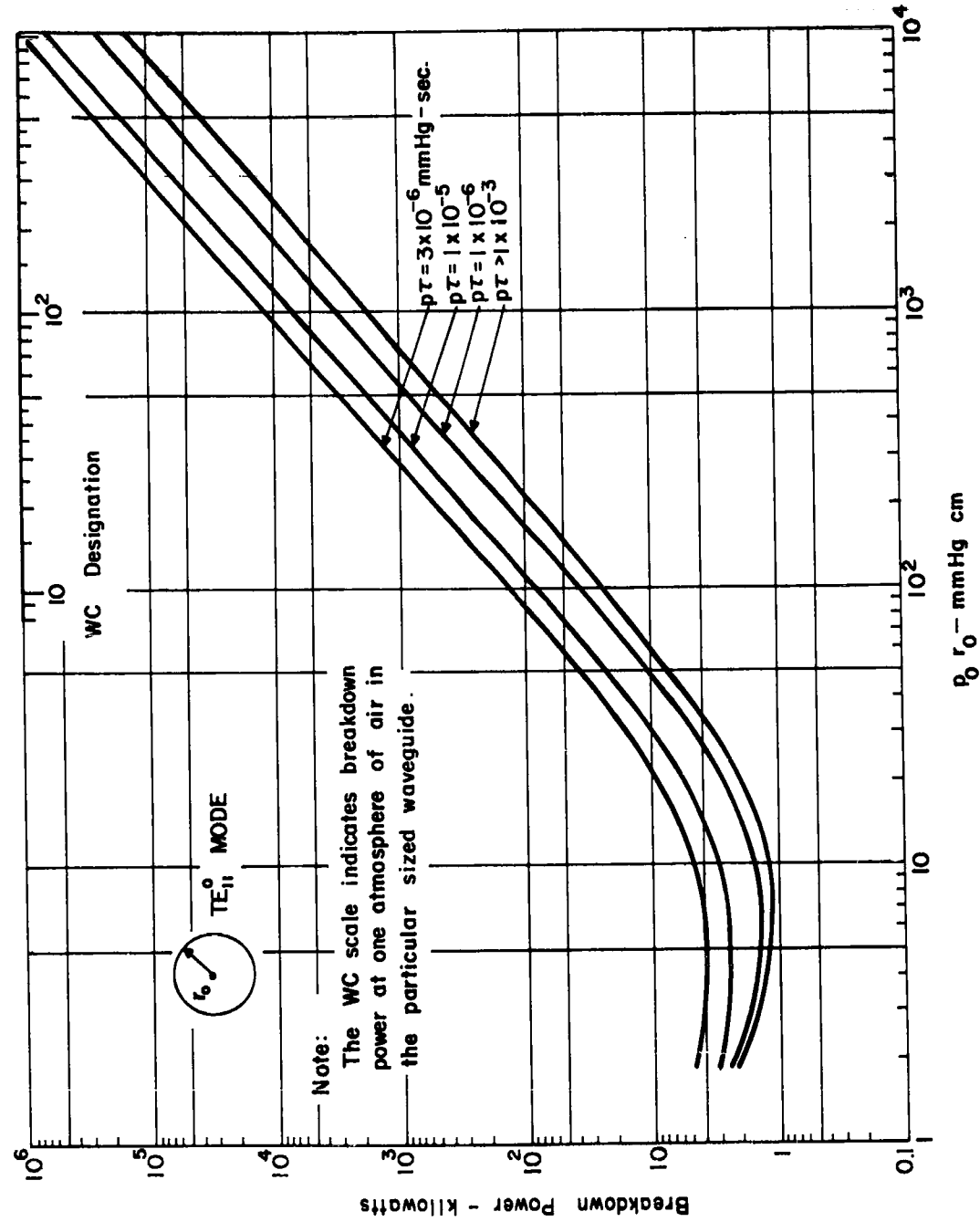


Figure 29 Single pulse breakdown power for air filled circular waveguides, TE_{11}^0 mode

Circular Waveguide - TE₀₁ Mode

The characteristics for rigid circular waveguide operating in the TE₀₁ mode are considered in this section. The electric field configuration for this mode in terms of the maximum rms field is

$$E = (E_{rms}/.582)J_1(3.83r/r_0) \quad (21)$$

The electric field is directed perpendicular to the radial direction, has a null at the center of the waveguide and at the walls and the maximum field intensity occurs at a value of radius equal to 0.48 times the conductor radius. The relation between the power carried by the waveguide and the maximum rms electric field is

$$P = 3.98 \times 10^{-3} (r_0)^2 (\lambda/\lambda_g) (E_{rms})^2 \quad (22)$$

The guide wavelength is determined from Equation 14 or Figure 53 where the cutoff wavelength for this mode, λ_c , is equal to $1.64r_0$.

The conditions of breakdown are determined from a numerical solution of the continuity equation, Equation 1, subject to the boundary condition that the electron density vanish at the walls. The coefficient ν_1 , ν_g and D are functions of radial distance because of the radial variation of E_{rms} . An approximate value for the diffusion length assuming that the coefficients are constant is

$$\Lambda = r_0/2.405. \quad (23)$$

The waveguide temperature curves were obtained from the material given in Section II.

The dimension, recommended frequencies and breakdown power at one atmosphere are given in Table VI. The breakdown power may be scaled from the tabulated values, the limitations for lower pressures are discussed in Section I, by multiplying by the square of the pressure ratio or the factors given in Table I for high dielectric strength gases. Additional information is given in Figures 30 through 33.

TABLE VI
STANDARD CIRCULAR WAVEGUIDES, TE_{01}^0 MODE
Dimensions, Recommended Frequencies and Breakdown Power

RETMA DESIGNATION	FREQUENCY RANGE (kmc/sec)		INSIDE DIAMETER (inches)	INSIDE RADIUS (cm)	CUT-OFF WAVELENGTH (cm)	CW BREAKDOWN POWER-760 mm Hg (megawatts)	
	f_1	f_2				f_1	f_2
WC-1590	1.10	1.57	15.9	20.2	33.2	347	489
WC-724	2.41	3.31	7.24	9.19	15.1	71.2	101
WC-240	7.25	9.98	2.40	3.055	5.01	8.10	12.0
WC-128	13.6	18.7	1.28	1.63	2.67	2.45	3.16
WC-94	18.6	25.6	0.938	1.19	1.95	1.35	2.1
WC-59	29.3	40.4	0.594	0.754	1.235	0.59	0.89
WC-33	53.1	73.1	0.328	0.416	0.682	0.20	0.29

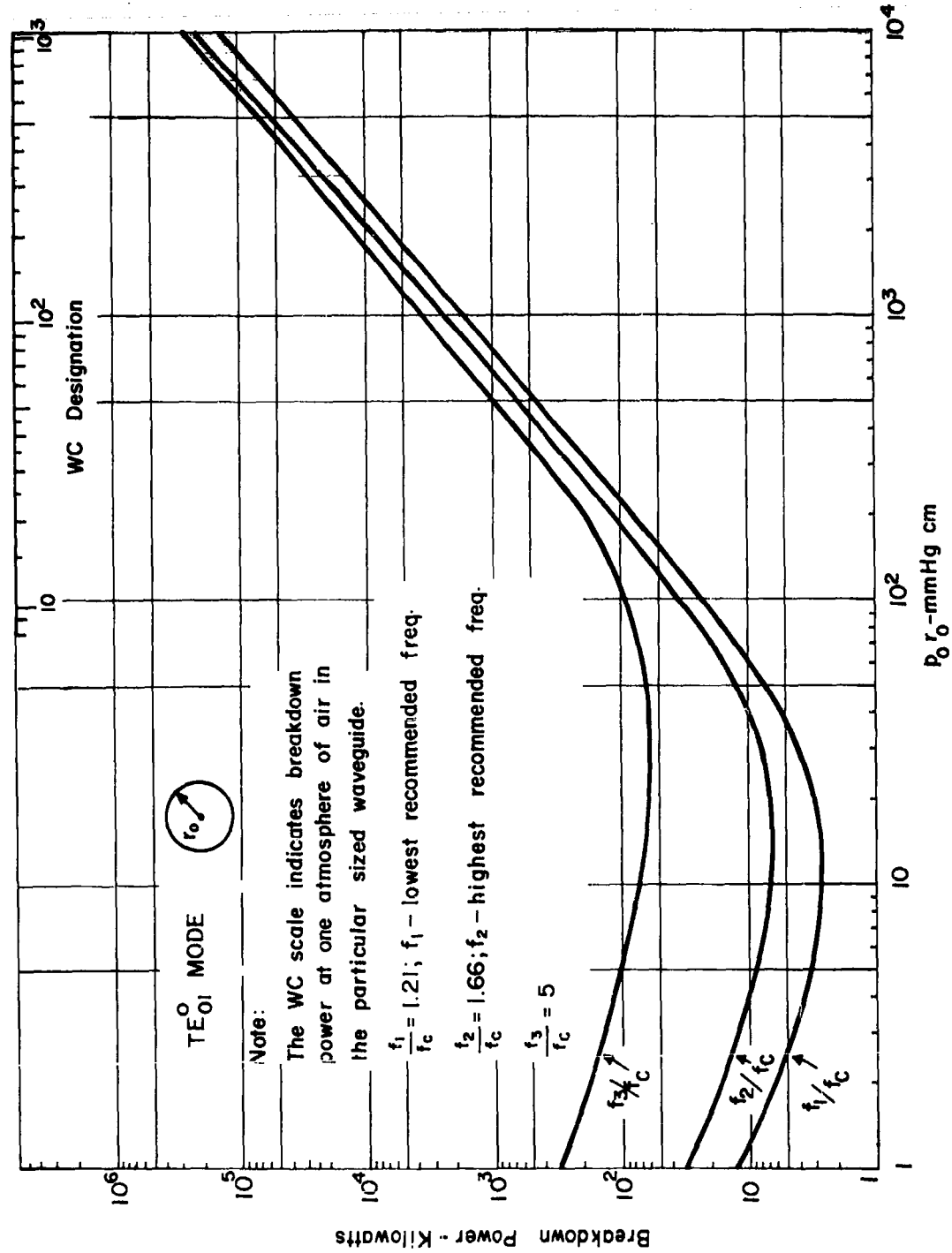


Figure 30 CW breakdown power for air filled circular waveguides
 TE₀₁ mode

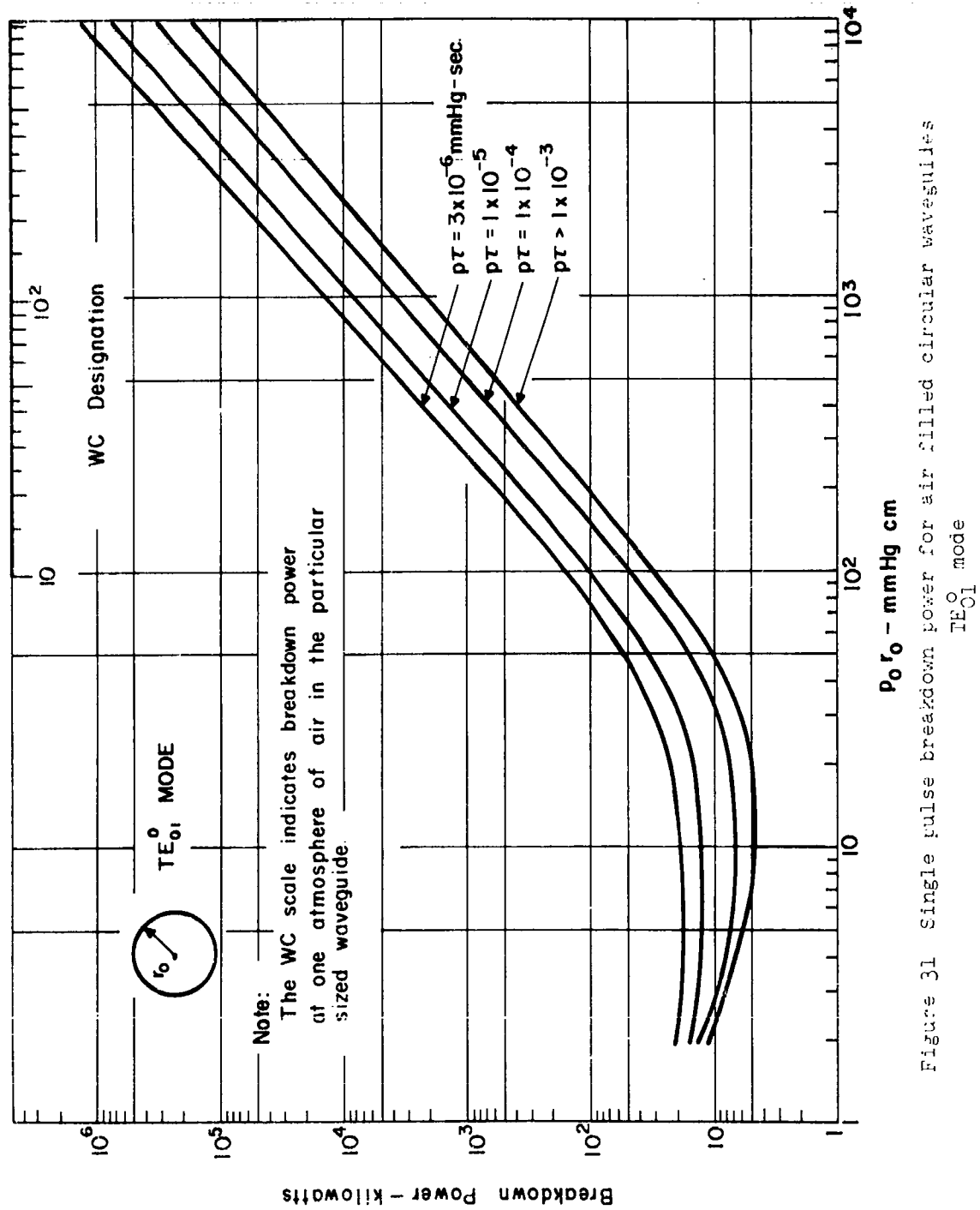


Figure 31 Single pulse breakdown power for air filled circular waveguides
 $TE_{01}^{(0)}$ mode

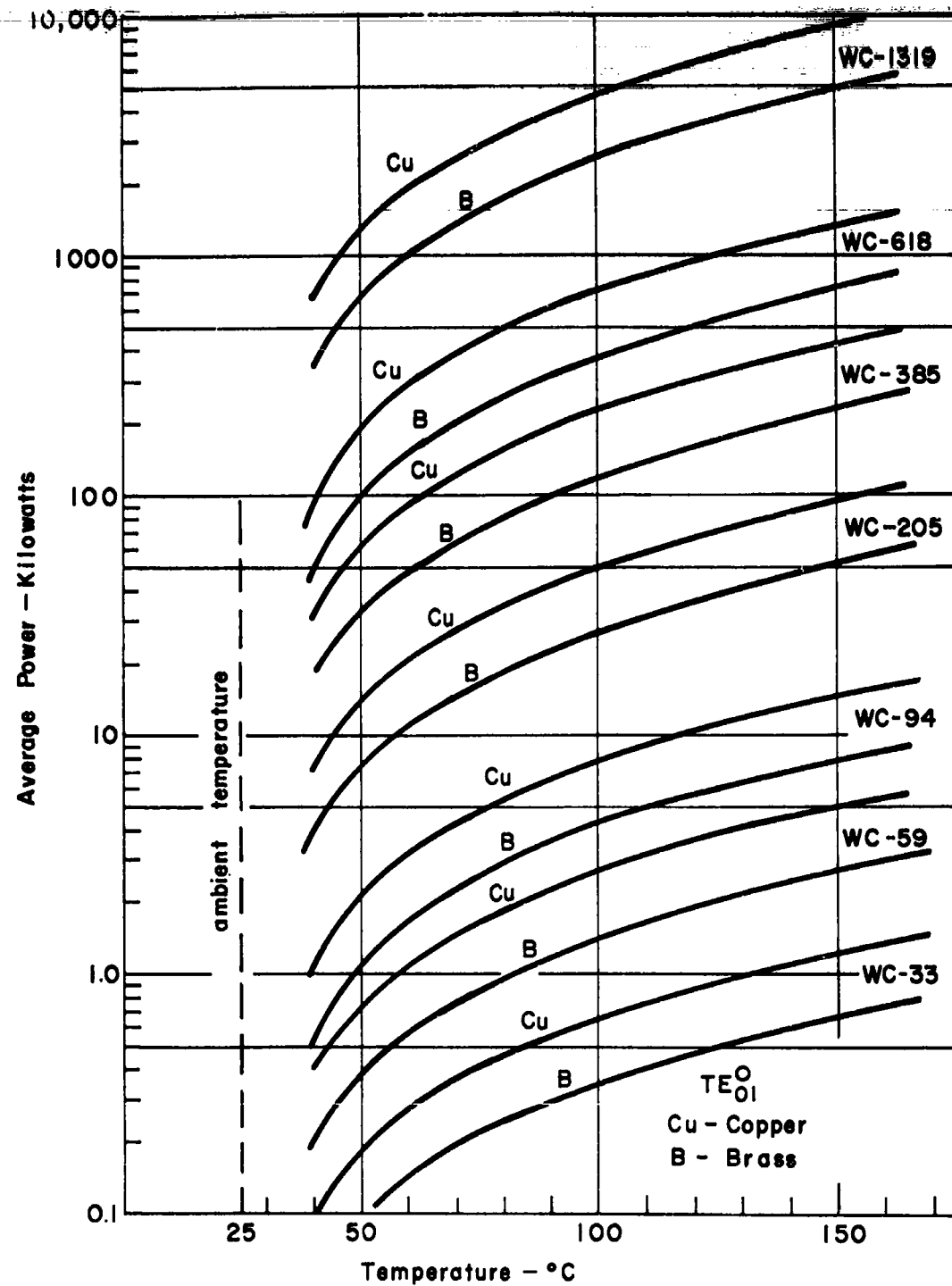


Figure 32 Average power capability of circular waveguides, TE_{01} mode, as a function of temperature

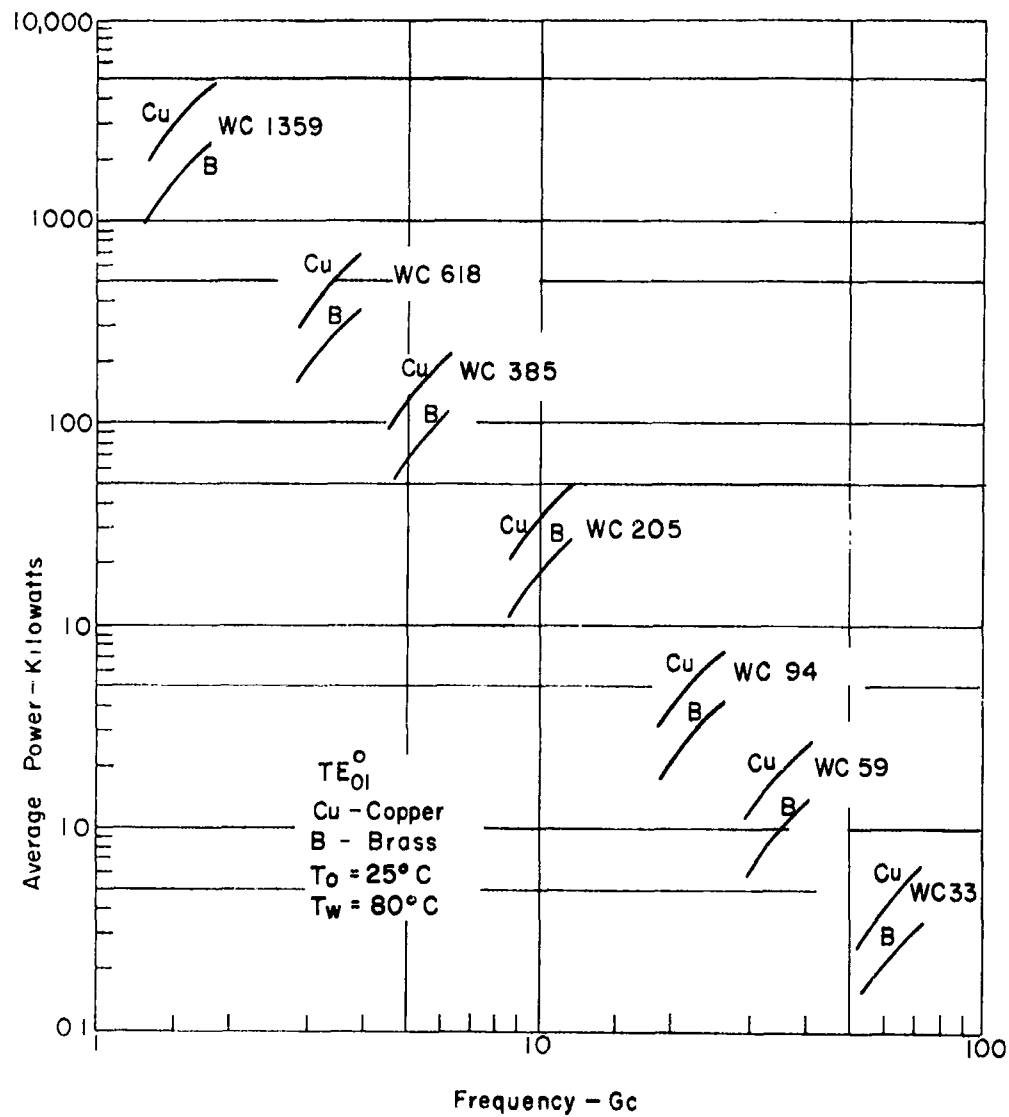


Figure 33 Average power capability of circular waveguides, TE_{01}^o mode, as a function of frequency

Circular Waveguide - TM₀₁ Mode

The characteristics of rigid circular waveguide operating in the TM₀₁ mode are considered in this section. The electric field configuration for this mode in terms of the maximum rms field is

$$E_z = E_{rms} J_0(2.405r/r_0) \quad (24)$$

$$E_r = E_{rms} (\lambda_c/\lambda_g) J_1(2.405r/r_0) \quad (25)$$

The electric field has components along the axis of the waveguide, E_z , and in the radial direction, E_r . For normal TM₀₁ mode operation the value of r_0/λ is less than 0.76, so the electric field which controls breakdown is the Z component directed along the waveguide axis, i.e., the maximum field intensity occurs in the center of the guide. The relation between the power carried by the waveguide and the maximum rms electric field is

$$P = 15.4 \times 10^{-3} (\lambda/\lambda_g) (r_0^4/\lambda^2) (E_{rms})^2 \quad (26)$$

The guide wavelength is determined from Equation 14 or Figure 53 where the cutoff wavelength for this mode is λ_c equal to $2.61r_0$.

The conditions of breakdown are determined from a numerical solution of the continuity equation, Equation 1, subject to the boundary condition that the electron density vanish at the walls

of the circular guide. The values of the coefficient ν_i , ν_a and D are functions of radial distance because of the radial variation of E . An approximate value for diffusion length assuming that the coefficients are constant is

$$\Lambda = r_0/2.405 \quad (27)$$

The waveguide dimensions, cutoff wavelength, and the cw power rating in air at atmospheric pressure are included in Table VII for common waveguide sizes. Additional information is given in Figures 34 and 35. Waveguide temperature was not computed for this mode because it is not commonly used for long waveguide runs.

TABLE VII

STANDARD CIRCULAR WAVEGUIDES, TM_{01}^0 MODE

Dimensions, Recommended Frequencies and Breakdown Power

BAND DESIGNATION	FREQUENCY (mc/sec)	INSIDE DIAMETER (inches)	INSIDE RADIUS (cm)	CUT-OFF WAVELENGTH (cm)	CW BREAKDOWN POWER-760 mm Hg (Megawatts)
X	9,375	1.165	1.48	3.87	1.63
K_u	16,000	0.683	0.867	2.26	0.58
K	24,000	0.455	0.578	1.51	0.28
K_a	35,000	0.312	0.396	1.03	0.14
4 mm	70,000	0.156	0.198	0.517	0.038

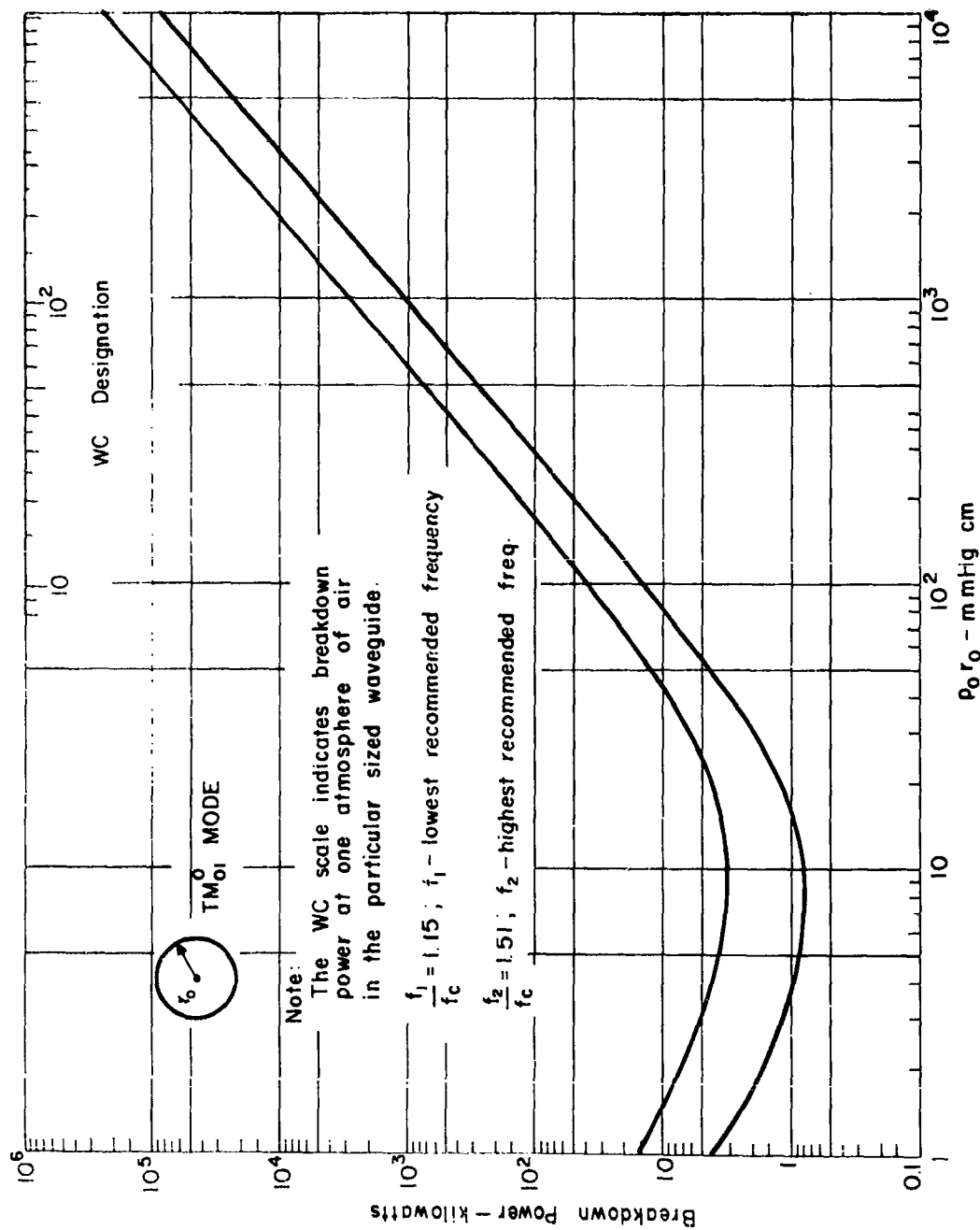


Figure 34 CW breakdown power for air filled circular waveguides.
TM₀₁ mode

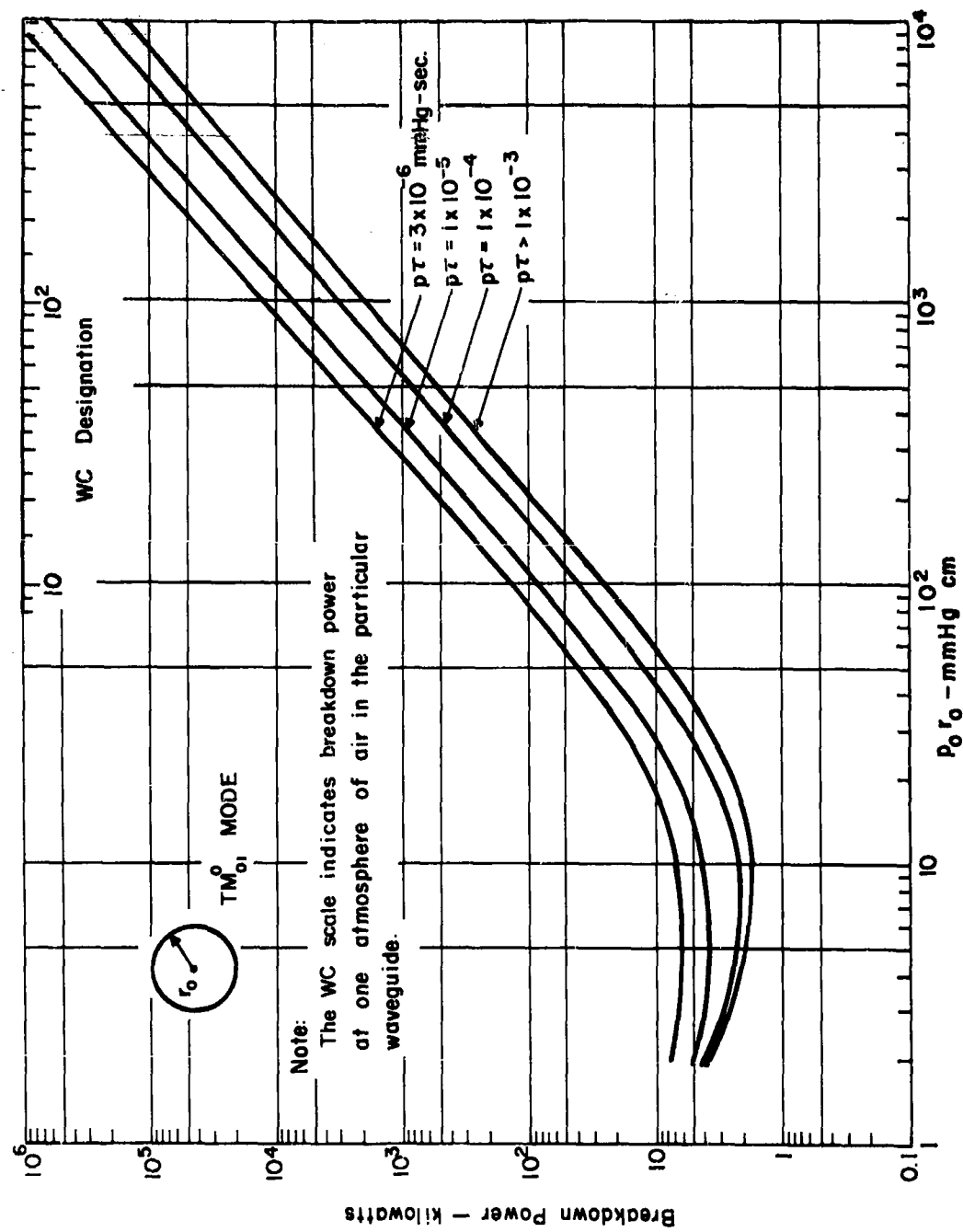


Figure 35 Single pulse breakdown power for air filled circular waveguides, TM₀₁ mode

Coaxial Waveguides

The characteristics of rigid coaxial waveguide operating in the dominant or TEM mode will be considered in this section. The electric field configuration for this mode in terms of the rms field is

$$E = E_{rms}(r_1/r) \quad (28)$$

The maximum field intensity occurs at the inner conductor radius, r_1 , and is represented by E_{rms} . The relation between the power carried by the waveguide and the maximum rms electric field is

$$P = (r_1)^2 \ln(r_2/r_1) (E_{rms})^2/30 \quad (29)$$

The calculations of breakdown power are for coaxial systems having an impedance of 50 ohms. This corresponds to a ratio of outer conductor to inner conductor, r_2/r_1 , of 2.3.

The conditions of breakdown are determined from a solution of the continuity equation, Equation 1 in cylindrical coordinates, subject to the boundary conditions that the electron density vanish at the walls. The coefficients ν_1 , ν_a and D are functions of radius since the electric field varies according to Equation 28.

The operating temperature of the coaxial waveguide has not been given because for long waveguide runs the critical parts of the waveguide are the thermal characteristics of the insulators and connectors.

Reference should therefore be made to manufacturer catalogues for average power limitations.

The dimensions, recommended frequencies and breakdown power are given in Table VIII and additional information in Figures 36 and 37.

TABLE VIII
STANDARD COAXIAL WAVEGUIDES, TEM MODE
Dimensions, Recommended Frequencies and Breakdown Power

WAVEGUIDE TYPE	FREQUENCY RANGE (mc/s)		IMPEDANCE (ohms)	OUTER CONDUCTOR DIAMETER (inches)	INNER CONDUCTOR RADIUS (cm)	CW BREAKDOWN POWER-760 mm Hg (megawatts) at f_2
	f_1	f_2				
RG152/U	0.5	650	50	6.13	3.30	110
RG154/U	0.5	1,300	50	3.13	1.67	29
RG153/U	0.5	2,700	50	1.61	0.843	7.35
RG155/U	0.5	3,300	50	0.875	0.432	2.10
RG151/U	0.5	10,000	50	0.375	0.159	0.350

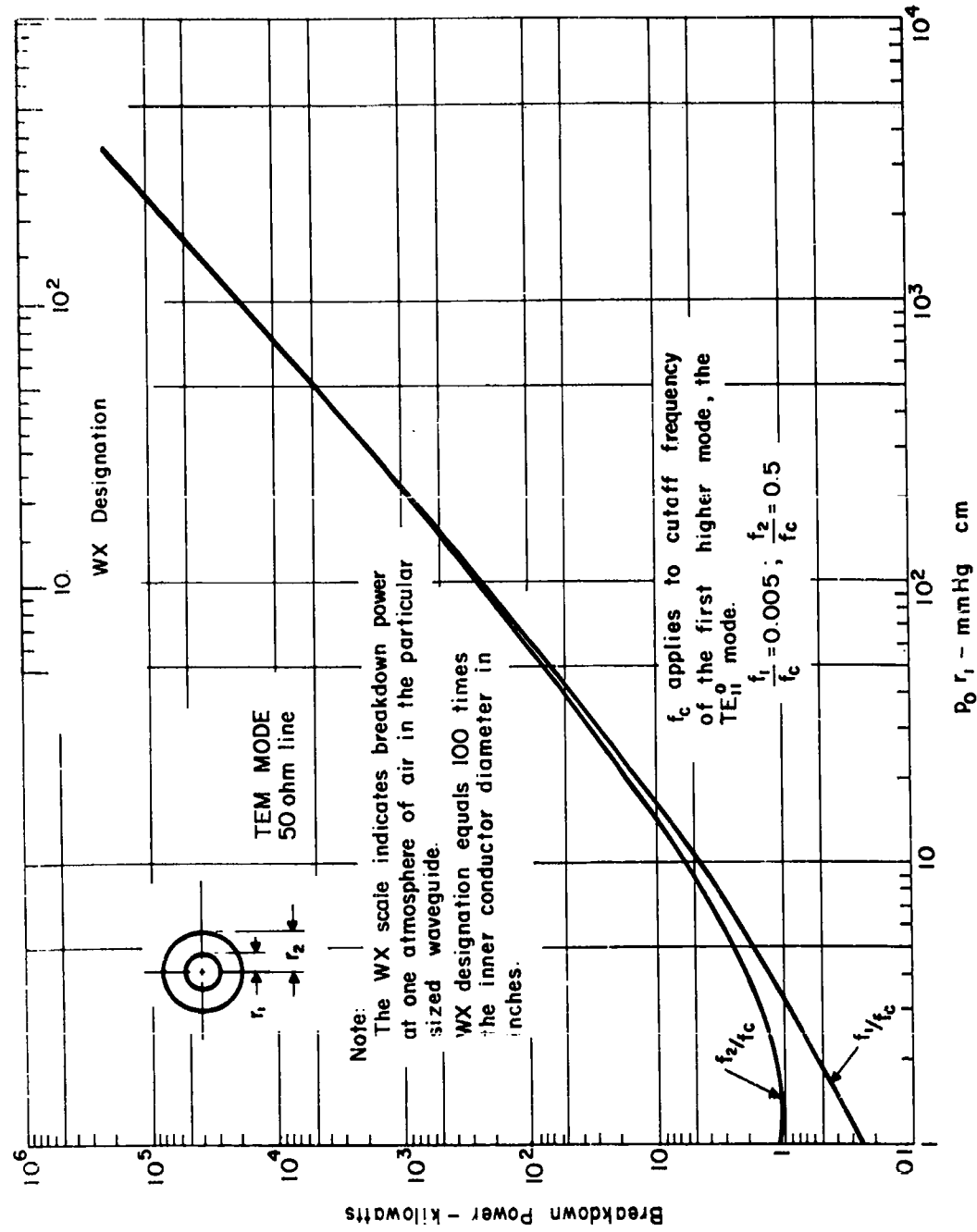


Figure 36 CW breakdown power for air filled coaxial lines,
TEM mode

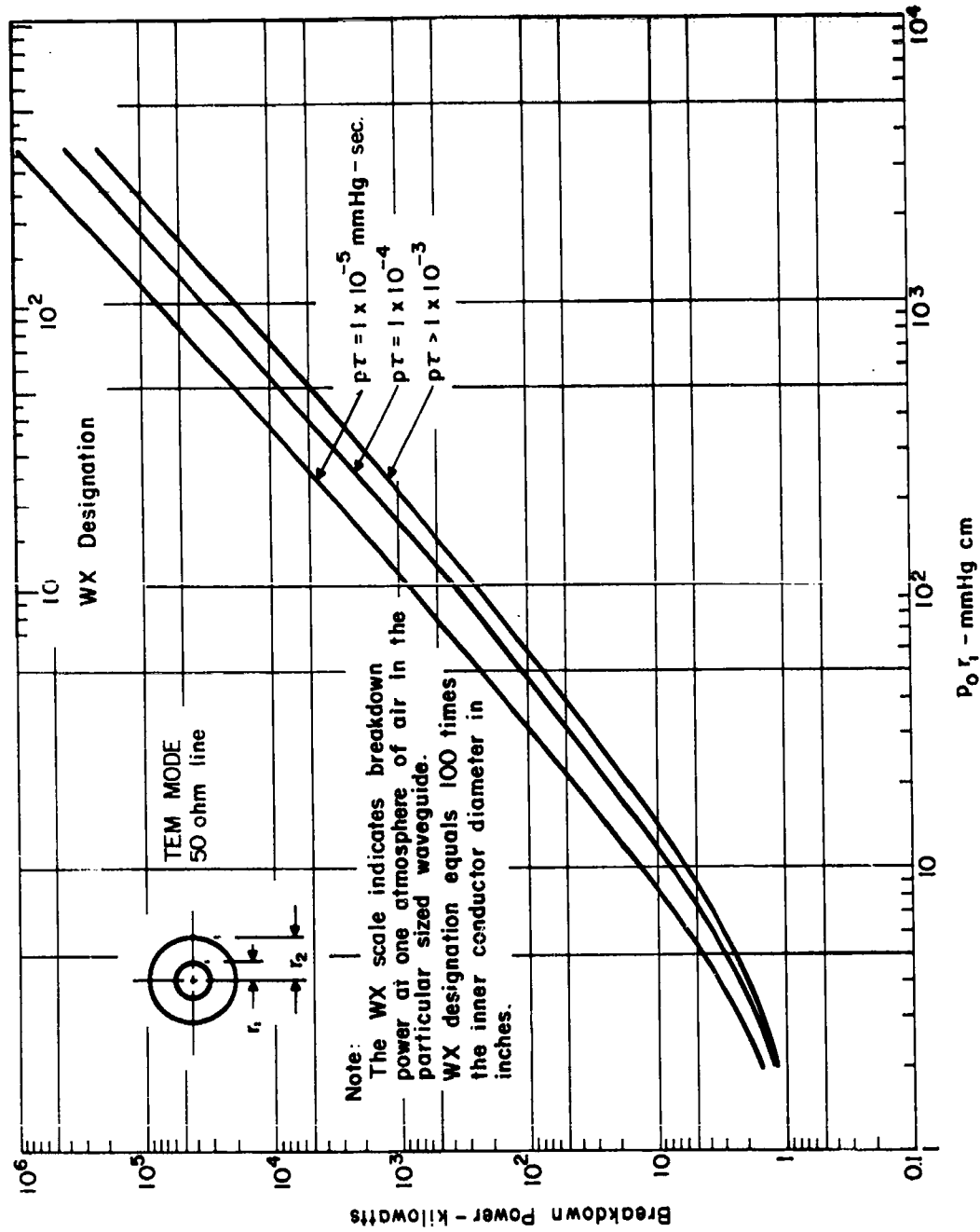


Figure 37 Single pulse breakdown power for air filled coaxial lines. TEM mode

IV. HIGHLY LOCALIZED BREAKDOWN, NON-UNIFORM CONDITIONS

Highly localized breakdown, generally associated with non-uniform conditions, becomes an increasingly important factor at high power levels. Degradation of a waveguide system due to their presence may not become important until the system has been highly pressurized to handle high power levels. At lower power levels pressurization gives the expected improvement. Two non-uniform conditions are distortion of the applied electric field and distortion of the ambient gas density, due to localized heating. In each case the value of E/p_0 becomes greater in the localized region and in accordance with Figure 2 the rate of ionization is increased.

A detailed examination of the breakdown theory shows that the electron continuity equation, Equation 1, remains valid for non-uniformities in electric field; but for non-uniformities in gas density it is no longer valid¹⁰. The correct, more general equation for cw breakdown is

$$\frac{v_{net}}{D} + \phi \nabla^2 \psi + (\nabla \phi) \cdot (\nabla \psi) = 0 \quad (30)$$

where ϕ is the inverse of the relative gas density and

$$\psi = Dn/\phi \quad (31)$$

is the normalized electron density. The other quantities were

introduced in Section I. The equation reduces to the more familiar one for ϕ a constant. In solving the above equation the usual boundary conditions, that n vanish at the walls, also applies to ϕ .

The electric field strength is increased locally by the presence of small metal objects or distortions of the waveguide walls. Examples for regular geometrical shapes are listed below¹¹

<u>Non-uniformity</u>	<u>Maximum increase in field strength</u>
hemisphere on a surface	3
sphere in space	3
sphere on surface	4.2
cylinder perpendicular to E field	2
hemicylinder	2

For the case of rounded corners and selected contours to minimize field enhancement, increased fields ranging to a maximum value of 3 are discussed by S. Cohn¹². For smoothly-varying bumpy surfaces the maximum field is increased by only a factor of 1.28,¹³

The above values of electric field enhancement are useful for estimating the reduction in peak power capability in components; however, it is the small inadvertent irregularity which is most troublesome. This type of irregularity may escape visual inspection and not lead to failure at modest values of pressurization. This is because the region is so small that rapid electron diffusion prevents breakdown. As the power level is increased, requiring additional pressurization, then the localized discharge becomes possible. An example

which was worked out theoretically for hemispheres¹⁴ can be used to compute the conditions for the transition from a volume to local breakdown. This transition is accompanied by a marked deviation in the linear relationship between breakdown power of the system and the square of pressure. Transition values of pressure for air as a function of radius are shown in Figure 38. As another example, small gaps at a waveguide joint due to warping or poor machining may develop field strengths exceeding those in the waveguide. Reference to Figure 4 makes it apparent that the maximum allowable gap should be given approximately by $pd/\pi < 1$ (mm Hg-cm).

The other form of non-uniformity arises from temperature gradients in the gas and thus in the gas density. The gradients arise as a result of particles or surfaces becoming heated. For very small heated regions even though the rate of ionization may become large the small size of the region allows the electrons to be lost rapidly by diffusion with the result that breakdown may become inhibited. An example of the temperature of a hot particle in a waveguide with only a modest loss tangent is shown in Figure 39. This was calculated assuming that radiation cooling predominates¹³.

To show the effect of gradients in gas density the solution to one dimensional problem, using Equation 30, for breakdown at a hot surface is shown in Figure 40.¹⁰ The solution is given in terms of the value of E_e/p_0 evaluated in the bulk of the gas remote from the hot surface and $p_0 l$ the normalized thickness of the layer of heated gas at the hot surface. For large film thickness the value of E_e/p_0 for breakdown

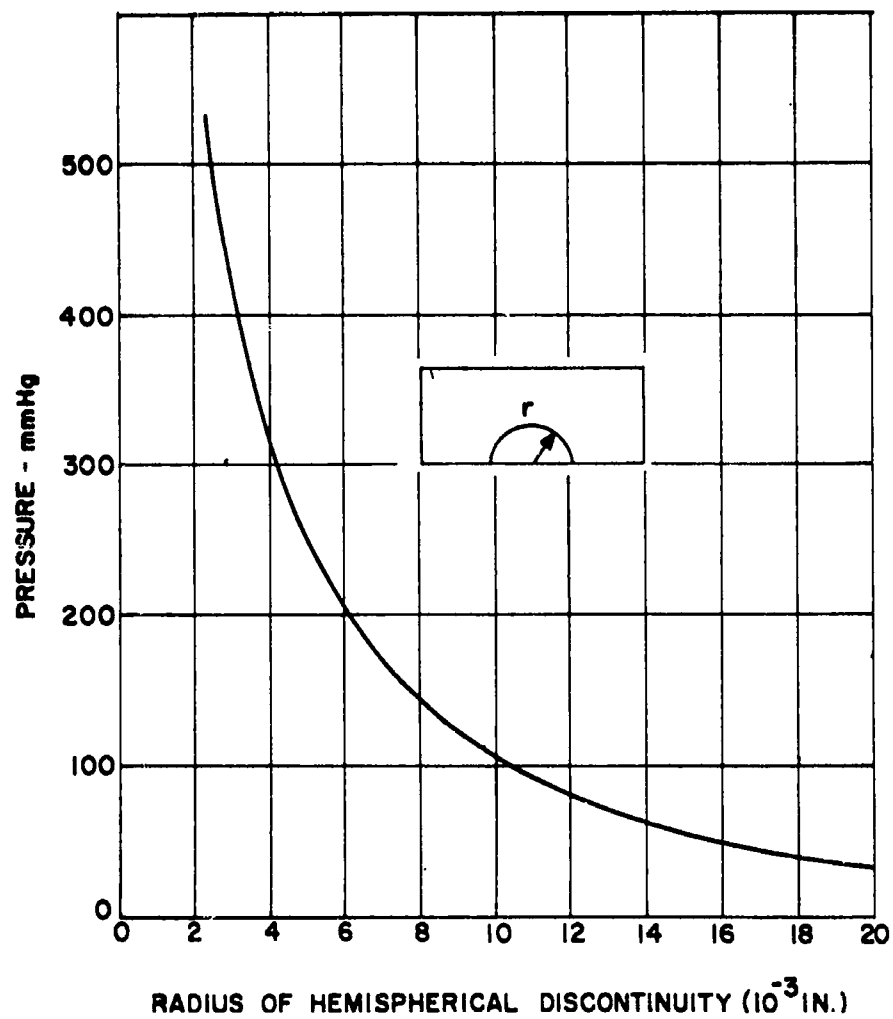


FIGURE 38
TRANSITION PRESSURE FOR HEMISPHERICAL DISCONTINUITY
IN AN AIR FILLED WAVEGUIDE

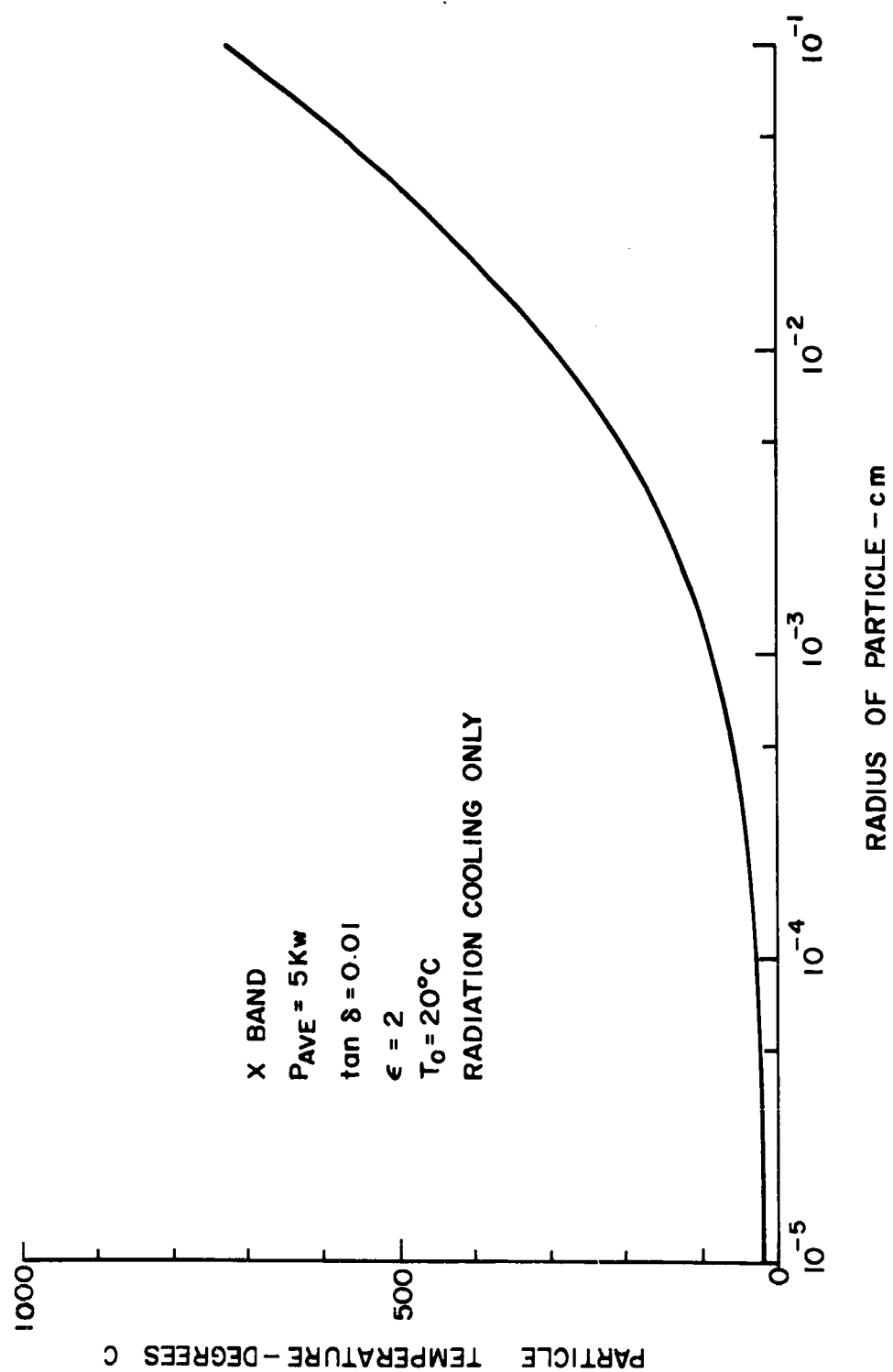


Figure 39
Temperature of Foreign Particle in a Waveguide

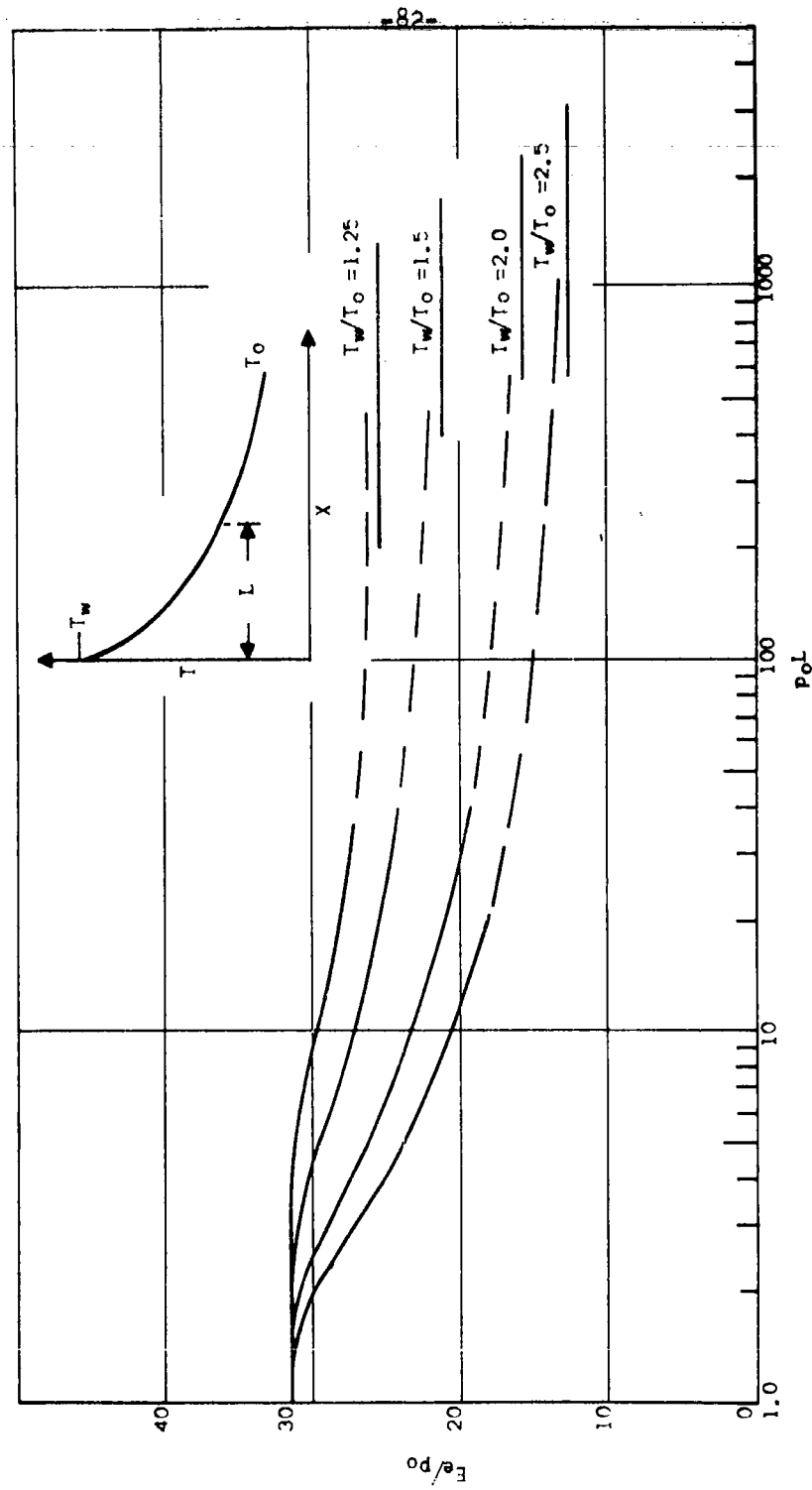


FIGURE 40
NORMALIZED SOLUTION FOR BREAKDOWN AT A HOT SURFACE
(EXACT DIGITAL COMPUTER SOLUTION)

decreases to the value given by the temperature ratio. If the normalized film thickness is small enough, $p_0 L$ about 10 or smaller the breakdown threshold is reduced only slightly by the presence of the hot surface.

There are several experimental verifications of localized breakdown to support the above discussion. The transition from a highly localized breakdown to a main volume breakdown is clearly shown by the measurements in Figure 41 for a small hemisphere¹⁰. The dashed lines represent the theoretical limits for the breakdown curve. Another cause for transitions is demonstrated by the set of breakdown measurements shown in Figure 42 for a number of different gases¹⁵. The departure of the curves from the linearity was found to be indicative of arcing at a joint in the test cavity. The interesting observation is that the breaks in the curves fell at about the same values of relative field strengths. This suggests a pressure independent effect; most likely it is due to excessive heating at the poor contact which causes breakdown when a critical power level is reached. The same effect accounts for the upper limits of $p_0 A$ plotted in the breakdown curves for various gases in Figure 7. These upper limits terminate approximately on a curve of constant power. A final example of localized breakdown is shown in Figure 43 for a small heated wire¹⁰. In this experiment the temperature of a 5 mil wire in a resonant cavity was varied in the presence of a flow of gas. The gas flow was used to vary the thickness of the film of heated gas at the wire. The value of flow rate $F = 15$ corresponds to 1240 centimeters per second. The

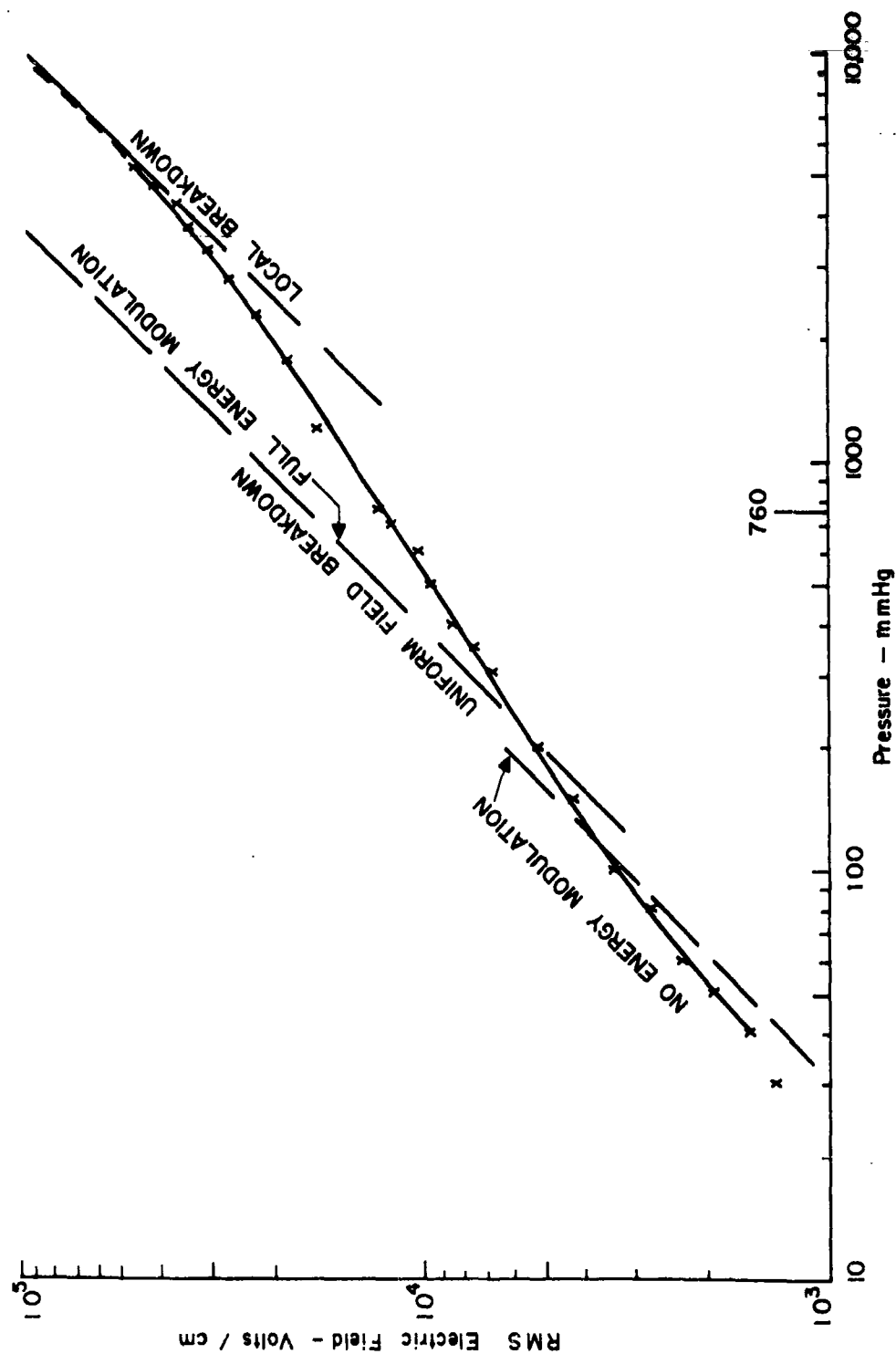


Figure 41
Breakdown of Air in TM_{010} Cavity .025 Hemisphere on Floor

50mC Co 60 SOURCE
POLISHED SURFACE

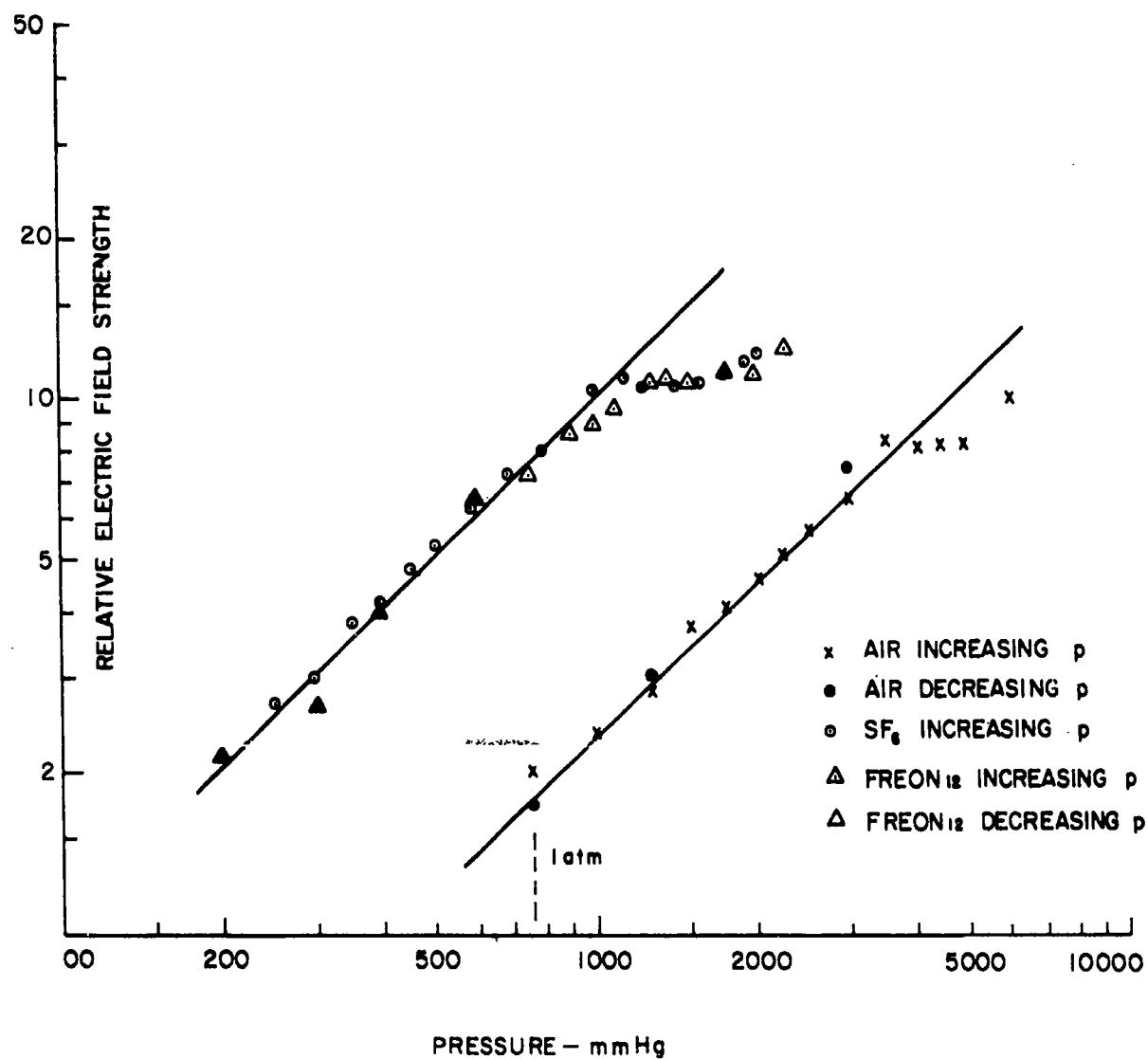


FIGURE 42
UNIFORM FIELD BREAKDOWN CHARACTERISTIC FOR
AIR, FREON 12, AND SF₆

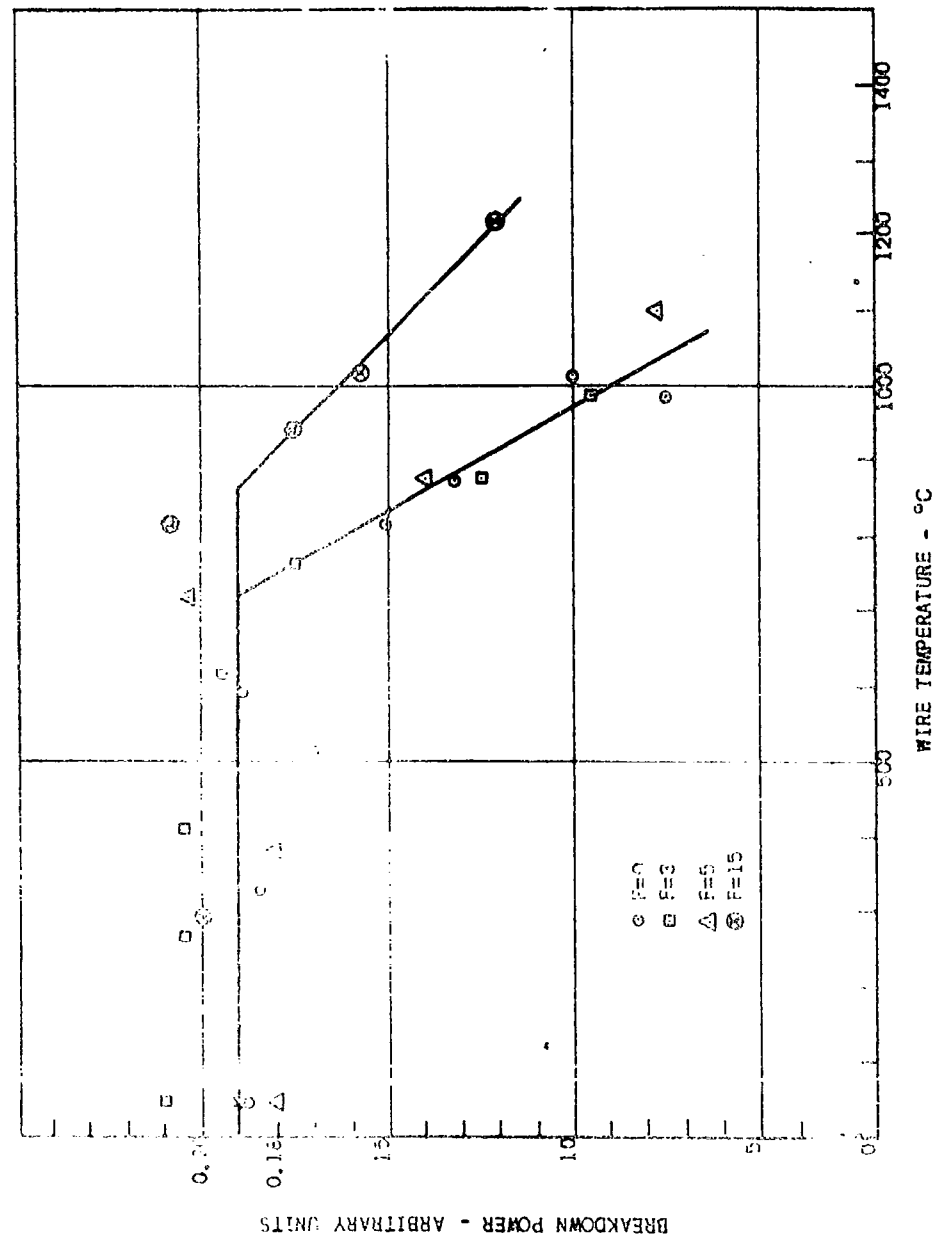


FIGURE 43
RESULTS OF BREAKDOWN MEASUREMENTS
WITH A HOT WIRE IN THE PRESENCE OF GAS FLOW

surprising result is that the breakdown threshold did not begin to drop until temperatures approaching 700°C were reached. At this temperature the breakdown threshold would be lowered by more than an order of magnitude under uniform conditions (see Section II). The eventual increase of the threshold due to the large gas flow and the eventual dropping off with temperature are examples of the importance of film thickness in controlling breakdown.

Although enhanced values of E/p generally occur at small discontinuities or localized heated regions, the effect on the breakdown threshold frequently does not appear until high pressures are reached where the electron diffusion rate has been sufficiently reduced. This points out that some care must be exercised in attempting to predict system failure from measurements made at lower power levels. The examples given in this section suggest important factors limiting the realization of the full power capability of waveguide systems.

V. DESIGN CONSIDERATION FOR
HIGH POWER WAVEGUIDE SYSTEMS

Frequently discrepancies are found between the rated power handling capabilities of components and the power levels at which the assembled system fails. Although the location of the point of failure in an operating system is difficult to find, experience indicates that it is generally inadvertent factors beyond the component designers control which are troublesome. In this section "good practice" for high power components will be discussed and then some of the inadvertent factors will be mentioned.*

The choice of a waveguide size and mode of operation has become more important as power levels have increased. In Section III detailed information was given regarding peak power and average power capabilities. In summarizing the information it is apparent that the breakdown power, in the high pressure range for a specific gas, is nominally proportional to the cross sectional area of the waveguide. The gas and its pressure determine the field strength at breakdown and the frequency is unimportant as long as it is not taken to be too close to cutoff. On the other hand, if a particular waveguide mode is chosen and an operating frequency range in terms of the ratio Area/λ^2 is given, then the breakdown power is proportional to λ^2 . A comparison of breakdown power for various modes at mid-band frequency is given in Table IX below:

*A discussion of this subject can also be found in Reference 18.

TABLE IX

Comparison of Breakdown Power for Various Modes

<u>Waveguide Mode</u>	<u>Breakdown Power</u>
TE ₀₁ rectangular	$1.03 \times 10^{-3} A E_{rms}^2$
Coaxial - 50 Ω	$2.10 \times 10^{-3} A E_{rms}^2$
TE ₁₁ circular	$1.20 \times 10^{-3} A E_{rms}^2$
TE ₀₁ circular	$0.92 \times 10^{-3} A E_{rms}^2$
TM ₀₁ circular	$2.05 \times 10^{-3} A E_{rms}^2$
Plane Wave	$2.66 \times 10^{-3} A E_{rms}^2$

The quantity A is the cross sectional area (cm²) of the waveguide and E_{rms} (volts/cm) is the breakdown field strength. The coefficient for the plane wave is largest indicating that in principle it can carry the greatest power per unit area. This follows because the power density is uniform throughout the cross section. A comparison can also be made to those modes of propagation which are possible on single wires and similar unbounded lines but not to the same degree of generality. At 100 Gc for a single wire line of 1 cm radius the breakdown power in terms of breakdown field strength is

$$P = 3.3 \times 10^{-2} E_{rms}^2$$

where 90% of the power is contained within a radius of 19 cm.¹⁸ If an enclosed rectangular waveguide of the same cross sectional area were used, then the breakdown power for the same maximum field strength would be

$$P = 1.2 E_{rms}^2$$

Thus, because the fields in the open wire line are concentrated at the single conductor, a rectangular waveguide of equivalent area can carry power levels almost two orders of magnitude greater.

The attenuation for various modes can be separated into the product of two factors: one geometric, including ratios of dimensions to wavelength, and one including the frequency to the 3/2 power and a coefficient depending upon the metal. The geometric factors for modes in rectangular and circular waveguide were tabulated in Table III and the expressions for resistivity of common metals were tabulated in Table II. For illustrative purposes Figure 44 contains the relative attenuation of several rectangular modes in square waveguide as a function of the ratio of size to wavelength. The low loss circular mode is plotted to show its superiority for large diameters. The case where just the height is increased is included to point out that no further significant decrease in attenuation occurs for values of b/λ greater than 2. Figure 45 contains the relative attenuation for circular waveguide modes.

In general the power handling capacity of a waveguide can be raised by increasing the cross sectional area. The final decision is an engineering compromise including such factors as cost, size, cooling techniques, pressurization, mode suppression and difficulty in realizing the required components.

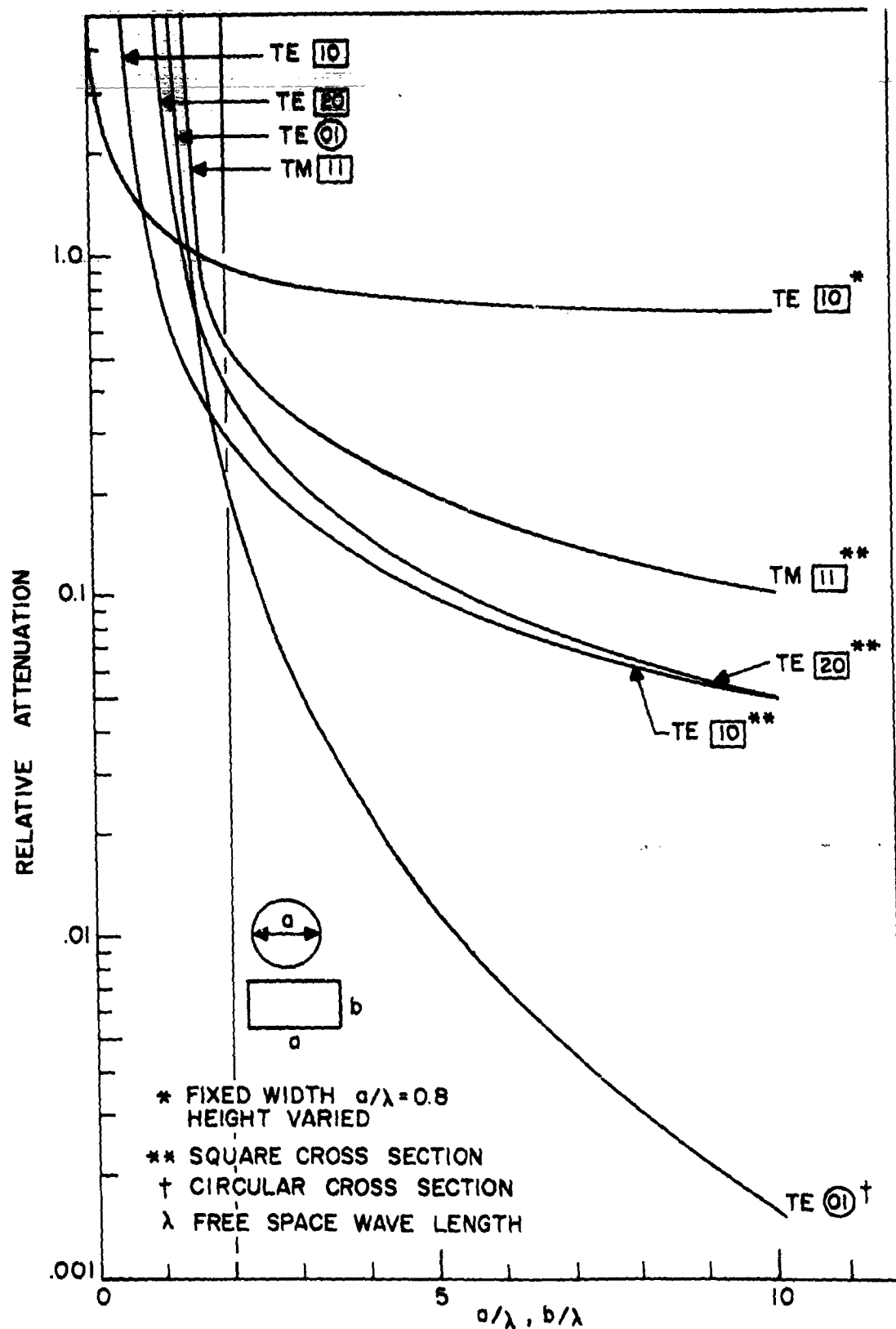


FIGURE 44 RELATIVE ATTENUATION OF MODES FOR RECTANGULAR WAVEGUIDE

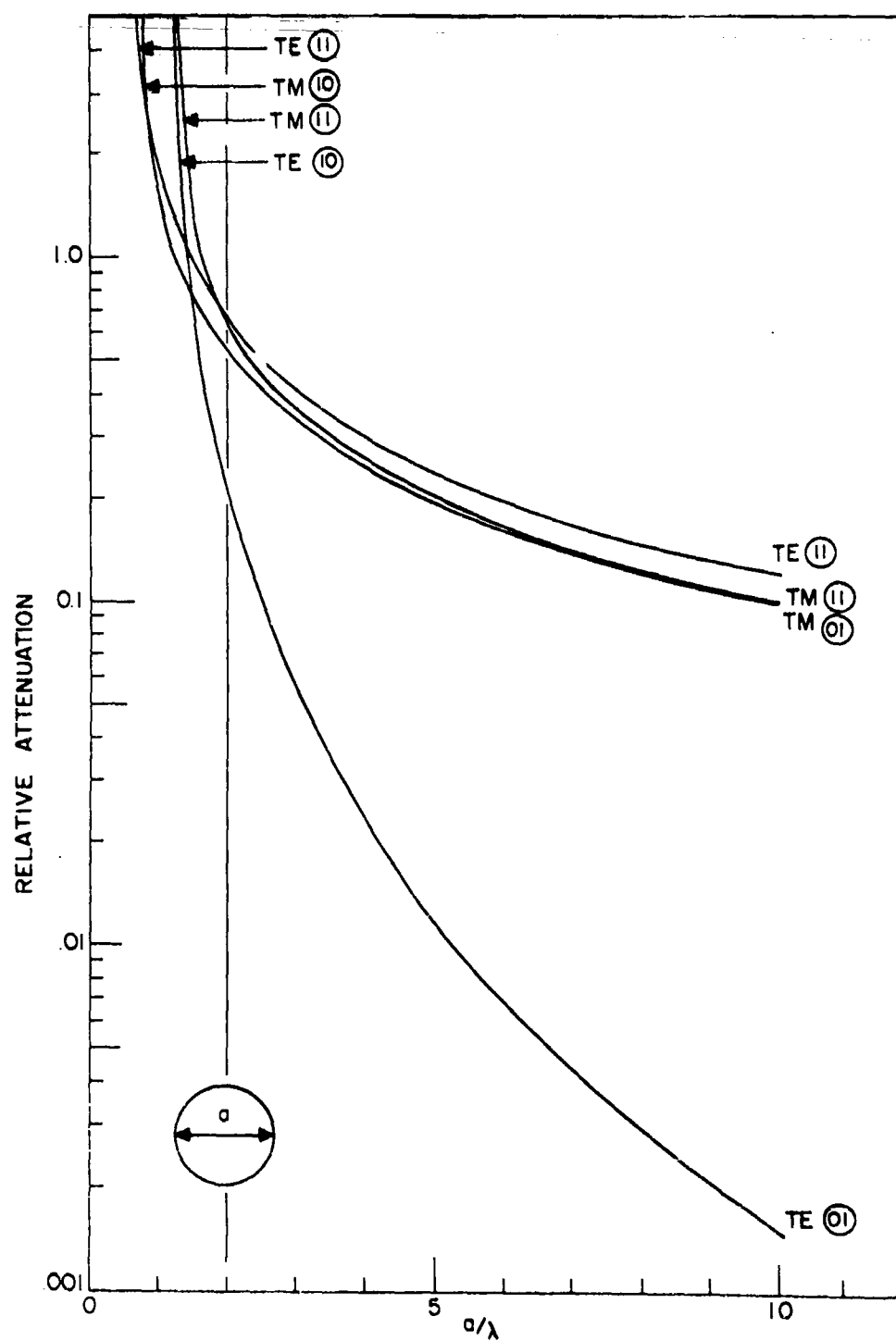


FIGURE 45 RELATIVE ATTENUATION OF MODES IN CIRCULAR WAVEGUIDE

There are a number of useful measures for obtaining acceptable high power performance. Pressurization with air or the high dielectric strength gases discussed in Section I can increase the peak power level by factors of 10 to 100. The power remains proportional to the square of pressure until other factors such as arcing joints or minor imperfections in the waveguide take over as the power levels are increased (see Section IV). The disadvantages of the high dielectric strength gases are the formation of corrosive and toxic products after a failure has occurred. In addition after arcing the Freon gases leave a carbon deposit while SF_6 leaves a deposit which does not appear to be as troublesome. Since the undesirable effects are a function of the power level and the duration of the arc, they can be minimized by a rapid turn-off of the transmitter at the onset of a failure and incidently reduce damage to the system from other causes. As an alternative evacuation can increase the power handling capability well beyond what can be achieved with pressurization when the pressure is reduced to the range of 10^{-4} to 10^{-5} mm Hg. One important advantage in the presence of rf fields is that even if there is a tendency for arcing there is normally not enough gas to lead to a destructive breakdown. On the other hand, since the electron mean free path is now long compared to the dimensions of the waveguide, multipactor discharges are likely to occur as well as electrons accelerated to high energies. This leads to serious problems with vacuum window failures. An evacuated system also requires much greater care and leaks which are negligible in high pressure systems become intolerable in evacuated systems.

Multipactor discharges occur for gap voltages in the range from 100 to perhaps 10,000. High field emission of electrons might begin at field strengths as low as 10^6 volts/cm.

Waveguide joints are generally required in systems and represent one of the most serious sources of failure problems. If line currents flow across small gaps introduced by poor tolerances, warping, etc. of flanges, then field strengths in excess of that in the main line can occur at the gap. If the line currents are forced to flow across resistive layers at joints, then localized heating can occur. Both of these effects lower the breakdown threshold of the entire system. A very approximate rule for gaps at flanges is that the tolerances should be such that the largest permissible value of gap distance, d , should be given by $pd/\pi \sim 1$ (mm Hg-cm). This condition emphasizes that as greater pressurization is used for higher power levels the tolerances for the flange faces must also be reduced. The resistance of thin coating on the flanges used to inhibit corrosion must be carefully evaluated; this is particularly true as pulse lengths and average power are increased. The restrictions on narrow gaps and lossy interfaces also apply more generally; for example, to ferrites cemented to waveguide walls.

Several obvious measures for insuring high power operation include minimizing electric field enhancement. This is done by avoiding high Q structures and large standing waves, by rounding all corners and maintaining smooth, scratch free surfaces. In addition the system should be free of foreign material such as metal particles or bits of

lossy material which can either increase fields to the breakdown point or heat excessively with breakdown following (see Section IV).

Other sources of failures are resonances associated with harmonics, spurious radiation and spurious modes of propagation. These resonances under the worst conditions can result in field strengths exceeding that of the main mode and absorption of as much as 50% of the line power in the resonant section. Resonance can occur in long sections of line or locally at choke joints, windows or ferrite phase shift sections. If spurious radiation or harmonics are present, filters should be used to remove them at the source. If spurious modes are present their effects can be reduced by careful design and by inserting mode filters or absorbers.

Heat removal is another important problem at high power levels. In Section III heat removal only by natural means was considered. It should be pointed out that black external surfaces contribute heat removal by radiation comparable to that by natural convection. Where convection cooling is absent, as at high altitudes, radiation cooling remains as the only natural means for heat removal. Liquid cooling is the most effective form and it is limited only by the expense and inconvenience of providing the required flow rate. Internal flow of gas, i.e., using the gas inside the waveguide as a coolant, is not as effective. When flow velocities reaching 30 or 40 miles per hour are used only limited length of waveguide (2-10 feet) can be cooled because of the low thermal capacity of gases¹⁰. In practice gas input and output ports would have to be distributed along the waveguide system.

Arc movements or transfer in a waveguide system can be a serious problem if the arc reaches a vulnerable component. In CW or high duty cycle systems where the power level is well below the breakdown threshold an arc travels towards the generator. At X-band, Figure 46, speeds of the order of 20 feet per second are found in air at atmospheric pressure¹⁰. Increasing the pressure or introducing high dielectric strength gases reduces the speed while increasing the power increases the speed. A useful fact is that the arc moves with a velocity relative to that of the gas and so it becomes possible to "blow" the arc back to the point of initiation with a counter flow of gas¹⁰. In low duty cycle systems where the peak power levels are near the breakdown threshold, an arc can transfer rapidly to a point near the source merely because of the increased field strength due to the resultant standing wave. In both high and low duty cycle operation at high power levels a localized arc may not move at all but nevertheless cause damage. An arc occurring at a poor joint may not seriously reduce the transmitted power, but would still be destructive. For adequate protection of a system, means for detecting and rapidly turning off the transmitter for both types of arcs are required. Arc detectors have been developed using sensors for light, sound and transmitted power level changes.

Waveguide components designed with the above principles should result in peak power capabilities within a factor of 2 or 3 of the associated waveguide and certainly within a factor of 10. Below are tabulated some peak power capabilities of high power components

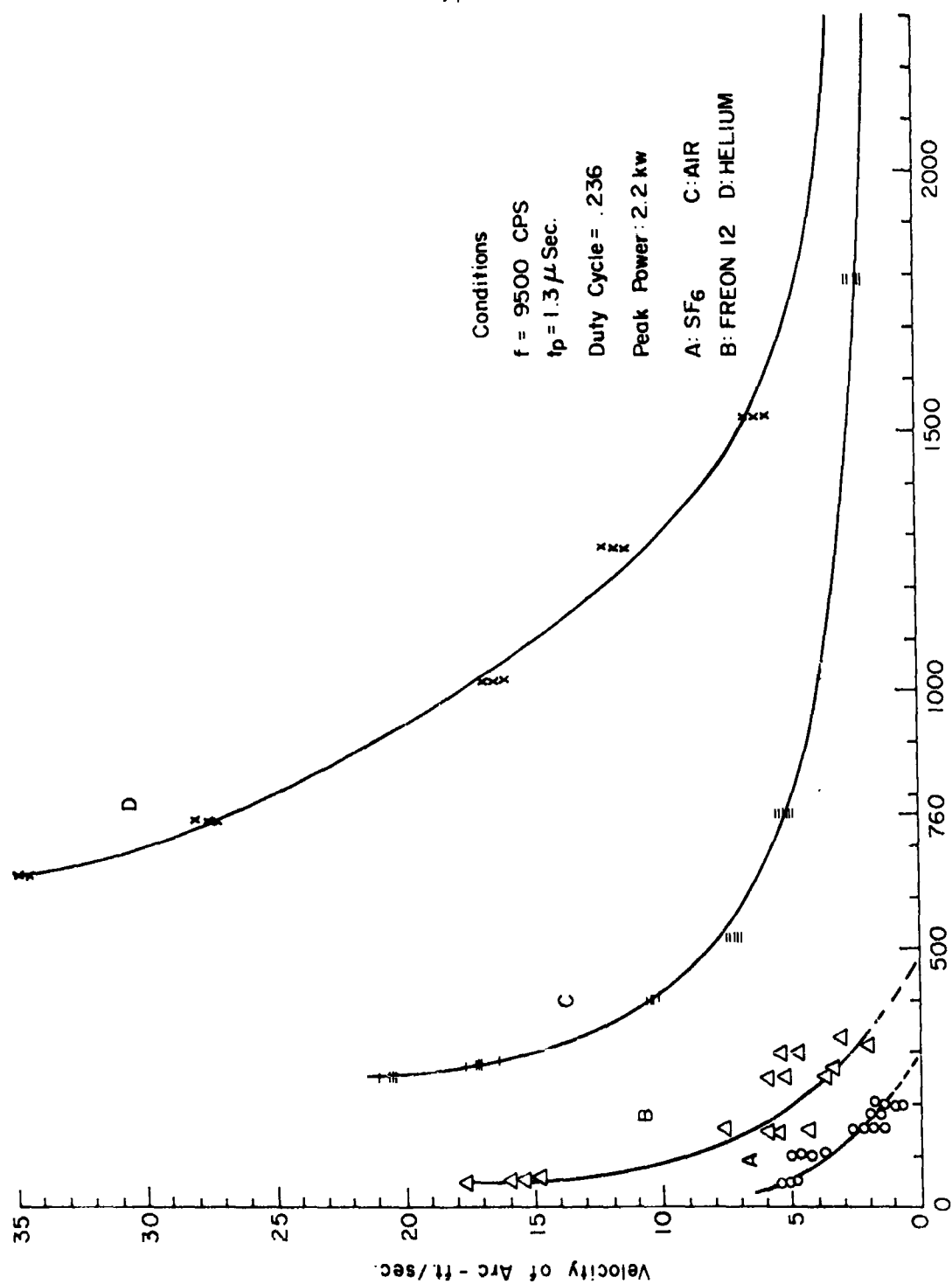


FIGURE 46 VELOCITY OF A TRAVELING ARC FOR SEVERAL DIFFERENT GASES

relative to a straight section of waveguide.

TABLE X

Relative Peak Power Capabilities
of High Power Components

<u>Component</u>	<u>Relative Capability</u>	<u>Frequency Evaluated</u>	<u>Pressure Range</u>
H plane bend*	.6 - .9	X-Band	air, 15 psi
E plane bend*	.97	"	air, 15 psi
H plane tee*	.80	"	air, 15 psi
90° twist*	.80 - .90	"	air, 15 psi
Magic tee*	.80	"	air, 15 psi
E plane tee*	.06	"	air, 15 psi
Cross guide coupler*	.21	"	air, 15 psi
Rotary Joints*-TM ₀₁	.14	"	air, 15 psi
-Coax	.15	"	air, 15 psi
Twists**	.25	S-Band	air, 15-35 psi
Folded Hybrid**			
Symetric arm	.63	"	air, 15-35 psi
Asymetric arm	.37	"	air, 15-35 psi
Short slot 3 db**	.26	"	air, 15-35 psi
Hybrid			

*The X-Band measurements were taken from Reference 17 where a 1.2 microsecond pulse length was used.

**Straight-section achieved only 50% of theoretical power where 12 microsecond pulse length was used.

APPENDIX I

Numerical Examples and Non-Standard Conditions

APPENDIX I

General breakdown curves for air filled waveguides are included in this section to allow direct solution of non-standard cases. These are curves of $(E_e/p_o)_n$ versus $p_o\tau$ where $p_o b$ or $p_o r$ are parameters. Figures 47 through 52 include rectangular, coaxial and circular waveguide modes. These curves represent solutions of the breakdown equation (Equation 1) which have taken into account the non-uniformities in the electric field for each mode.

Examples of the procedure to follow in computing the breakdown power for a given set of conditions will be presented by outlining several solutions in detail.

Problem 1: Compare the single pulse breakdown power of WR-112 and WR-90 waveguides at 40 mm Hg using a rectangular power pulse of 1/2 microsecond pulse width and a frequency of 9000 megacycles/sec at 20°C.

		<u>WR-112</u>	<u>WR-90</u>
a) Using Table IV compute the following	(ab)	3.59	2.33
quantities	(λ/λ_c)	0.584	0.728
	$p_o b$	50.5	40.8
	$p_o \lambda$	133	133
	$p_o \tau$	2×10^{-5}	2×10^{-5}
b) From Figure 53 determine	(λ/λ_g)	0.810	0.682
c) From Figure 47 determine	$(E_e/p_o)_n$	51	51
d) From Figure 3 determine	Δ	0.5	0.5
and using Eq. 3	E_e/p_o	50.5	50.5

		<u>WR-112</u>	<u>WR-90</u>
e) Multiply by p_o to obtain	E_e	2020	2020
f) From Figure 1 determine and compute	E_{rms}/E_e	1.03	1.03
g) From Eq. 14 compute	P	16.7 kw	9.2 kw

For the conditions of the problem the breakdown power of WR-112 is 16.7 kilowatts and the breakdown power of WR-90 is 9.2 kilowatts.

Problem 2: Compare the cw breakdown power of WR-187 for both full height and 1/8 height waveguide at 5000 megacycles/sec. The pressure is 20 mm Hg at 100°C.

		<u>Full Height</u>	<u>1/8 Height</u>
a) Normalize the pressure according to Eq. 8 to 20°C	p_o	15.7	15.7
b) Using Table IV compute the following quantities	(ab)	10.5	5.25
	(λ/λ_c)	0.632	0.632
	$p_o b$	34.8	4.35
	$p_o \lambda$	95	95
c) From Figure 53 determine	(λ/λ_g)	0.773	0.773
d) From Figure 48 determine $(p_o \tau \rightarrow \infty)$	$(E_e/p_o)_n$	33	
From Figure 49 determine $(p_o \tau \rightarrow \infty)$		-	44
e) From Figure 3 determine and using Eq. 3	Λ	0.3	0.3
	E_e/p_o	32.7	43.7
f) Multiply by p_o to obtain	E_e	514	686
g) From Figure 1 determine and compute	E_{rms}/E_e	1.07	1.07
	E_{rms}	550	735

I-3

		<u>Full Height</u>	<u>1/8 Height</u>
h) From Eq. 14 compute	P	3.24 kw	0.72 kw

For the conditions of the problem the breakdown power for full height guide is 3.25 kilowatts and for 1/8 height guide, 0.72 kilowatts.

I-4

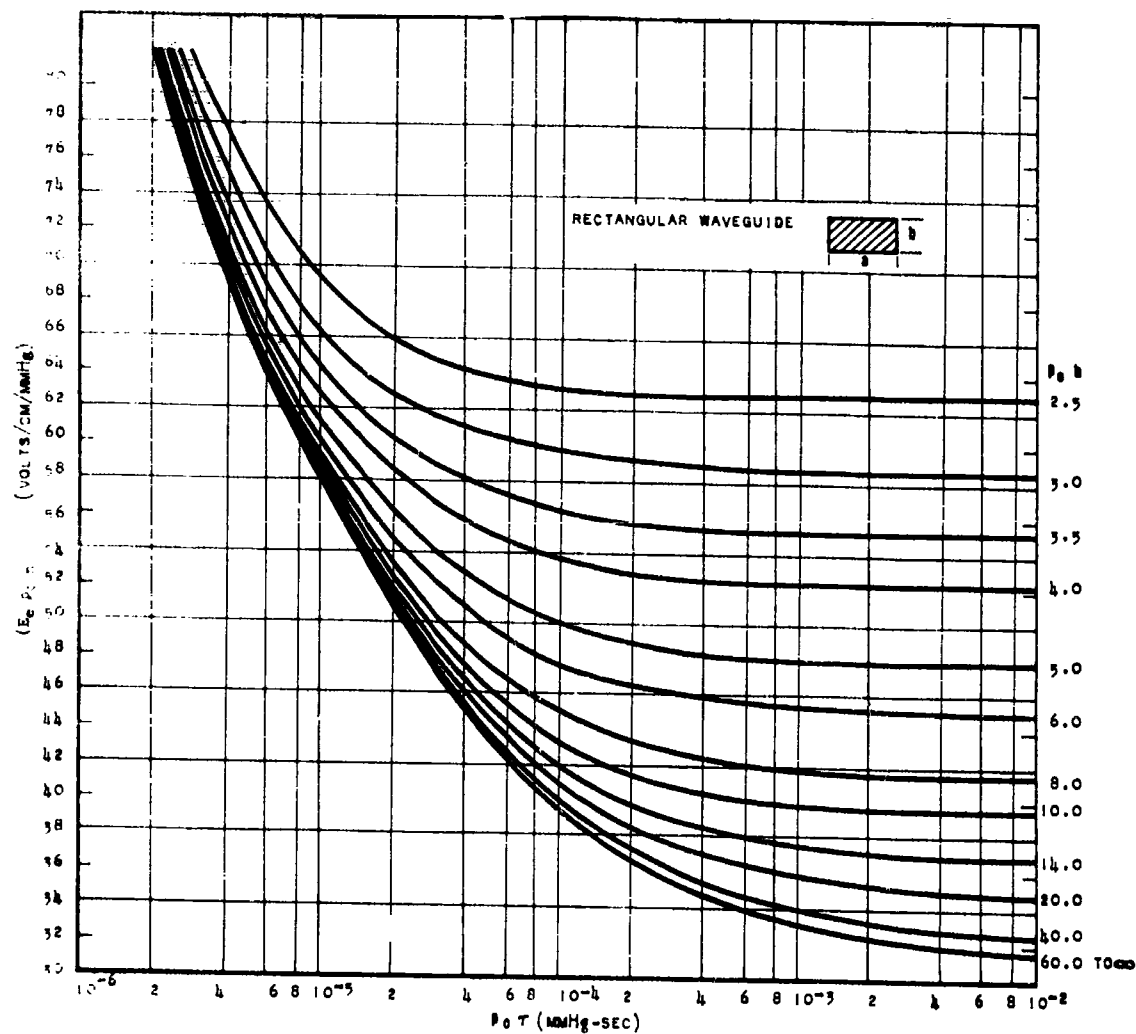


FIGURE 4. RATIO OF NORMALIZED SINGLE PULSE BREAKDOWN FIELD TO PRESSURE AS A FUNCTION OF PRESSURE TIMES PULSE WIDTH FOR VARIOUS VALUES OF PRESSURE TIMES WAVEGUIDE HEIGHT AND FOR $a/b = 2$

I-5

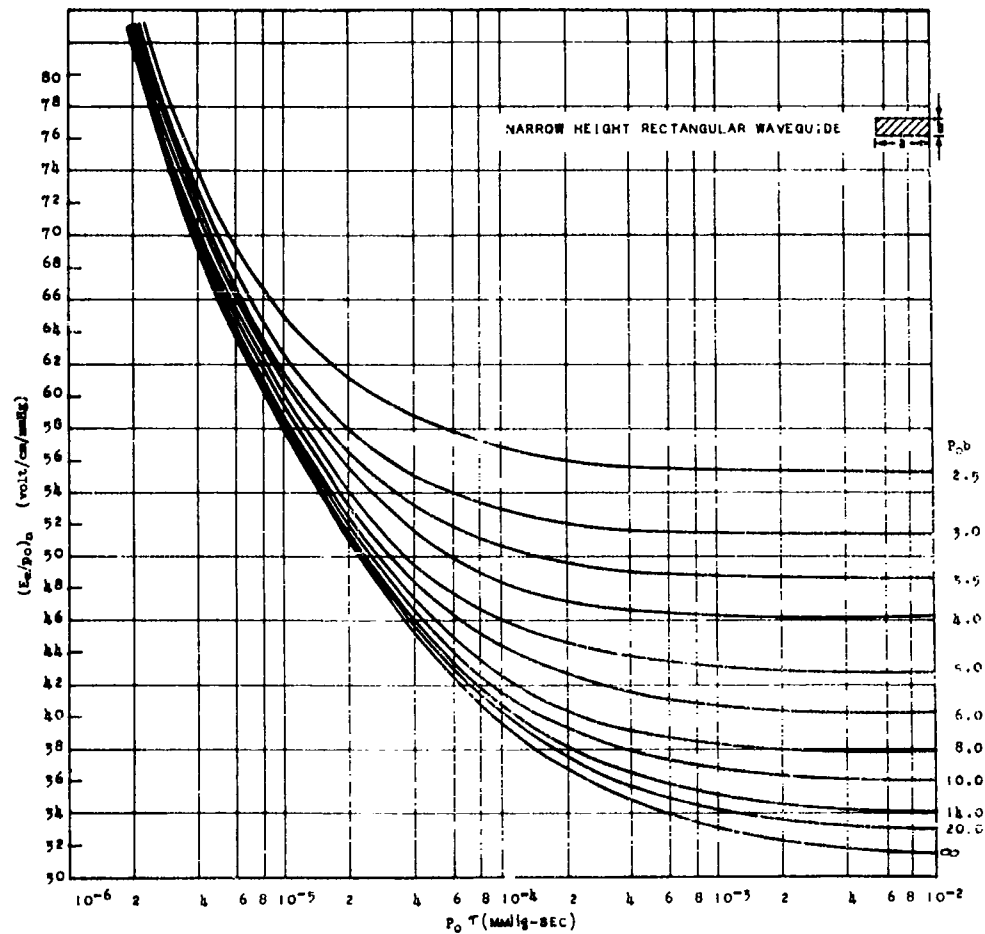


FIGURE 1-5 RATIO OF NORMALIZED SINGLE PULSE WAVEFORM FIELD TO PRESSURE AS A FUNCTION OF PRESSURE TIME PULSE WIDTH FOR VARIOUS VALUES OF PRESSURE TIME AVERAGE HEIGHT AND FOR $\alpha = 2$

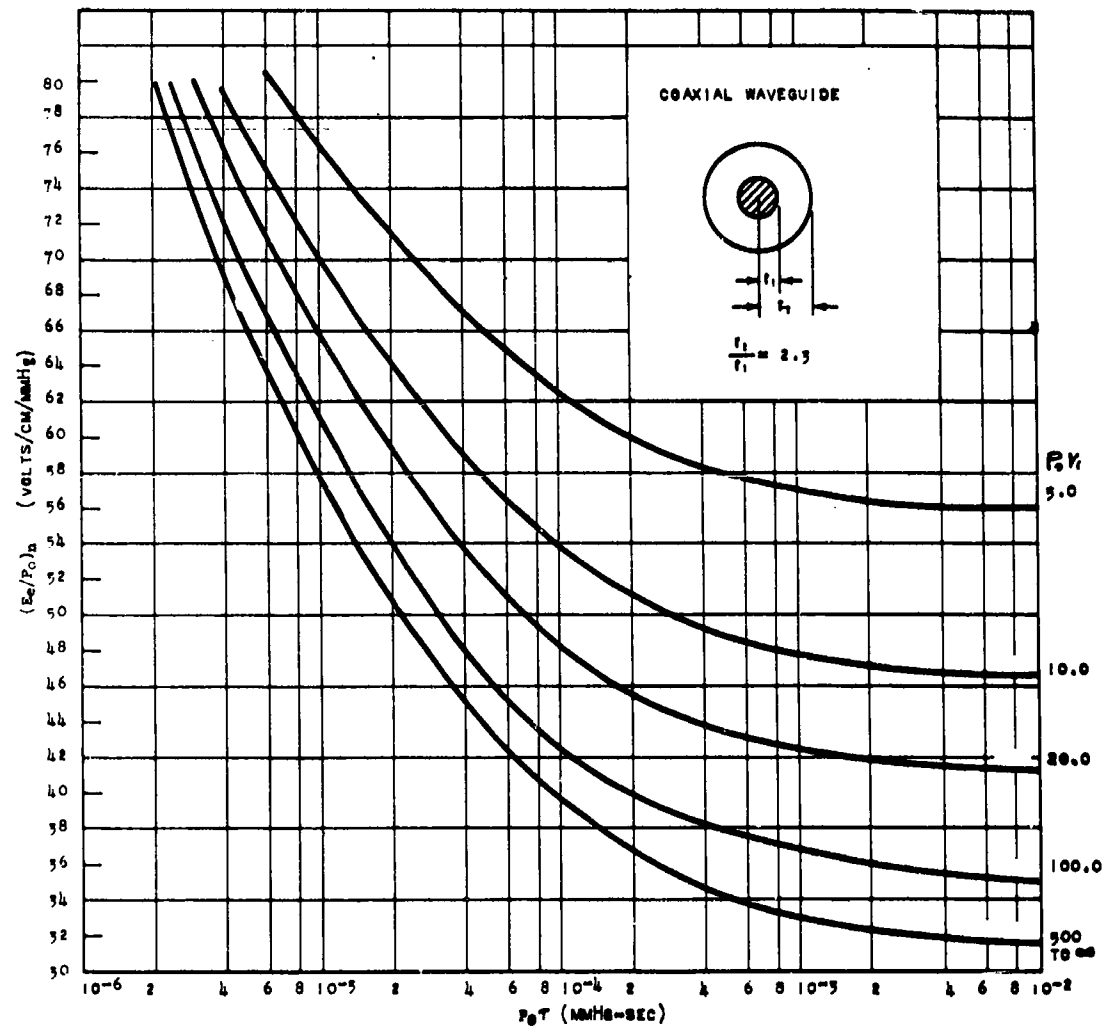


FIGURE 49 RATIO OF NORMALIZED SINGLE PULSE BREAKDOWN FIELD TO PRESSURE AS A FUNCTION OF PRESSURE TIMES PULSE WIDTH FOR VARIOUS VALUES OF PRESSURE TIMES INNER CONDUCTOR RADIUS

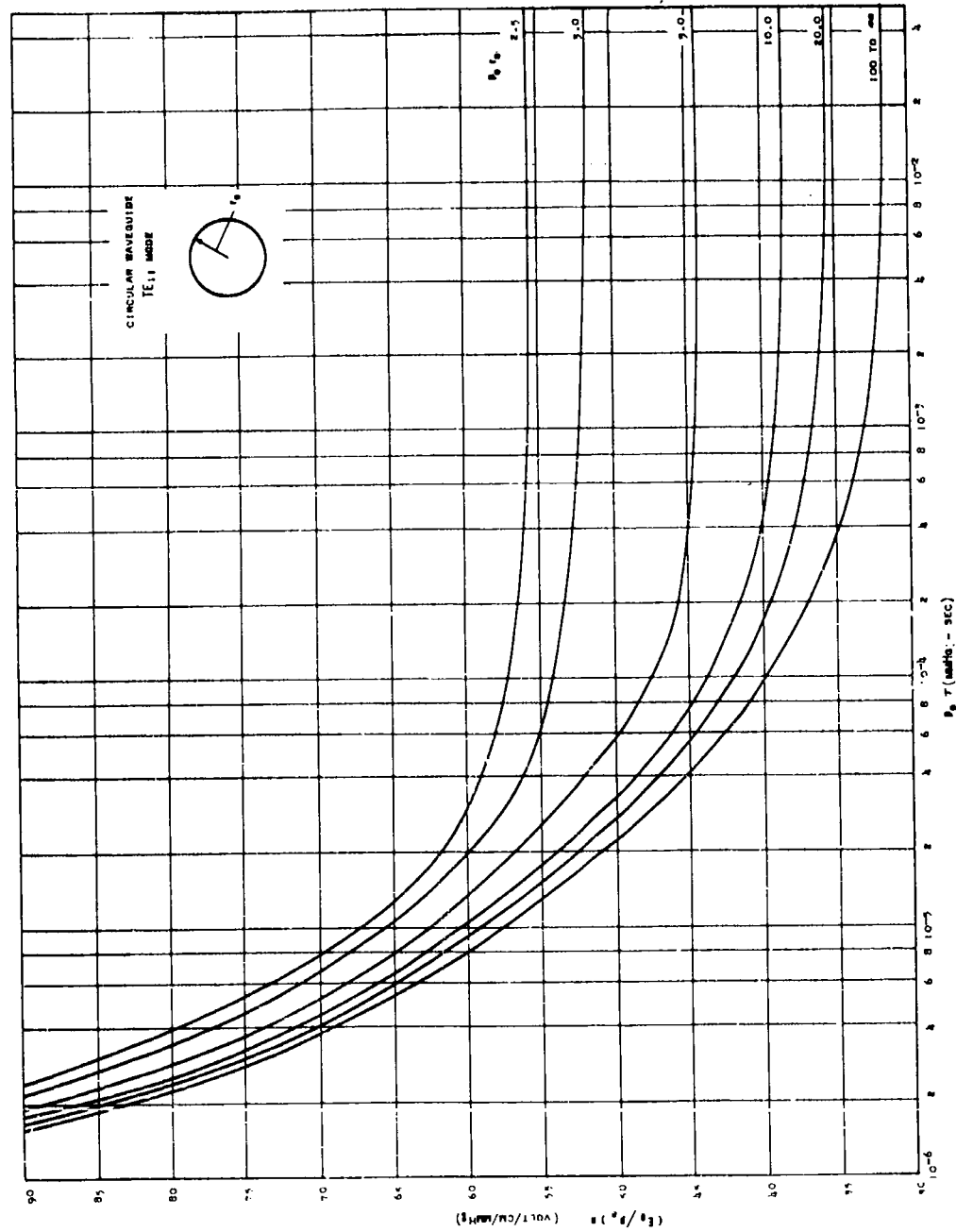


FIGURE 50 RATIO OF NORMALIZED SINGLE PULSE BREAKDOWN FIELD TO PRESSURE AS A FUNCTION OF PRESSURE TIMES PULSE WIDTH FOR VARIOUS VALUES OF PRESSURE TIMES RADIUS FOR CIRCULAR WAVEGUIDES OPERATING IN THE TE_{11} MODE

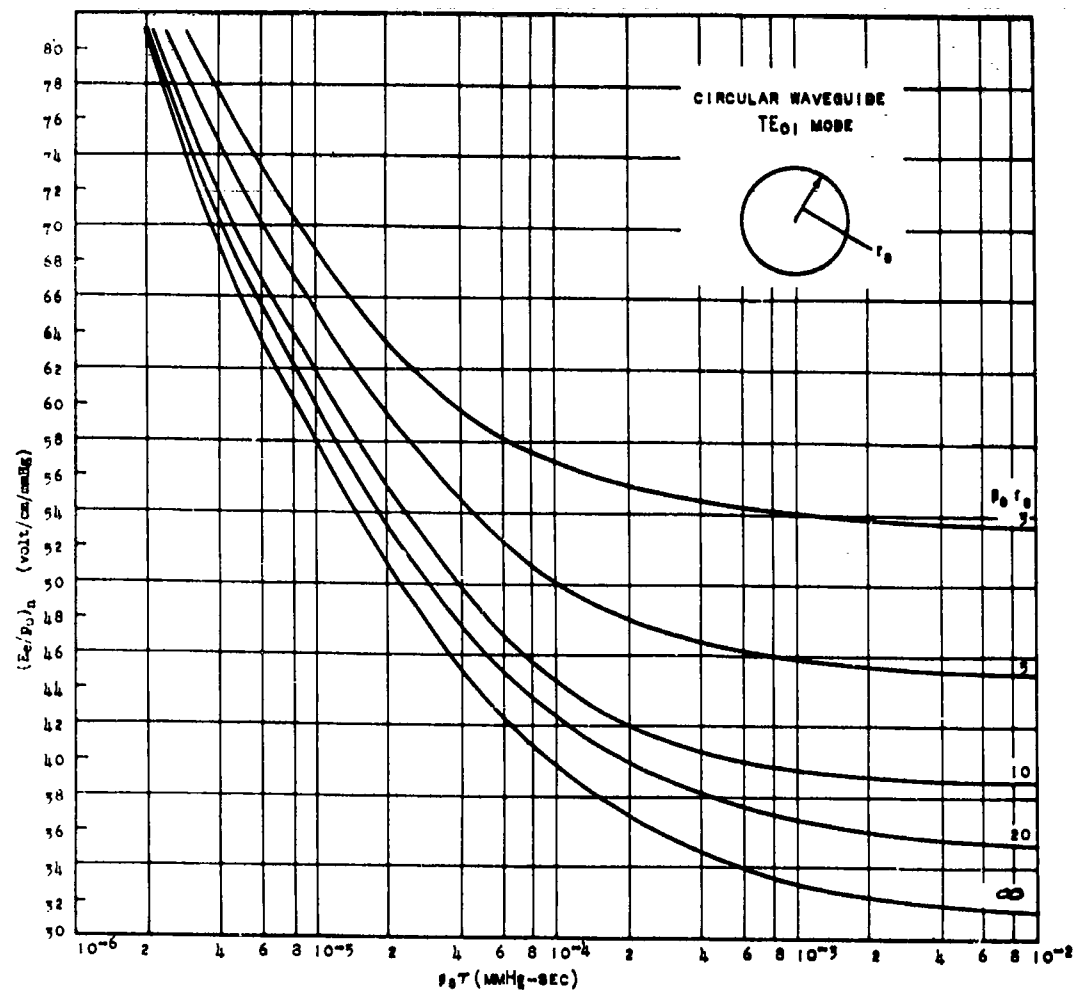


FIGURE 51 RATIO OF NORMALIZED SINGLE PULSE BREAKDOWN FIELD TO PRESSURE AS A FUNCTION OF PRESSURE TIMES PULSE WIDTH FOR VARIOUS VALUES OF PRESSURE TIMES RADIUS FOR CIRCULAR WAVEGUIDES OPERATING IN THE TE_{01} MODE

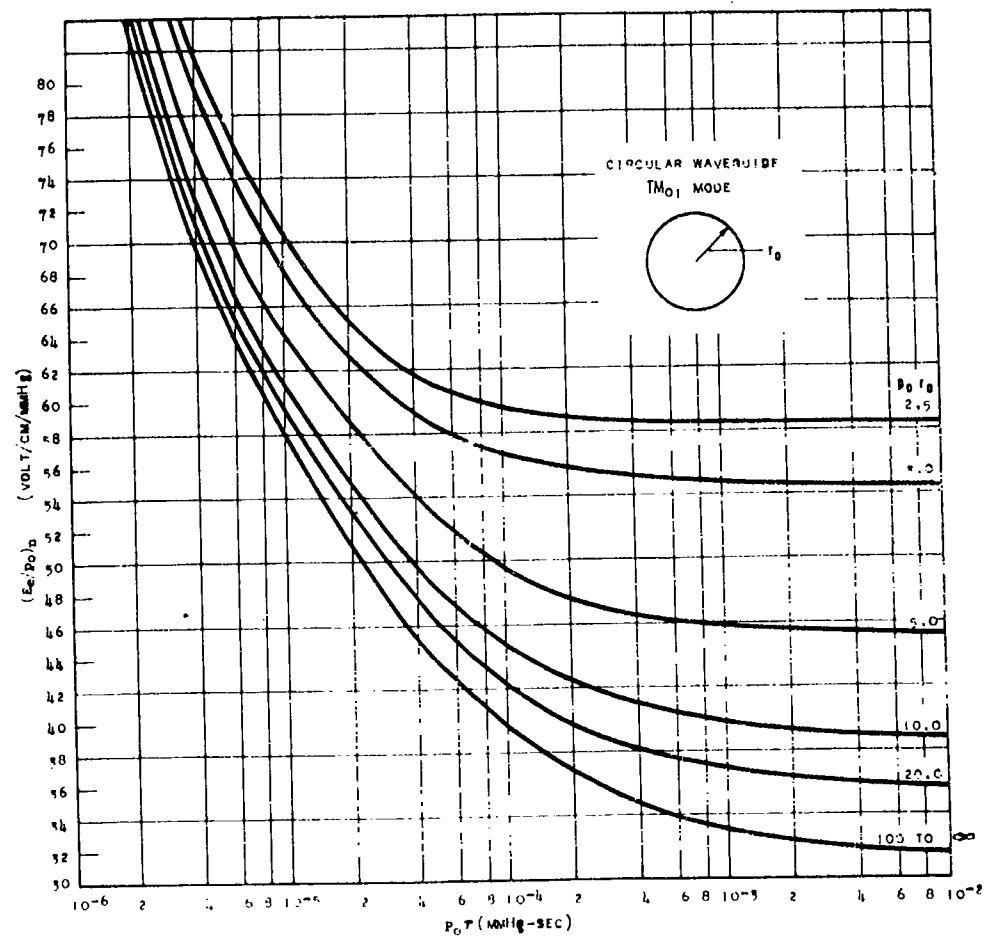


FIGURE 5-2 RATIO OF NORMALIZED SINGLE PULSE BREAKDOWN FIELD TO PRESSURE AS A FUNCTION OF PRESSURE-TIME PRODUCT FOR VARIOUS VALUES OF PRESSURE-TIME PRODUCT FOR CIRCULAR WAVEGUIDE OPERATING IN THE TM₀₁ MODE

I-10

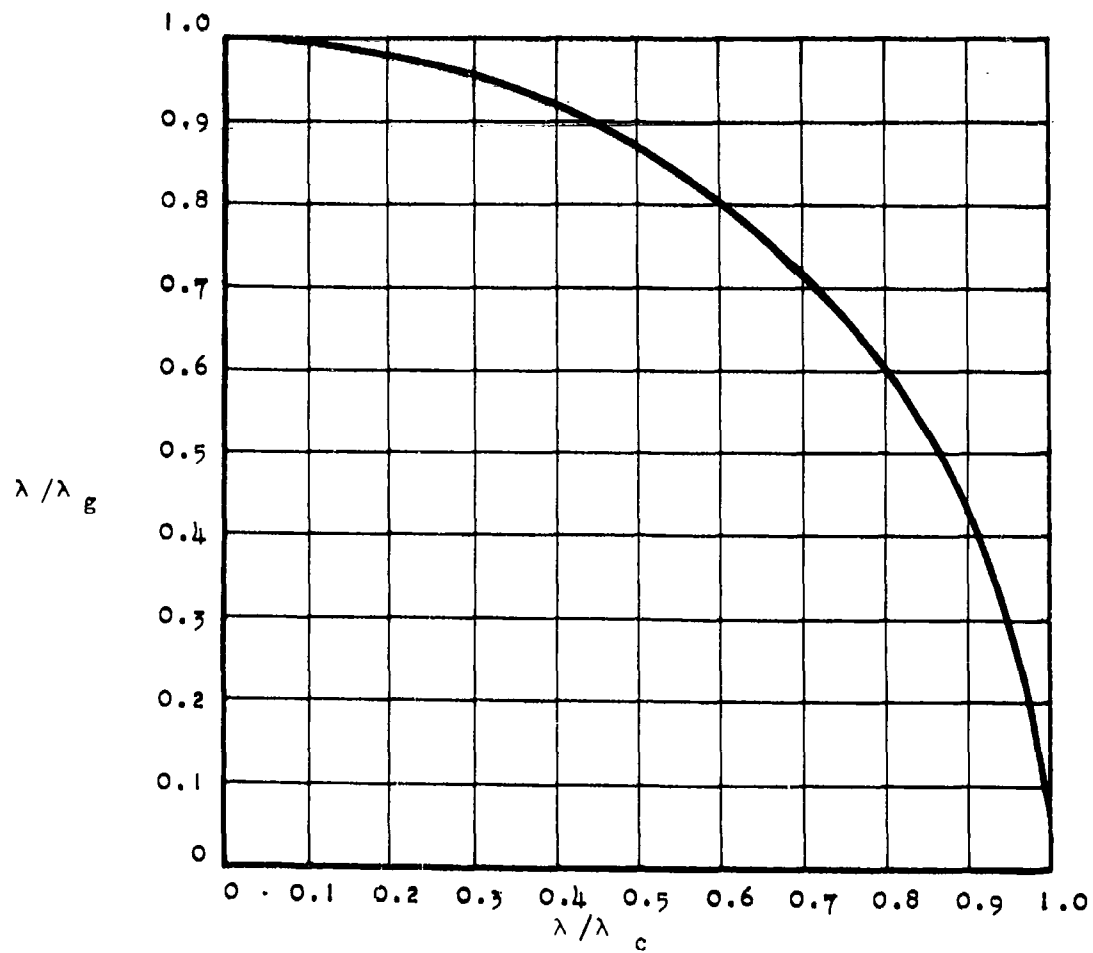


FIGURE 53 λ/λ_g AS A FUNCTION OF λ/λ_c

APPENDIX II
Diffusion Lengths

APPENDIX II

The diffusion length is a length parameter which is indicative of the size of the breakdown region and consequently of the rate of electron loss during breakdown. As discussed in Section I the ionization grows exponentially as the factor

$$\exp \left[\nu - D/\Lambda^2 \right] t,$$

where Λ is the diffusion length. Decreasing values of Λ lead to decreasing growth rates. In a volume which contains uniform fields the diffusion length depends only upon the dimensions of the volume. For any specific case where the fields vary the diffusion length is a function of geometry as well as the maximum value of $(E/p)_n$ because the maximum value determines the size of the region in which ionization is taking place. Breakdown solutions for air filled waveguide yield the curves shown in Figures 54 and 55 for relative diffusion lengths in rectangular and circular waveguide. The quantity Λ_0 is the diffusion length corresponding to uniform fields; but, it corresponds to a non-physical situation since a region bounded by conducting walls cannot sustain a uniform field configuration. The diffusion length is seen to be small near the threshold for ionization, 31.5 volts/cm mm Hg, as expected, because of the relatively small size of the region of ionization.

The significance of these curves is that, under non-uniform field conditions, the rate of build up is considerably reduced near the

II-2

ionization threshold where only a small portion of the region experiences ionization. The curves also suggest the rule that Λ may be approximated by a value equal to one third the smallest dimension of the region in which ionization is dominant.

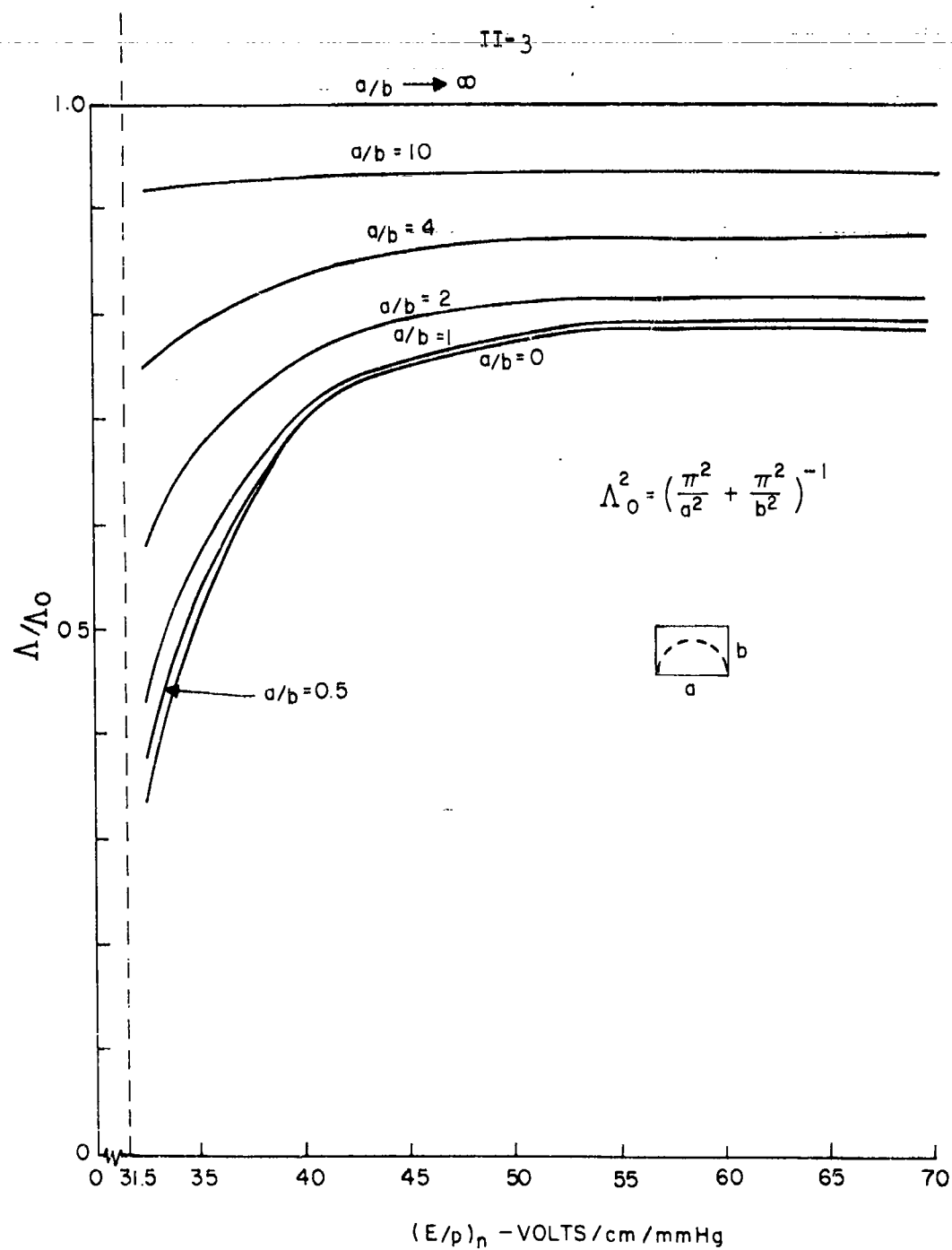


FIGURE 54
DIFFUSION LENGTHS FOR AIR FILLED RECTANGULAR
WAVEGUIDE TE_{10} MODE

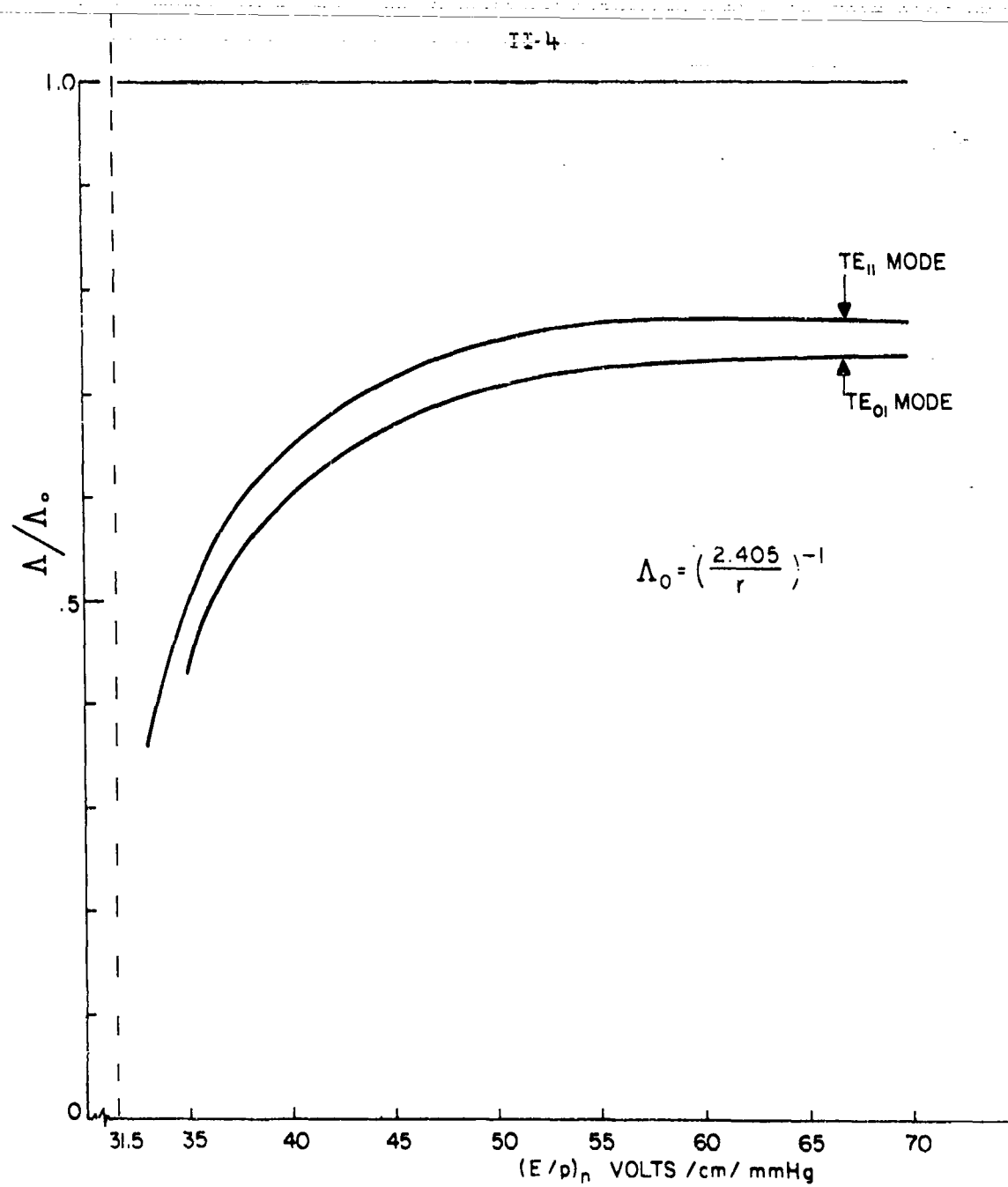


FIGURE 55
DIFFUSION LENGTHS FOR AIR FILLED CIRCULAR WAVEGUIDE

REFERENCES

1. L. Gould and L. W. Roberts, "Breakdown of Air at Microwave Frequencies", Jour. App. Phy. 27, 1162 (Oct. 1956).
2. S. C. Brown, "Basic Data of Plasma Physics", John Wiley and Sons, New York, N. Y., 1959.
3. S. C. Brown, "High Frequency Gas Discharge Breakdown", Handbuch der Physik XXII, 1955.
4. C. Buntschuh, H. B. Salkins and M. Gilden, "Nanosecond Pulse Breakdown Study", Rome Air Development Center - RADC-TDR-63-82, Microwave Associates, Feb. 1963.
5. P. R. Howard, "Processes Contributing to the Breakdown of Electro-negative Gases in Uniform and Non-uniform Electric Fields", Proc. of Institution of Elect. Engs. 104 part A, 139 (April 1957).
6. R. Cooper, "Experiments on the Electrical Strength of Air at Centimeter Wavelengths", Jour. of Inst. of Elect. Engs. 96 part III, 315 (1947).
7. W. H. McAdams, "Heat Transmission" (Third Edition), McGraw-Hill Book Co., 1954.
8. Handbook of Chemistry and Physics, 34th Edition (1952-1953).
9. S. J. Miller, Lincoln Laboratory, private communication, (1962).
10. M. Gilden, "Ultra High Power Transmission Line Techniques", Second Technical Note, Rome Air Development Center, RADC-TDR-62-208, Microwave Associates, June 1962 and Final Technical Note, March 1963.
11. R. D. Wengenroth, "The Waveguide Spark Gap as a Standard for Microwave High Voltages," Wheeler Laboratories, Report 953 P, June 1960.
12. S. B. Cohn, "Rounded Corners in Microwave High-Power Filters and Other Components", IRE Trans MTT-9, 389, (September 1961).
13. M. Gilden, "Ultra High Power Transmission Line Techniques", First Technical Note, Rome Air Development Center, RADC-TDR-62-208, Microwave Associates, December 1961.
14. P. M. Platzman and E. Huber-Solt, "Microwave Breakdown in Non-uniform Electric Fields", Phy. Rev. 119, 1143 (August 1960).

15. M. Gilden, "High Power Capabilities of Waveguide Systems", Fifth Quarterly Report, NObsr 85190, Microwave Associates, April 30, 1962.
16. M. J. King and J. C. Wiltse, "Surface Wave Propagation on Coated or Uncoated Metal Wires at Millimeter Wavelengths", IRE Trans. AP-10, 246, (May 1962).
17. Sperry Gyroscope Company, Report No. 7220-13004, "Study of Techniques for Measuring Microwave High-Power Breakdown in Waveguide Transmission Lines", June 1956.
18. R. M. White and R. H. Stone, "Gaseous Breakdown in Pressurized Microwave Components", Electronics, p 45, April 20, 1962.